INORGANIC COMPONENTS OF ATMOSPHERIC AEROSOLS

Thesis by:

Anthony S. Wexler

In Partial Fulfillment of the Requirements

for the Degree of

Doctor of Philosophy

California Institute of Technology

Pasadena, CA 91125

1991

(Defended December 5, 1990)

ACKNOWLEDGEMENTS

There are a number of individuals who contributed directly and indirectly to the completion of this thesis. First I would like to thank Dr. John Seinfeld who provided technical advice, financial support, and academic freedom to pursue my research. I would like to thank Dr. Donald Marsh of the University of Southern California for directing me towards an academic career and helping me remain financially solvent during my years at Caltech. I would also like to thank Dr. Glen Cass who provided technical advice during numerous informal discussions and Dr. Spyros Pandis who provided the wall that first bounced back most of the ideas in this thesis.

I will be forever grateful for the moral support of the members of my family: my parents, Art and Trudy Wexler, for their encouragement; my in-laws, Sherman and Hannah Stein, for their advice; and my wife, Rebecca, for her support. Finally I want to thank my children, Jason and Rachel, for the distractions they provide from the rigors of academic life.

ABSTRACT

The inorganic components comprise 15% to 50% of the mass of atmospheric aerosols and, these along with the relative humidity, control the aerosol water content. For about the past 10 years the mass of the inorganic components of atmospheric aerosol was predicted assuming thermodynamic equilibrium between the volatile aerosol-phase inorganic species, NH_4NO_3 and NH_4Cl, and their gas-phase counterparts, NH_3, HNO_3, and HCl. In this thesis I examine this assumption and prove that 1) the time scales for equilibration between the gas and aerosol phases are often too long for equilibrium to hold, and 2) even when equilibrium holds, transport considerations often govern the size distribution of these aerosol components.

Water can comprise a significant portion of atmospheric aerosols under conditions of high relative humidity, whereas under conditions of sufficiently low relative humidity atmospheric aerosols tend to be dry. The deliquescence point is the relative humidity where the aerosol goes from a solid dry phase to an aqueous or mixed solid-aqueous phase. Previous to this thesis little had been known about the temperature and composition dependence of the deliquescence point. In this thesis I first derive an expression for the temperature dependence of the deliquescence point and then prove that in multicomponent solutions the deliquescence point is lower than in the deliquescence point of the individual single component solutions.

These theories of the transport, thermodynamic, and deliquescent properties of atmospheric aerosols are integrated into an aerosol inorganics model, AIM. The equilibrium predictions of AIM compare well to fundamental thermodynamic measurements. Comparison of the prediction of AIM to those of other aerosol equilibrium models show substantial disagreement in the predicted water content at lower relative humidities. The difference is due to the improved treatment of the deliquescence properties of mixed solute aerosols that is contained in AIM.

In the summer and fall of 1987 the California Air Resources Board conducted the Southern California Air Quality Study, SCAQS. During this study the atmospheric aerosols were measured at nine sites in the Los Angeles air basin. The measurements determined the size and composition distributions of the components of the aerosol and the concentrations of their gas phase counterparts during a series of intensive study periods. The comparison of these SCAQS measurements to the predictions of AIM have so much scatter that a departure from equilibrium, that can be attributed to transport limitations, cannot be discerned. When the measured size distributions are compared as another indication of transport-limited departure from equilibrium, we find that different size aerosol particles are not in mutual equilibrium. Although the SCAQS data do not indicate a transport-limited departure from equilibrium, they do support our hypothesis that transport considerations are essential to predicting the size distribution of the volatile inorganic species.

TABLE OF CONTENTS

LIST OF TABLES

Section 2

Section 3

Section 4

Section 5

LIST OF FIGURES

Section 3

Section 4

Section 5

SECTION 1

INTRODUCTION

Pollutants in urban atmospheric environments exist in either the gas or aerosol phases. In the past most attention has been directed toward controlling emissions that result in the formation of the gas-phase pollutants, such as ozone, NO_2, and carbon monoxide. Recently the U.S. Environmental Protection Agency has required local governments to place more emphasis on controlling the emissions that lead to the formation of aerosol-phase pollutants. These aerosol pollutants reduce visibility, damage thoracic airways, and cause plant and materials damage.

Urban atmospheric aerosol particles are liquid or solid, or a combination of the two. They are composed primarily of crustal material, elemental carbon, organic compounds, and inorganic electrolytes or salts. The inorganic species consist primarily of ammonium, sodium, nitrate, sulfate, and chloride, and account for 25-50% of the fine aerosol mass in polluted urban environments. The physical and chemical processes that determine their aerosol-phase concentration and their particle-size distribution are the subject of this thesis.

Aerosol sodium originates in sea spray over the ocean as sodium chloride, and since it can be assumed to be nonvolatile, remains in the aerosol phase. Aerosol chloride also originates as sodium chloride in sea spray, but the chloride may be displaced by other strong acids, in which case it evaporates as HCl. Under polluted atmospheric conditions, the strong acids that displace chloride are HNO_3 and H_2SO_4. HNO_3 is primarily formed by gas-phase oxidation of NO_x, and H_2SO_4 is formed by either gas- or aqueous-phase oxidation of SO_2. The vapor pressure of sulfuric acid is extremely low so any gas-phase H_2SO_4 will tend to condense on aerosol particles. Nitric acid is highly volatile, but will condense as NH_4NO_3(s)

or NH_4NO_3(aq) if its partial pressure product with NH_3(g) is exceeded. Ammonia is ubiquitous in terrestrial air masses as it is emitted from bacterial action in soil, animal husbandry operations, and some industrial processes.

Depending on the ambient relative humidity and temperature, atmospheric aerosol particles may also contain a substantial fraction of water. The inorganic components of atmospheric aerosols are hygroscopic and thus their concentration determines, along with the ambient conditions, the aerosol mass of water. At sufficiently low relative humidities the inorganic components form solid salts, and water is either absent or bound up in hydrated salts. At high relative humidities, the inorganic components are dissolved in an aqueous solution. The relative humidity at which a solid salt is in equilibrium with its aqueous solution is termed the deliquescence point.

Previous to this thesis, a few standard assumptions were employed to calculate the aerosol mass of the inorganics and water. First it was assumed that the gas and aerosol phases are in thermodynamic equilibrium with respect to the volatile inorganic compounds ammonia, nitric acid, and hydrochloric acid. Second, this equilibrium assumption was used to partition the volatile compounds among different size particles. And third, it was assumed that at relative humidities below the single-solute deliquescence point, the aerosol particles were in the solid phase. This thesis examines these assumptions, shows when they apply and when they fail, and sets out to redefine the set of physical and chemical principles that govern the aerosol mass and size distribution of the inorganic components and water.

The free energy of formation of NH_4NO_3(s) has been measured by a number of investigators over the years, but the accuracy of these measurements and the resulting accepted value have recently been called into question. Section 2 of the thesis reexamines the determination of the free energy of formation value reported

by the National Institutes of Standards and Technology. This value becomes relevant in Section 4 where I show that the equilibrium constant for the reaction $NH_4NO_3(s) \rightleftharpoons NH_3(g) + HNO_3(g)$ has been off by a factor of two in previous atmospheric work.

Section 3 investigates the physical processes that govern the aerosol mass and size distribution of NH_4NO_3 and NH_4Cl. In previous work the mass and size distribution of these ammonium salts was determined by assuming thermodynamic equilibrium between the gas and aerosol phases. Thermodynamic equilibrium is a good assumption if the time scales for equilibration between the phases are short. In this work I derive expressions for these time scales and evaluate them under typical atmospheric conditions. The physical and chemical processes that govern the size distribution of these ammonium salts are also examined.

In Section 4 a new aerosol inorganics model (AIM) of the processes that determine the aerosol mass and size distribution of the inorganic compounds is described, and its predictions are compared with fundamental thermodynamic measurements and the predictions of previous models. The model was created to account for transport limitations that may inhibit equilibration between the gas and aerosol phases and also may govern the size distribution of the inorganics. New theories are developed and incorporated into AIM that show how the deliquescence point depends on temperature and composition of the particles.

In Section 5 I use the model and theoretical developments in the previous sections to predict the inorganic composition of the aerosol during the summer and fall of 1987, when a large body of meteorological and pollutant data was gathered during the Southern California Air Quality Study. The predicted gas-phase concentrations of ammonia and nitric acid are compared to the measured concentrations to determine departures from equilibrium. Correlations between these departures

and other physical and chemical quantities measured during SCAQS are examined in an effort to explain the observed lack of equilibrium. The size distributions of aerosol ammonium and nitrate were measured during SCAQS and it is shown that these distributions can be compared to determine the degree of equilibrium that exists between aerosol particles of differing size and composition.

The appendix to the thesis describes the aerosol inorganics model, AIM. It includes a full calling tree, and documentation of the arguments to and the purpose of each subroutine.

SECTION 2

THE AMMONIUM NITRATE EQUILIBRIUM CONSTANT REVISITED

ABSTRACT

In this note we review the current state of the literature on the thermodynamic properties of ammonium nitrate and address the concerns of Jaffe (1988) regarding the equilibrium constant of ammonium nitrate developed by Stelson et al. (1979). We also provide a new calculation of the equilibrium constant of the reaction $NH_4NO_3(s) \rightleftharpoons NH_3(g) + HNO_3(g)$.

INTRODUCTION

The equilibrium constant between the gas phase concentrations of ammonia and nitric acid and solid ammonium nitrate is of primary importance to accurately predicting the quantity of ammonium nitrate aerosol in the atmosphere. Jaffe (1988) provides a summary of some of the research to date that employs this constant. In Jaffe's letter, he points out that the agreement that Stelson et al. (1979) found between their calculation and the data of Brandner et al. (1962) does not necessarily confirm the accuracy of the calculation. He suggested that the value of the free energy of formation of $NH_4NO_3(s)$ that Stelson obtained from Wagman et al. (1968) was most likely inferred from Brandner's experimental data. Furthermore, Jaffe pointed out some possible flaws in the experimental procedures and assumptions employed by Brandner.

In this note we re-examine the $NH_4NO_3(s) \rightleftharpoons NH_3(g) + HNO_3(g)$ equilibrium constant calculation of Stelson et al. (1979) and Stelson and Seinfeld (1982), describe the independent measurements that have been made to determine the free energy of formation of $NH_4NO_3(s)$, and provide a recalculation of the value of the equilibrium constant using more up-to-date data.

HEAT OF FORMATION AND HEAT CAPACITIES

Stelson et al. (1979) used three sets of thermodynamic parameters in their calculations: standard Gibbs free energy of formation, heat of formation, and heat capacity. The heat of formation and heat capacity data were available before the experiment of Brandner in, for instance, NBS Circular 500 (Rossini et al., 1952). The slope of the log K vs $1/T$ curve in Stelson's Figure 2 is dependent solely on the heat of formation. Since the slope of the curve found by Stelson et al. (1979) is practically identical to that through Brandner's data, we have an indication of the accuracy of Brandner's measurements. In fact, Brandner et al. point out the

Table 1

Thermodynamic data of the ammonium nitrate system

at 298.15 K

Species	C_p° J/mol – K	S_f° J/mol – K	ΔH_f° kJ/mol
$NH_3(g)$	35.630	192.659	−45.940
$HNO_3(g)$	54.115	266.783	−133.912
$NH_4NO_3(s)$	139.08	150.810	−365.6

Source: Glushko (1978)

close agreement between the heat of formation inferred from their data and the heats of formation then available in the literature. Heats of formation found in the most recent literature (listed in Table 1) are in close agreement to that employed by Stelson et al. (1979).

FREE ENERGY OF FORMATION

A number of researchers have independently arrived at the value of the free energy of formation of $NH_4NO_3(s)$ by different means. Some of these calculations are referred to in the latest CODATA publication (Cox et al., 1989). We will provide a brief review of these calculations.

Stephenson et al. (1955) calculated the free energy of formation of $NH_4NO_3(s)$ by two independent means. First, using measurements and theoretical determinations of the heat capacity of $NH_4NO_3(s)$, Stephenson et al. (1955) integrated C_p/T

from 0 K to 298 K to obtain 151.1 ± 0.2 J/mol – K as the entropy under standard conditions. Denbigh (1981, Section 13.11) discusses the theoretical foundation of this calculation. Using heat of formation and entropy data from NBS Circular 500 (Rossini et al., 1952), Stephenson et al.'s first determination of free energy was found to be −183.5 kJ/mol.

Second, Wishaw and Stokes (1953) measured concentration and activity of a saturation solution of NH_4NO_3(aq). Applying these data in a similar fashion as Stephenson (1944) had done for NH_4Cl(s), Stephenson et al. (1955) determined the free energy of formation of NH_4NO_3(s) to be −183.9 kJ/mol.

Third, Feick (1954) deduced the entropy of formation of NH_4NO_3(s) at 298 K to be 151 J/mol – K from vapor pressure measurements. This is in agreement with Stephenson's entropy determination.

Finally, Brandner et al. (1962) measured vapor pressure over NH_4NO_3(s) and from his correlation the free energy change is found to be −183.3 kJ/mol under standard conditions without taking into account the solid-solid phase changes that NH_4NO_3 undergoes at 357.25 K and 305.38 K (Nagatani et al., 1967).

Later experimental determinations by Eichenauer and Liebscher (1965) did not support the heat capacity measurements of Stephenson et al. (1955) above 256.2 K, but subsequent measurements by Nagatani et al. (1967) confirmed Stephenson's results.

There is some question as to the degree of dissociation of the vapor in the experiments of Feick (1954) and Brandner et al. (1962) as has been demonstrated by de Kruif (1982). Furthermore, the usual mode of dissociation of liquid ammonium nitrate is $NH_4NO_3(l) \rightarrow 2H_2O + N_2O$ (Ray and Jana 1913; Andersen et al., 1958) which may bias Feick's (1954) results. These uncertainties concerning the vapor phase do not affect the two determinations by Stephenson et al. (1955).

CONCLUSIONS

The thermodynamic properties of NH_4NO_3(s) at 298 K have been determined by a number of independent methods all of which are found to be in relative agreement. As can be ascertained by examining the extensive notes and bibliography in Cox et al. (1989), there are many independent checks of the thermodynamic properties of a given substance. Thermodynamic properties from different sources may not be in complete agreement and thus the most accurate equilibrium constant determination will be obtained by using a self-consistent set of thermodynamic data. The most recent set that includes all of the necessary property values is that in Glushko (1978). The values for NH_3(g), HNO_3(g), and NH_4NO_3(s) are presented in Table 1.

The expression for the equilibrium constant in terms of these thermodynamic parameters is

$$\ln K_p = \frac{\Delta S - \Delta C_p}{R} - \frac{\Delta H - 298.15\Delta C_p}{RT} + \frac{\Delta C_p}{R} \ln\frac{T}{298.15}$$

where K_p is the equilibium constant in atm^2 and $R = 8.31448$ J/mol – K is the gas constant (Cox, 1989). Evaluating this expression gives

$$\ln K_c = 70.685 - \frac{24110}{T} - 5.934 \ln(\frac{T}{298.15})$$

where K_c is in ppm^2. At 298 K this value is within 2% of that obtained using equation 4 of Stelson et al. (1979).

Since pure dry NH_4NO_3(IV) crystals are not likely to exist under typical atmospheric conditions, any remaining inaccuracy in this expression should be small compared to uncertainties due to measurement error or modelling approximations.

ACKNOWLEDGEMENT

This work supported by the State of California Air Resources Board.

REFERENCES

Anderson W. H., Bills K. W., Dekker A. O., Mishuck E., Moe G. and Schultz R. D. (1958) The gasification of solid ammonium nitrate. *Jet Propulsion* **28** 831-832.

Brandner J. D., Junk N. M., Lawrence J. W. and Robins J. (1962) Vapor pressure of ammonium nitrate. *J. Chem. Engng Data* **7**, 227-228.

Cox J. D., Wagman D. D. and Medvedev V. A. (1989) CODATA key values for thermodynamics. Hemisphere, New York.

de Kruif C. G. (1982) The vapor phase dissociation of ammonium salts: ammonium halides, ammonium rhodanide, ammonium nitrate, and ammonium bicarbonate. *J. Chem. Phys.* **77** 6247-6250.

Feick G. (1954) The dissociation pressure and free energy of formation of ammonium nitrate. *J. Am. Chem. Soc.* **76** 5858-5860.

Glushko V. P. (1978) Termodinamicheskie svoistva individual'nykh veshchestv: spravochnoe izdanie v chetyrekh tomakh. Izd. 3-e. Moskva.

Jaffe D. A. (1988) Accuracy of measured ammonium nitrate equilibrium values. *Atmospheric Environment* **22** 2329-2330.

Nagatani M., Seiyama T., Sakiyama M., Suga H. and Seki S. (1967) Heat capacities and thermodynamic properties of ammonium nitrate crystal: phase transitions between stable and metastable phases. *Bull. Chem. Soc. Japan* **40** 1833-1844.

Ray P. C. and Jana S. C. (1913) The vapour density of ammonium nitrate, benzoate, and acetate. *J. Chem. Soc* **103** 1565-1568.

Rossini F. D., Wagman D. D., Evans W. H., Levine S. and Jaffe I. (1952) Selected values of chemical thermodynamic properties. Circular of the National Bureau of Standards 500.

Stelson A. W., Friedlander S. K. and Seinfeld J. H.(1979) A note on the equilibrium relationship between ammonia and nitric acid and particulate ammonium

nitrate. *Atmospheric Environment* **13** 369-371.

Stelson A. W. and Seinfeld J. H. (1982) Relative humidity and temperature dependence of the ammonium nitrate dissociation constant. *Atmospheric Environment* **16** 983-992.

Stephenson C. C. (1944) The dissociation of ammonium chloride. *J. Chem. Phys.* **12** 318-319.

Stephenson C. C., Bentz D. R. and Stevenson D. A. (1955) The heat capacity of ammonium nitrate from 15K to 315K. *J. Am. Chem. Soc.* **77** 2161-2164.

Wagman D. D., Evans W. H., Parker V. B., Harlow I., Baily S. M. and Schunm R. H. (1968) Selected values of chemical thermodynamic properties; tables for thirty-four elements in standard orders of arrangement. NBS Tech. Note 270-3.

Wishaw B. F. and Stokes R. H. (1953) The osmotic and activity coefficients of aqueous solutions of ammonium chloride and ammonium nitrate at 25 K. *Trans. Faraday Society* **49** 27-31.

SECTION 3

THE DISTRIBUTION OF AMMONIUM SALTS AMONG A SIZE AND COMPOSITION DISPERSED AEROSOL

ABSTRACT

The chemical and physical processes that govern the distribution of ammonium salt condensate over a size- and composition-dispersed aerosol particle population are considered. From an analysis of the concentration profiles of ammonia, nitric acid, and hydrochloric acid vapors surrounding an aerosol particle, the single particle fluxes of these species are derived. By evaluating the time scales for equilibration of the vapor-phase species with a population of aerosol particles, it is found that ammonium salts in the gas and aerosol phases are not always in equilibrium, especially under less polluted and cooler conditions. The principles that govern the distribution of ammonium salts on aerosol particles of different size and composition are identified, and it is found that thermodynamic equilibrium often does not uniquely determine the distribution of ammonium salt condensate. Thus it is concluded that both transport and thermodynamic properties of the aerosol population govern the distribution of ammonium salt condensate.

INTRODUCTION

In a polluted urban environment, the ammonium salts NH_4NO_3 and NH_4Cl account for 10% to 30% of the fine aerosol mass, and the total inorganic salts account for 25% to 50% of the fine aerosol mass (Gray et al., 1986; Heintzenberg, 1989). Stelson et al. (1979) postulate that these ammonium salts are in thermodynamic equilibrium with their vapor-phase components, NH_3, HNO_3, and HCl. This equilibrium postulate is supported by ambient measurements (Hildemann et al., 1984; Doyle et al., 1979; Tanner, 1982; Grosjean, 1982), and the equilibrium constants for ammonium nitrate and ammonium chloride in the solid and aqueous phases have been calculated as a function of ambient temperature, relative humidity, and particle composition (Stelson et al., 1979; Stelson and Seinfeld 1982a; Pio and Harrison 1987). A number of researchers (Russell et al., 1983; Saxena et al., 1983, 1986; Bassett and Seinfeld, 1983; Russell and Cass, 1986; Russell et al., 1988) employ the equilibrium postulate to calculate the total mass of ammonium salt aerosol and others (Bassett and Seinfeld 1984; Pilinis et al., 1987; Pilinis and Seinfeld 1987, 1988) use an extension of this postulate to partition the condensed ammonium salts over a size- and composition-dispersed aerosol. Recently, this postulate was questioned in an experimental investigation (Allen et al., 1989).

Since accurate prediction of the quantity of ammonium salts in the aerosol phase and their distribution with respect to particle size is essential to a full understanding of the source-receptor relations that govern the formation of atmospheric aerosol, a study of the physical and chemical principles governing this partitioning is undertaken here. Atmospheric aerosol particles are considered to be composed of inorganic species in the solid and/or aqueous phases, perhaps coated by organic surface active agents. NH_3, HNO_3, and HCl condense or evaporate from each particle depending on the relative concentrations of these species in the background gas and

at the particle surface. The vapor-phase species are depleted from the gas phase in response to condensation on the aerosol particle, which results in a tendency for the particle population and the gas phase to equilibrate. Simultaneously, but at a slower rate, condensation and evaporation may occur such that individual aerosol particles tend to equilibrate with each other.

The analysis we are about to present is divided into three sections. To further our understanding of aerosol growth via condensation of ammonium salts, we first analyze the physical and chemical processes that govern transport of NH_3 and HX, the vapor-phase components of a general ammonium salt NH_4X, between the gas phase and a single aerosol particle. The processes that we consider are the reversible gas-phase reaction $NH_4X(g) \rightleftharpoons NH_3(g) + HX(g)$, the reversible particle surface accommodation reactions $NH_4X(a) \rightleftharpoons NH_3(g) + HX(g)$ and $NH_4X(a) \rightleftharpoons NH_4X(g)$, and diffusion of $NH_3(g)$, $HX(g)$, and $NH_4X(g)$ between the background gas and the particle surface. By solving the differential equations that describe conservation of mass for the diffusing species, we obtain expressions for the net flux of NH_3 and HX to and from aerosol particles.

The equations describing the flux to a single particle enable us to answer a number of questions concerning populations of aerosol particles in the second section. We begin by identifying the characteristic times for a population of aerosol particles to equilibrate with the gas phase and, using these time scales, examine the atmospheric conditions under which the equilibrium assumption is valid. Next we identify the characteristics of aerosol particles that enable the equilibrium assumption to be used to partition ammonium salt condensate among the aerosol population. As a consequence, we also identify the characteristics of aerosol particles such that transport properties govern the distribution of ammonium salt condensate and equilibrium considerations play little or no role.

In the final section, we estimate the likely uncertainties in the relevant physical properties of aerosol particles and the resulting inherent uncertainty that we expect in the predicted size distribution of ammonium salts.

TRANSPORT OF $NH_3(g)$, $HNO_3(g)$, AND HCl(g) TO A SINGLE PARTICLE

Let us consider the equations governing mass transport of NH_3 and HX, the vapor-phase components of a general ammonium salt NH_4X, between gas and aerosol phases. The physical and chemical processes that we consider are 1) molecular diffusion of the gas-phase species $NH_3(g)$, HX(g) and $NH_4X(g)$, 2) the reversible gas-phase reaction $NH_3(g) + HX(g) \rightleftharpoons NH_4X(g)$, and 3) the surface reactions $NH_3(g) + HX(g) \rightleftharpoons NH_4X(a)$ and $NH_4X(g) \rightleftharpoons NH_4X(a)$, where $NH_4X(a)$ is an ammonium salt in the aqueous or solid aerosol phase.

The transport of $NH_3(g)$, HX(g), and $NH_4X(g)$ between the gas and an aerosol particle is governed by the differential equations for mass conservation in the gas phase

$$\frac{\partial C_{NH_4X}}{\partial t} - \frac{D_{NH_4X}}{r^2}\frac{\partial}{\partial r}(r^2\frac{\partial C_{NH_4X}}{\partial r}) = -\frac{\partial C_{NH_3}}{\partial t} + \frac{D_{NH_3}}{r^2}\frac{\partial}{\partial r}(r^2\frac{\partial C_{NH_3}}{\partial r}) =$$
$$-\frac{\partial C_{HX}}{\partial t} + \frac{D_{HX}}{r^2}\frac{\partial}{\partial r}(r^2\frac{\partial C_{HX}}{\partial r}) = k_+ C_{NH_3} C_{HX} - k_- C_{NH_4X}$$

where C_i are the gas-phase concentrations, D_i are the molecular diffusivities, t is time, r is the radial distance from the center of the aerosol particle with radius R_p, and k_+ and k_- are the forward and reverse rate constants for the reversible gas-phase reaction. We proceed in steps to consider the magnitude of each of the terms in this equation and then to solve it. The first step is to consider the time derivative terms.

Gas-phase diffusion and reaction time scales

Let us consider a solid- or aqueous-phase particle of NH_4X in chemical equilibrium with the surrounding gas phase. Suppose the concentrations of either or

both of the gas-phase species, $NH_3(g)$ and $HX(g)$, far from the particle are instantaneously increased, resulting in condensation on the particle as new equilibrium conditions are approached. The initial changes in the gas-phase concentrations far from the particle are propagated toward the particle until a steady state concentration profile is established. There are two time scales associated with this relaxation to a steady state profile: one associated with the time, τ_D, required for the gas-phase concentration profile to reach a steady state by molecular diffusion, and the other associated with the time, τ_K, required for the concentration profile to reach a steady state with respect to the reversible gas-phase chemical reaction.

We assume that far from the particle the gas-phase concentrations of NH_3 and HX are known and that at the particle surface there is condensation of these species. For species that do not undergo a significant gas-phase reaction, the characteristic time for establishment of the steady state profile due to molecular diffusion is $\tau_D \sim R_p^2/D_i$ (Seinfeld, 1986), which under typical atmospheric conditions and particle sizes is less than 10^{-6} s.

The characteristic time for equilibration of the gas-phase reaction $NH_3(g) + HX(g) \rightleftharpoons NH_4X(g)$ is $\tau_K = [k_+(C_{NH_3,e} + C_{HX,e}) + k_-]^{-1}$, where $C_{NH_3,e}$ and $C_{HX,e}$ are the equilibrium concentrations of the gas-phase species (Hill, 1977). Since the equilibrium constant is given by $K_{NH_4X(g)} = k_-/k_+$, we can express this time scale as

$$\tau_K = \frac{1/k_+}{C_{NH_3,e} + C_{HX,e} + K_{NH_4X(g)}}.$$

Determination of the equilibrium constant, $K_{NH_4Cl(g)}$, for the reaction $NH_3(g) + HCl(g) \rightleftharpoons NH_4Cl(g)$ was an active area of research around the turn of the century. Most of the investigations were carried out at temperatures much higher than atmospheric (see Table 1). The data concerning the dissociation of NH_4Cl are usually expressed in terms of the dissociation constant, b_{NH_4Cl}, for the reaction

Table 1

Dissociation Constant and Equilibrium Constant of $NH_4Cl(g)$

Investigator	Temperature [K]	$b_{NH_4Cl}(g)$ [%]	K_p [atm]
Ramsay and Young (1886)	553	70 – 80	–
Smith and Lombard (1915)	> 553	60 – 70	3×10^{-7} at 300 K*
Rodebush and Michalek (1929)	562	100	–
Stephenson (1944)	–	100	–
Clementi and Gayles (1967)	< 2000	100	1.3×10^{-4} at 300 K*
Shibata (1970)	523	~ 60	–
de Kruif (1982)	352	85	1×10^{-5}

* Inferred from data available in these papers

$$NH_3(g) + HCl(g) \rightarrow b_{NH_4Cl}NH_3(g) + b_{NH_4Cl}HCl(g) + (1 - b_{NH_4Cl})NH_4Cl(g).$$

The equilibrium constant can be expressed in terms of the dissociation constant as

$$K_{NH_4Cl(g)} \equiv \frac{p_{NH_3}p_{HCl}}{p_{NH_4Cl}} = \frac{b^2_{NH_4Cl}}{1 - b^2_{NH_4Cl}}p_t$$

where p_t is the total pressure of $NH_3(g)$, $HCl(g)$, and $NH_4Cl(g)$ (de Kruif, 1982).

There are no reported measurements of the dissociation constant of $NH_4Cl(g)$ at typical atmospheric temperatures and pressures. At elevated temperatures and somewhat lower pressures numerous measurements and calculations have been performed and are in substantial disagreement. Since the data of de Kruif (1982) are

by far closest to atmospheric temperature of any of the measurements or computations in the literature and since he finds that the dissociation constant is relatively insensitive to temperature, we use 85% as the dissociation constant of NH_4Cl at 352 K along with the total pressure of 0.4 Pa to obtain

$$K_{NH_4Cl(g)} = 1 \times 10^{-5} \text{ atm}$$

under atmospheric conditions.

In the same set of experiments, de Kruif (1982) finds the dissociation constant for $NH_4NO_3(g)$ at 352 K to be 66%. Again assuming that the dissociation constant is a weak function of temperature along with the measured total pressure of 0.40 Pa, we find

$$K_{NH_4NO_3(g)} \equiv \frac{p_{NH_3} p_{HNO_3}}{p_{NH_4NO_3}} = 3 \times 10^{-6} \text{ atm.}$$

We can estimate the maximum likely concentration of $NH_4Cl(g)$ and $NH_4NO_3(g)$ by assuming that the maximum concentration of the dissociated species are each 100 ppb. Using these concentrations with the equilibrium constants $K_{NH_4Cl(g)}$ and $K_{NH_4NO_3(g)}$ results in $p_{NH_4Cl} = 1$ ppb and $p_{NH_4NO_3} = 3$ ppb. A more typical concentration for the dissociated species is 10 ppb, which results in $p_{NH_4Cl} = 0.01$ ppb and $p_{NH_4Cl} = 0.03$ ppb. Thus we find that under atmospheric conditions the concentration of the associated species is considerably less than the concentrations of the dissociated species. This is used in a later section when the boundary conditions are developed.

Returning to evaluation of τ_K, under typical atmospheric conditions the concentrations of $NH_3(g)$, $HCl(g)$, and $HNO_3(g)$ are considerably less than the values of $K_{NH_4Cl(g)}$ and $K_{NH_4NO_3(g)}$, so the time constant for the concentration profiles to reach a steady state due to the reaction $NH_3(g) + HX(g) \rightleftharpoons NH_4X(g)$ can be

simplified to

$$\tau_K \sim \frac{1}{k_+ K_{\mathrm{NH_4X(g)}}}.$$

To evaluate the time constant, τ_K, for the reaction to reach steady state, the values of the forward or reverse rate constants for these reactions are needed. Countess and Heicklen (1973) measure the number concentration of NH_4Cl(s) particles formed in a nucleation experiment. From the initial rate of particle formation, they infer the forward rate constant to be $k_+ = 467$ atm^{-1}s^{-1}. In a check of this rate constant, they measured the rate of disappearance of NH_3(g) from a batch reactor containing NH_3(g), HCl(g), and N_2(g). Also in a nucleation experiment, Henry et al. (1983) find double the value of this rate constant fit their data better.

An upper limit for k_+ for NH_4X is given by the collision rate:

$$k_+ \leq \sqrt{\frac{8kT}{\pi\mu}} \frac{\pi\sigma^2}{kT}$$

where k is the Boltzmann constant, T is the temperature, $\mu = 1.93 \times 10^{-26}$ Kg/molecule and $\pi\sigma^2 = 1.5 \times 10^{-19}$ m^2 are the reduced mass and cross section for NH_3 and HCl collisions, while $\mu = 2.23 \times 10^{-26}$ kg/molecule and $\pi\sigma^2 = 1.8 \times 10^{-19}$ m^2 are the same quantities for NH_3 and HNO_3 collisions. Evaluating this expression at 298 K gives $k_+ \leq 2.7 \times 10^9$ atm^{-1}s^{-1} for NH_4Cl and $k_+ \leq 3.0 \times 10^9$ atm^{-1}s^{-1} for NH_4NO_3. Clementi and Gayles (1967) predict that the energy barrier for the reaction forming NH_4Cl(g) is small, which suggests that the collision theory estimate may not be too many orders of magnitude from the actual value. There are a number of possible explanations for the large discrepancy between the three measured values and the maximum value calculated from collision theory.

The rate constant based on collision theory is high because the actual reaction

probably requires a third molecule, M, to stabilize the $NH_4X(g)$ molecule:

$$NH_3 + HX \rightarrow NH_4X^*$$

followed by

$$NH_4X^* + M \rightarrow NH_4X + M.$$

In both experiments the total pressures are nearly atmospheric, so concentrations of M are representative of atmospheric values. The experimental data may be low simply due to limitations in the rate of mixing of the two gas streams, as in both experiments the flow was laminar; thus the measured reaction rate may not be limited by the chemical kinetics but rather by the rate of diffusion.

Using the equilibrium and rate constants, we can evaluate the time constant for the gas-phase concentration profiles to reach steady state due to the gas-phase chemical reaction. For the forward rate constant based on collision theory, we obtain $\tau_K > 10^{-5}$ s, and for the forward rate constant based on the experimental data of Countess and Heicklen (1973) and Henry et al. (1983), we obtain $\tau_K \sim 3.5$ min.

Either characteristic time is probably short compared to those of the other processes affecting the ambient concentrations of $NH_3(g)$, HX(g), and $NH_4X(g)$. We assume this is the case and thus that transport of $NH_3(g)$ and HX(g) to and from an aerosol particle in response to changes in background gas-phase concentrations occurs with the gas-phase concentration profiles in steady state. This assumption is supported by other findings in a later section.

For aqueous-phase particles there are additional time scales related to 1) attaining interfacial equilibrium and 2) diffusion in the liquid phase. For the species being considered here, both of these time scales are less than one second (Seinfeld, 1986).

Thus the gas-phase concentration profiles of $NH_3(g)$, $HX(g)$, and $NH_4X(g)$ are governed by the steady state form of the continuity equation

$$\frac{D_{NH_4X}}{r^2}\frac{d}{dr}(r^2\frac{dC_{NH_4X}}{dr}) = -\frac{D_{NH_3}}{r^2}\frac{d}{dr}(r^2\frac{dC_{NH_3}}{dr}) = -\frac{D_{HX}}{r^2}\frac{d}{dr}(r^2\frac{dC_{HX}}{dr}) = k_-C_{NH_4X} - k_+C_{NH_3}C_{HX}.$$

It is worth emphasizing here that although the gas-phase concentrations are in steady-state they are not necessarily in chemical equilibrium. In the vicinity of the particle, molecular diffusion to and from the particle perturb the gas-phase concentrations, driving the species out of equilibrium, while the reversible chemical reaction $NH_4X(g) \rightleftharpoons NH_3(g) + HX(g)$ drives these concentrations toward equilibrium. Steady-state is reached when molecular diffusion and chemical reaction balance.

The diffusion-reaction length scale

If we non-dimensionalize the above differential equation, we find that the characteristic thickness of the diffusion-reaction boundary layer surrounding the particle is

$$\lambda = \sqrt{D_{NH_4X}/k_-} \equiv \sqrt{D_{NH_4X}/K_{NH_4X(g)}k_+}.$$

The square of the ratio of the particle radius over the diffusion-reaction boundary layer thickness is the so called Damköhler number, $\gamma = R_p^2/\lambda^2$ (Schultz et al., 1974). When there are no gas-phase reactions, $NH_3(g) + HX(g) \rightleftharpoons NH_4X(g)$, the concentration profile is governed exclusively by molecular diffusion, λ is infinite, and γ is zero. When k_- and k_+ are small but non-zero, λ is large, γ is small, and the gas-phase reaction slightly perturbs the concentration profile due to molecular diffusion alone. When k_- and k_+ are large, λ is small, γ is large, and the gas-phase reactions have a significant effect upon the concentration profiles. These three cases are illustrated qualitatively in Figure 1.

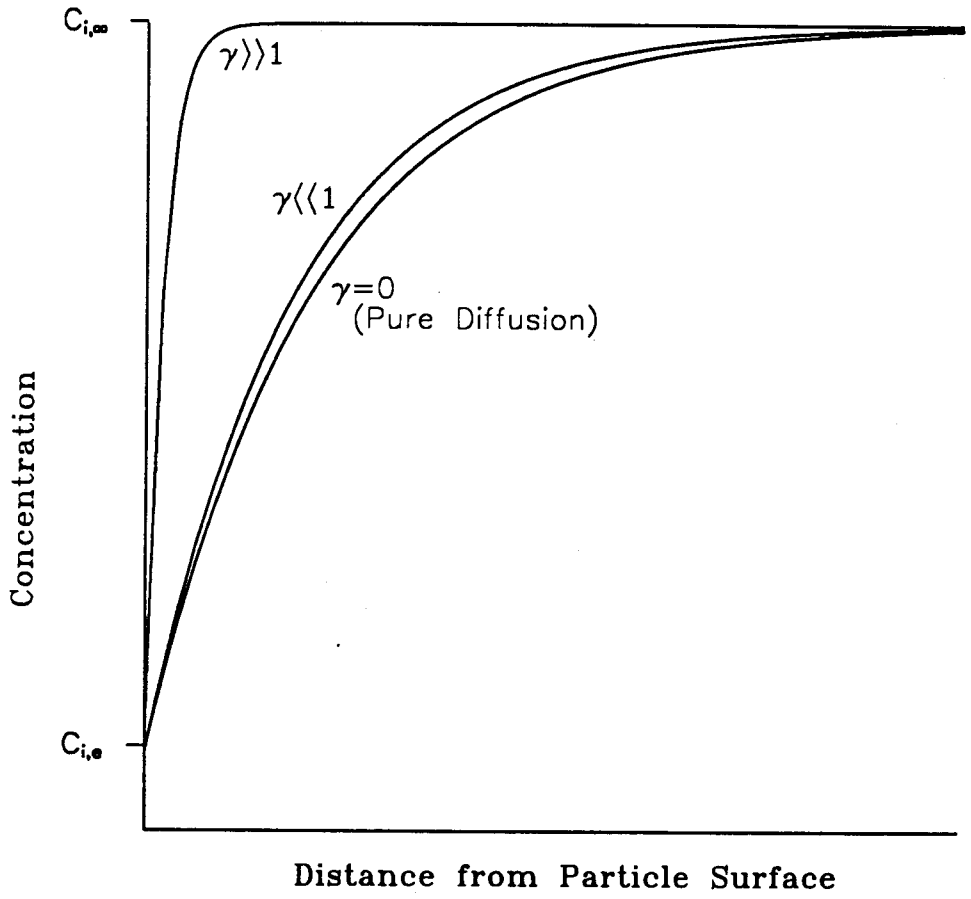

Figure 1. Typical concentration profile as a function of Damköhler number, γ.

Before we proceed, let us try to obtain a greater physical understanding of the diffusion-reaction boundary layer thickness, λ. Imagine a control volume surrounding the particle and encompassing this boundary layer. There are two competing processes that are at balance within the control volume: the gas-phase chemical reaction, which drives the local concentrations toward equilibrium, and molecular diffusion of the gas-phase species through the surface of the control volume, which drives the concentrations out of chemical equilibrium. The thickness of the diffusion-reaction boundary layer defines a spherical shell surrounding the particle where in a qualitative sense the molecular diffusion through the surface of the shell balances the gas-phase chemical reactions occuring within the volume of the shell.

To illustrate the effect of the gas-phase reaction, let us consider condensation of $NH_3(g)$, HX(g), and $NH_4X(g)$ on a solid NH_4X particle. If, for example, surface accommodation is via NH_4X only, and if the Damköhler number is large, $NH_3(g)$ and HX(g) will diffuse toward the particle along with $NH_4X(g)$. In the thin boundary layer near the particle surface, the reaction $NH_3(g)+HX(g) \rightarrow NH_4X(g)$ takes place, and the $NH_4X(g)$ is accommodated. Without the chemical reaction, only diffusion of $NH_4X(g)$ may contribute to overall transport to the particle, since there is no gas-phase mechanism for forming NH_4X and only NH_4X can be accommodated, but with the chemical reaction, the overall transport is augmented by diffusion of $NH_3(g)$ and HX(g) toward the particle in addition to the diffusion of $NH_4X(g)$.

If the Damköhler number is small, an insufficient amount of $NH_3(g)$ and HX(g) are converted to $NH_4X(g)$ in the vicinity of the particle to affect the gas-phase concentration profiles or the overall transport. Furthermore, if accommodation is via $NH_3(g)$ and HX(g) instead of $NH_4X(g)$, even a large Damköhler number does not have a significant effect on the concentration profiles or the transport because under typical atmospheric conditions the concentrations of $NH_3(g)$ and HX(g) are

considerably greater than the concentration of $NH_4X(g)$. We will now estimate the magnitude of the Damköhler number and, in the following section, the mode of accommodation onto solid and aqueous-phase particles.

The length of the diffusion-reaction boundary layer can be expressed in terms of the characteristic time for the gas-phase reaction as $\lambda = \sqrt{D_{NH_4X}\tau_K}$. Assuming that $D_{NH_4X} \sim 10^{-5}$ m^2/s, this expression can be evaluated at the τ_K value obtained from the experimentally determined kinetics of Countess and Heicklen (1973) and Henry et al. (1983) to obtain $\lambda \sim 5$ cm, or at the collision theory value of τ_K to obtain $\lambda > 10$ μm. Thus, for both of these time constant values we find that the Damköhler number, γ, is probably much less than unity, and we are led to the conclusion that, at the size of typical atmospheric aerosol particles, diffusion governs the concentration profiles surrounding the particle.

We have now determined that the concentration profile surrounding the particle is in steady state and that the gas-phase reaction $NH_3(g) + HX(g) \rightleftharpoons NH_4X(g)$ does not significantly affect these concentration profiles. The resulting continuity equations governing the concentrations are

$$\frac{D_{NH_4X}}{r^2}\frac{d}{dr}(r^2\frac{dC_{NH_4X}}{dr}) = -\frac{D_{NH_3}}{r^2}\frac{d}{dr}(r^2\frac{dC_{NH_3}}{dr}) = -\frac{D_{HX}}{r^2}\frac{d}{dr}(r^2\frac{dC_{HX}}{dr}) = 0.$$

To solve these equations, we now develop the boundary conditions.

Accommodation of NH_3, HX, *and* NH_4X *on the particle surface*

$NH_3(g)$, HX(g), and $NH_4X(g)$ can sublime or condense on the particle surface according to the reactions $NH_3(g) + HX(g) \rightleftharpoons NH_4X(s)$, $NH_3(g) \rightleftharpoons NH_3(aq)$, $HX(g) \rightleftharpoons HX(aq)$, or $NH_4X(g) \rightleftharpoons NH_4X(a)$. Since the concentration of $NH_4X(g)$ is considerably less than the concentrations of $NH_3(g)$ and HX(g), the predicted rate of mass transport to and from the particle may differ by an order of magnitude or more, depending on whether sublimation and condensation is via the associated or

dissociated species. Also, the rate of this accommodation reaction governs whether the accommodation rate or gas-phase diffusion dominates transport to and from the particle. We will now address these questions.

Chaiken et al. (1962) measure the sublimation rate of NH_4Cl(s) tablets and strands and find results in agreement with those of Schultz and Dekker (1956) in the temperature range 420 K to 1000 K, giving an Arrhenius form of the sublimation rate, B, in terms of the rate of change of the particle radius:

$$B = 0.6 \exp\left(\frac{-13,200 \text{ cal/mol}}{RT}\right) \text{ [m/s]}.$$

Sturges and Harrison (1988) measure the evaporation rate of solid NH_4Cl particles and find $B = 1.3 \times 10^{-10}$ m/s. Unfortunately, they do not state the temperature at which the experiment was performed, but imply 293 K. Evaluating Chaiken's expression at 293 K gives $B = 0.85 \times 10^{-10}$ m/s and at 298 K gives $B = 1.25 \times 10^{-10}$ m/s, which are both in excellent agreement with the Sturges and Harrison value.

Schultz and Dekker (1956) propose that the dissociation $NH_4Cl \rightarrow NH_3 + HCl$ occurs on the surface of NH_4Cl(s) so that dissociated vapor leaves the solid during sublimation. This proposal is confirmed by Tang and Fenn (1973) at 358 K. Countess and Heicklen (1973) and Dahlin et al. (1981) infer that nucleation and condensation occur via the associated species so that the surface reaction is $NH_4Cl(g) \rightarrow NH_4Cl(s)$. Since the sublimation experiments were carried out at elevated temperatures and the nucleation experiments at elevated concentrations compared to typical atmospheric conditions, we are left with an indefinite conclusion regarding the appropriate mode for the surface reaction.

If we assume that the accommodation reaction occurs via the dissociated species, we can estimate the maximum sublimation rate from kinetic theory. The

maximum condensation rate occurs when every NH_3 and HCl molecule that strikes the particle surface is accommodated. Then the maximum rate of condensation, R_{max}, is governed by the species with the lower rate of collision with the particle:

$$R_{max} = \sqrt{\frac{8kT}{\pi m_{\mathrm{NH_3}}}} \min\left(\frac{p_{\mathrm{NH_3}}}{RT}, \sqrt{\frac{m_{\mathrm{NH_3}}}{m_{\mathrm{HCl}}}} \frac{p_{\mathrm{HCl}}}{RT}\right),$$

where $m_{\mathrm{NH_3}}$ and m_{HCl} are the masses of the corresponding molecules. For $p_{\mathrm{NH_3}} = p_{\mathrm{HCl}}$, which corresponds to most of the experimental data,

$$R_{max} = \sqrt{\frac{8kT}{\pi m_{\mathrm{HCl}}}} \frac{p_{\mathrm{HCl}}}{RT}.$$

If the gas phase is not far from equilibrium with the aerosol phase, the partial pressure of HCl(g) is approximately the equilibrium partial pressure, $p_{\mathrm{HCl}} \sim \sqrt{K_{\mathrm{NH_4Cl(s)}}}$. Pio and Harrison (1987) calculate the equilibrium constant, $K_{\mathrm{NH_4Cl(s)}} \equiv p_{\mathrm{NH_3}} p_{\mathrm{HCl}}$, for this reaction from accepted thermodynamic data and find

$$\ln K_{\mathrm{NH_4Cl(s)}} = 2.2358 \ln\left(\frac{T}{298}\right) - \frac{21,320}{T} + 36.729 - 8.167 \times 10^{-3} T + 4.644 \times 10^{-7} T^2 - 1.105 \times 10^{-10} T^3$$

where $K_{\mathrm{NH_4Cl(s)}}$ is in atm^2.

Near equilibrium the condensation rate is approximately the same as the sublimation rate, $R_{max} \sim B_{max}$, and we find

$$B_{max} \sim \sqrt{\frac{8kT}{\pi m_{\mathrm{HCl}}}} \frac{\sqrt{K_{\mathrm{NH_4Cl(s)}}}}{RT}.$$

Evaluating this expression at 298 K gives $B_{max} = 59 \times 10^{-10}$ m/s, a factor of 45 higher than the observed rate.

If we now assume that the accommodation occurs via $NH_4Cl(g)$, we can use the assumption that the gas phase is not far from equilibrium with the aerosol phase in

order to estimate the maximum sublimation rate:

$$R_{max} = \sqrt{\frac{8kT}{\pi m_{NH_4Cl}}} \frac{p_{NH_4Cl}}{RT}.$$

Near equilibrium, we have $p_{NH_4Cl} = K_{NH_4Cl(s)}/K_{NH_4Cl(g)} = 6.9 \times 10^{-12}$ atm at 298 K. Evaluating R_{max} at 298 K gives $B_{max} = 0.035 \times 10^{-10}$ m/s, a factor of 30 lower than the observed rate. Thus we are able to eliminate $NH_4Cl(g) \rightleftharpoons NH_4Cl(s)$ as the gas-solid aerosol accommodation mechanism under atmospheric temperature and pressure.

There are far fewer data available for sublimation of $NH_4NO_3(s)$ than are available for $NH_4Cl(s)$. Andersen et al. (1958) measure the evaporation rate of $NH_4NO_3(s)$ strands at surface temperatures above the melting point, 443 K, using the same procedures employed by Chaiken et al. (1962) for NH_4Cl. The data fit the Arrhenius form, but a sharp change in the kinetics occurs in the neighborhood of the melting point—a not unexpected finding—and insufficient data were obtained below the melting point to arrive at a sublimation rate. It is clear from their data that the sublimation rate expressed in terms of the rate of change of particle radius is many orders of magnitude lower than 10^{-5} m/s at atmospheric temperatures.

Richardson and Hightower (1987) measure the sublimation rate of solid ammonium nitrate particles and find the rate to be initially 0.23×10^{-10} m/s, but after four hours it is only 0.06×10^{-10} m/s. Later these same investigators (Hightower and Richardson, 1988) obtain a rate of about 0.4×10^{-10} m/s with mixed ammonium nitrate - ammonium sulfate salts and a value of 22×10^{-10} m/s when extrapolated to pure NH_4NO_3. When these particles were exposed to relative humidities of 20% to 60%, the rate for mixed salts was about 4×10^{-10} m/s.

Let us assume that dissociation into NH_3 and HNO_3 occurs at the particle surface and that the equilibrium constant is not changed substantially by the NH_4NO_3

being in the same crystal lattice or solid solution with $(NH_4)_2SO_4$. We can then evaluate the expression for the maximum sublimation rate using the equilibrium constant (Stelson et al., 1979)

$$\ln K_{NH_4NO_3(s)} = 43.054 - \frac{24,110}{T} - 5.93 \ln(\frac{T}{298.15}),$$

where $K_{NH_4NO_3(s)} \equiv p_{NH_3} p_{HNO_3}$ is in atm^2, to obtain $B_{max} = 36 \times 10^{-10}$ m/s, 1.5 to 600 times higher than the observed rates.

If we assume the accommodation occurs via $NH_4NO_3(g)$ and the gas and solid phases are not far from equilibrium, the maximum sublimation rate is $B_{max} = 0.065 \times 10^{-10}$ m/s at 298 K, which corresponds to the lowest reported experimental value. Although the case is not as conclusive here as for ammonium chloride, we conclude that the mechanism for accommodation is most likely $NH_3(g) + HNO_3(g) \rightleftharpoons NH_4NO_3(s)$.

The laboratory data of Hightower and Richardson (1988) suggest a unity accommodation coefficient for $NH_3(g)$ and $HNO_3(g)$ on aqueous-phase particles. Under atmospheric conditions, Gill et al. (1983) suggest that aerosol particles are likely to be completely coated by organic surface active agents that reduce the sticking coefficient of water molecules on water to $\frac{1}{300}$ or less. In a subsequent work (Graedel et al., 1983), a sticking coefficent of $\frac{1}{500}$ for other atmospheric constituents is assumed. If we assume that the sticking coefficient is relatively independent of which species is being accommodated, transport to and from the aqueous phase is dominated by $NH_3(g)$ and $HX(g)$, since their gas-phase concentrations are much higher than those of $NH_4X(g)$. Thus we can conclude that sublimation and condensation occur primarily via the dissociated species for both solid- and aqueous-phase aerosol particles.

For solid particles, the experimentally determined surface rate constants are 10

to 50 times smaller than the value based on collision theory, and thus we assume that the accommodation coefficient is in the range of $\frac{1}{10}$ to $\frac{1}{50}$ for solid particles. For aqueous-phase particles, we will explore the effect of the accommodation coefficient on transport, considering values between 1 and $\frac{1}{500}$. Since 1) accommodation is via the dissociated species and 2) the gas-phase reactions do not significantly affect the concentration profiles, the concentration profile of $NH_4X(g)$ does not affect the transport process. These conclusions also support the steady state assumption made earlier. The continuity equations can be further simplified to

$$\frac{D_{NH_3}}{r^2}\frac{d}{dr}(r^2\frac{dC_{NH_3}}{dr}) = \frac{D_{HX}}{r^2}\frac{d}{dr}(r^2\frac{dC_{HX}}{dr}) = 0.$$

The boundary conditions for these differential equations state that 1) far from the particle the concentrations of $NH_3(g)$ and $HX(g)$ are known

$$C_{NH_3}(r \rightarrow \infty) = C_{NH_3,\infty}$$

$$C_{HX}(r \rightarrow \infty) = C_{HX,\infty}$$

and 2) at the particle surface, surface reactions govern the accommodation of only the dissociated species, $NH_3(g)$ and $HX(g)$, into the aerosol phase. For solid-phase particles, the flux of NH_3 must balance the flux of HX so the boundary conditions are

$$D_{NH_3}\frac{dC_{NH_3}}{dr}\bigg|_{R_p} = D_{HX}\frac{dC_{HX}}{dr}\bigg|_{R_p} = \alpha k_{coll,NH_4X(s)}(C_{NH_3}(R_p)C_{HX}(R_p) - K_{NH_4X(s)}),$$

where $k_{coll,NH_4X(s)}$ is the collision-limited surface reaction rate constant and α is the sticking coefficient. For aqueous-phase particles, the boundary conditions are

$$D_{NH_3}\frac{dC_{NH_3}}{dr}\bigg|_{R_p} = \alpha k_{coll,NH_3}(C_{NH_3}(R_p) - C_{e,NH_3})$$

$$D_{HX}\frac{dC_{HX}}{dr}\bigg|_{R_p} = \alpha k_{coll,HX}(C_{HX}(R_p) - C_{e,HX})$$

and $k_{coll,i}$ is the mean speed of molecules of the condensing vapor-phase species, NH_3 and HX.

The appropriate non-dimensionalization of these boundary conditions yields for solid particles

$$\sqrt{\frac{D_{NH_3}}{D_{HX}}}\frac{\beta_{NH_4X(s)}}{\bar{C}}\frac{dC_{NH_3}}{d\rho}\bigg|_{\rho=1} = \sqrt{\frac{D_{HX}}{D_{NH_3}}}\frac{\beta_{NH_4X(s)}}{\bar{C}}\frac{dC_{HX}}{d\rho}\bigg|_{\rho=1} = \frac{C_{NH_3}(\rho=1)C_{HX}(\rho=1) - K_{NH_4X(s)}}{\bar{C}^2},$$

where $\beta_{NH_4X(s)} = \sqrt{D_{NH_3}D_{HX}}/\alpha k_{coll,NH_4X(s)}R_p\bar{C}$ is the dimensionless surface accommodation factor which indicates whether gas-phase diffusion or surface accommodation limit transport to and from a solid particle, $\rho = r/R_p$ is the dimensionless radial coordinate, and $\bar{C} = (D_{NH_3}C_{NH_3,\infty} + D_{HX}C_{HX,\infty})/\sqrt{D_{NH_3}D_{HX}}$ is a diffusion weighted average of the concentrations far from the particle. For aqueous-phase particles, non-dimensionalizing yields

$$\beta_{NH_3}\frac{dC_{NH_3}}{d\rho}\bigg|_{\rho=1} = C_{NH_3}(\rho=1) - C_{e,NH_3}$$

$$\beta_{HX}\frac{dC_{HX}}{d\rho}\bigg|_{\rho=1} = C_{HX}(\rho=1) - C_{e,HX}$$

where $\beta_i = D_i/\alpha k_{coll,i}R_p$ is the surface accommodation factor for aqueous-phase particles. If α is unity, every molecule that strikes the particle surface is accommodated, and β_i is at its minimum for a given species. Transport to the particle must be limited by diffusion, since surface accommodation is ideal. As α decreases, β_i increases, and the transport of species to the particle becomes more limited by the surface accommodation. Eventually, α is so small that diffusion no longer limits transport and the vapor concentration profiles surrounding the particle are flat (see Figure 2). As will be seen in subsequent derivations, when $\beta_i \sim 1$, both diffusion and surface accommodation affect transport to the particle.

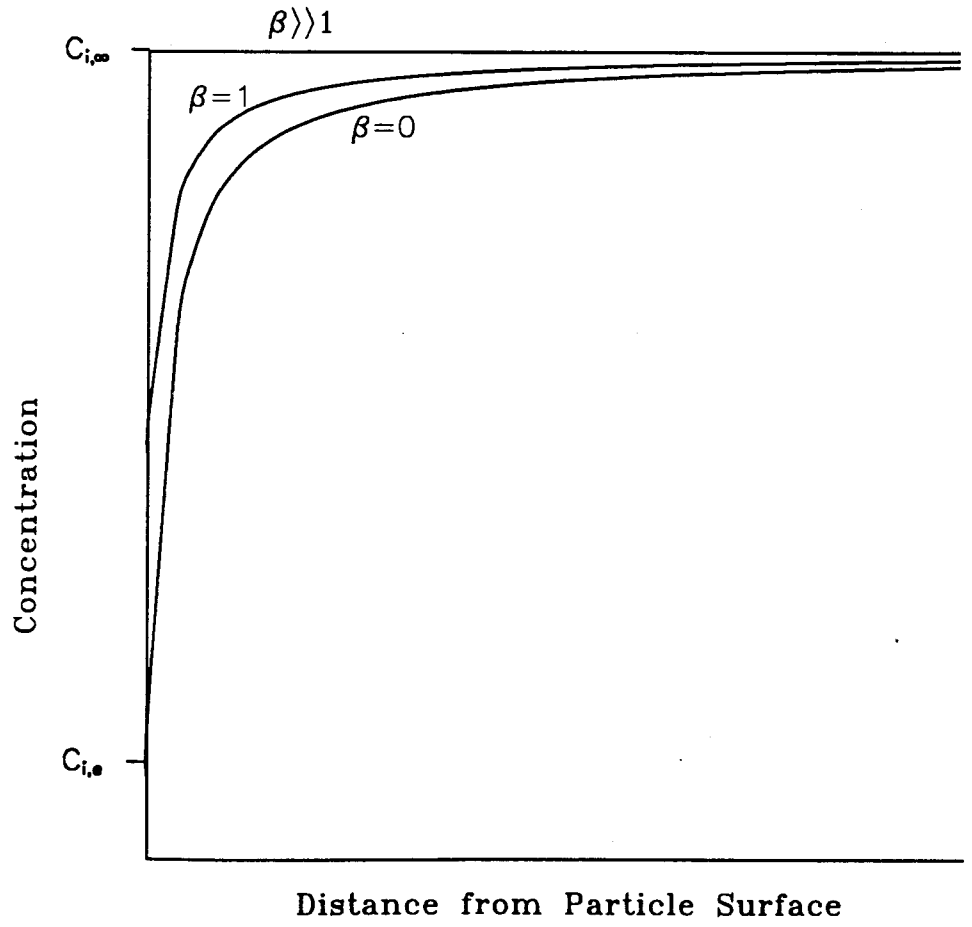

Figure 2. Typical concentration profile as a function of surface accommodation factor, β.

Evaluating $\bar{D}/\alpha k_{coll,NH_4X(s)}\sqrt{K_{NH_4X(s)}}$ for $NH_4Cl(s)$ gives ~ 0.5 μm, whereas evaluating it for $NH_4NO_3(s)$ gives 0.01 μm to 10 μm. For aqueous-phase particles with surface accommodation coefficient, α, in the range 0.1 to 0.01, we find $D_i/\alpha k_{coll,i}$ in the range of 0.3 to 3 μm. In all of these cases we find $\beta_i \sim 1$ and thus transport is in the realm where diffusion and surface kinetics are both significant.

Why is it that for the fastest experimentally determined surface reaction rates (corresponding to an accommodation coefficient of 0.7), the transport is not diffusion limited? As we now demonstrate, this is due to the fact that the radii of typical atmospheric aerosol particles are not much larger than the mean free path of the diffusing species. Let us evaluate $\beta \sim D/kR_p$ for transport of hypothetical condensible molecules to and from an aerosol particle. The diffusivity can be approximated by $D = \lambda_{i,air}\bar{c}_i\frac{3\pi}{32}(1+\frac{M_i}{M_{air}})$ (Flagan and Seinfeld, 1988), where $\lambda_{i,air}$ is the mean free path of molecules of species i in air, $\bar{c}_i$ is the mean speed of molecules of species i, M_i is the molecular weight of species i, and M_{air} is the mean molecular weight of air. We can relate the mean free path of a dilute species i in air to the mean free path of air molecules in air by $\lambda_{i,air} = \lambda_{air}\sqrt{\frac{2M_{air}}{M_i+M_{air}}}\frac{\sigma_{air}^2}{\sigma_{i,air}^2}$, where σ_{air} is the collision diameter for air molecules with each other and $\sigma_{i,air}$ is the collision diameter for molecules of species i with air molecules (Adamson, 1979). The rate constant can be expressed in terms of the mean molecular speed by $k = \alpha\bar{c}_i$ for condensation on aqueous-phase particles, where α is the accommodation coefficient (Moore, 1972). For condensation on solid particles an appropriately weighted mean speed is used. Combining gives

$$\beta \sim \frac{\lambda_{air}}{\alpha R_p}\frac{3\pi}{32}\sqrt{2\frac{M_{air}+M_i}{M_{air}}}\frac{\sigma_{air}^2}{\sigma_{i,air}^2}.$$

Since the mean free path of molecules in air at STP is about 0.065 μm and

$\frac{3\pi}{32}\sqrt{2\frac{M_{air}+M_i}{M_{air}}}\frac{\sigma_{air}^2}{\sigma_{i,air}^2}$ is of order unity, we can evaluate β at STP to obtain

$$\beta \sim \frac{0.065\ \mu\text{m}}{\alpha R_p}.$$

For 10 μm particles and accommodation coefficient near unity, the transport is diffusion limited, $\beta \ll 1$. For 0.1 μm particles, this limit does not hold even for unity accommodation coefficient, since particles this small challenge the continuum approximation. Thus we see that since the size of fine aerosol particles ($0.1 - 1$ μm radius) are about the same as the mean free path, λ_{air}, small deviations from unity in the accommodation coefficient of these particles can shift the transport out of the diffusion limited regime.

Whether transport is governed by molecular diffusion, surface accommodation, or both is not only central to determining the rate of mass transport; it also determines the distribution of condensate with respect to particle size. To first order, if condensation is diffusion limited, the distribution of condensate is proportional to the first moment of the aerosol size distribution, whereas, if the condensation is surface accommodation limited, the distribution of condensate is proportional to the second moment of the aerosol size distribution.

At this point, we have been able to simplify the continuity equations and boundary conditions such that they describe the essential physics and chemistry of the mass transport of volatile inorganics between the gas and aerosol phases. We will now solve these equations for the flux of the chemical species under consideration.

Mass transport between the gas and aerosol phases

The concentration profiles of NH_3(g) and HX(g) that satisfy the differential equations and the boundary conditions at infinity are

$$C_i = C_{i,\infty} - A_i\frac{R_p}{r}$$

where the A_i are arbitrary constants that depend on the boundary conditions at the particle surface.

Applying the boundary conditions for solid-phase particles gives

$$J_i = 4\pi r^2 D_i \frac{dC_i}{dr}$$

$$= 2\pi R_p \sqrt{D_{NH_3} D_{HX}} \bar{C} (\beta_{NH_4X(s)} + 1) \left[1 - \sqrt{1 - 4 \frac{C_{NH_3,\infty} C_{HX,\infty} - K_{NH_4X(s)}}{\bar{C}^2 (\beta_{NH_4X(s)} + 1)^2}} \right]$$

where $J_i = J_{NH_3} = J_{HX}$.

Applying the boundary conditions for aqueous-phase particles gives the flux of ammonia as

$$J_{NH_3} = 4\pi r^2 D_{NH_3} \frac{dC_{NH_3}}{dr}$$

$$= 4\pi R_p D_{NH_3} \frac{(C_{NH_3,\infty} - C_{NH_3,e})}{\beta_{NH_3} + 1}$$

and the flux of acid as

$$J_{HX} = 4\pi r^2 D_{HX} \frac{dC_{HX}}{dr}$$

$$= 4\pi R_p D_{HX} \frac{(C_{HX,\infty} - C_{HX,e})}{\beta_{HX} + 1}$$

where $C_{i,e}$ signifies the equilibrium gas-phase concentration of NH_3 or HX at the particle surface. Algorithms for calculating $C_{i,e}$ are given in Stelson and Seinfeld (1982b) for an ammonium nitrate and nitric acid solution. For more complex solutions, the methods described in Pilinis and Seinfeld (1987) can be used.

These expressions allow us to calculate the fluxes of NH_3 and HX to a single particle. There are other considerations that may affect this mass flux, such as 1) surface heating due to the latent heat of condensation and 2) motion of the particle with respect to the background gas due to settling and turbulent shear. These processes have all been considered and can be shown to be negligible.

With these expressions for the single particle mass fluxes, we are now able to address the problems of determining the mass flux to a population of aerosol particles and thus assessing the ultimate distribution of ammonium salt condensate.

AEROSOL POPULATION MASS TRANSFER

We have derived expressions that describe the fluxes of $NH_3(g)$, $HNO_3(g)$, and HCl(g) between the background gas and a single aerosol particle. Using these expressions, we now address the question: what are the physical and chemical processes that govern the distribution of ammonium salt condensate over a size- and composition-dispersed aerosol? We approach this problem by first examining the time scales for equilibration between the gas-phase concentrations and those at the aerosol surface. Then we address the more qualitative question of when there is a preference for condensate to appear on one particle size instead of another.

Equilibrium between the vapor phase and a population of aerosol particles

As we have just shown, transport between the gas and aerosol phases is in part determined by the concentrations of NH_3 and HX at the particle surface and these concentrations in the background gas. Let us examine the situation where at first these concentrations are in equilibrium and then the background concentrations are suddenly increased so that condensation ensues. In general, the gas-phase concentrations decrease and the concentrations at the particle surface increase until equilibrium is attained. The decrease in background concentrations is due to depletion of species from the gas phase as they condense. The characteristic time, τ_∞, for the two phases (aerosol and gas) to equilibrate due to this depletion is proportional to the total flux of gas-phase species to the aerosol phase.

For solid-phase aerosol particles, the surface concentrations are constant and τ_∞ is the only relevant time scale for the relaxation to equilibrium. For aqueous-phase particles, the gas-phase concentrations at the surface of the particles may increase as condensation proceeds, and this increase also tends to equilibrate the two phases. This change in gas-phase concentrations at the surface of a particle is due to changes in the chemical composition of the particle as condensation proceeds.

We assume here that the gas-phase particle surface concentrations respond rapidly to changes in particle composition (Seinfeld, 1986). The characteristic time, τ_p, for the two phases to equilibrate due to the increase in particle surface concentration is proportional to the total flux of gas-phase species to the aerosol phase and, in addition, to the chemical composition of the aerosol phase.

The magnitude of τ_p is related to the ability of the aerosol phase to absorb NH_3 and HX. For solid particles, this absorptive capacity is infinite, since as ammonium salts condense, the surface equilibrium concentrations remain constant. The absorptive capacity of aqueous-phase particles is dependent on the composition of the particles. For certain compositions, the absorptive capacity is infinite, but for other compositions the absorptive capacity is finite. In the next section, we relate the composition of aqueous-phase particles to their absorptive capacity. In the remainder of this section, we estimate the magnitude of these two time scales, τ_∞ and τ_p.

The evolution of the background gas-phase concentration, $C_{i,\infty}$, due to transport to a monodisperse aerosol can be described by

$$\frac{dC_{i,\infty}}{dt} = -NJ_i$$

where J_i is the single particle flux (which is defined in the previous section for both solid- and aqueous-phase particles), i is NH_3 or HX, and N is the number concentration of aerosol particles. The characteristic time for gas-phase concentrations to change in the presence of transport to solid- or aqueous-phase particles is

$$\tau_\infty \sim \frac{\beta + 1}{4\pi N R_p \bar{D}}$$

where $\bar{D}$ is an average diffusivity of the gas-phase species.

For solid aerosol particles, the surface concentrations remain constant as condensation proceeds and thus τ_p is irrelevant. For aqueous-phase particles, the sur-

face concentration of condensing species may or may not change as condensation proceeds. In the next section we will discuss the cases where 1) water and ammonium salt condense on particles together to maintain constant molality and 2) the water content of the particle remains constant so that the molality changes during condensation. At this juncture, it is sufficient to state that both of these cases exist, but particle surface concentrations change most if the particle water content remains constant as inorganic species condense. In this case, the evolution of the liquid-phase molality, m_i, is given by

$$\frac{dm_i}{dt} \sim \frac{1}{m_W} N J_i$$

where m_W is the liquid water mass of the aerosol per unit volume of air.

The gas-phase surface equilibrium concentration, $C_{i,e}$, is related to the liquid-phase molality by an equilibrium constant, K_i [kg/m^3], which is a function of the composition of the particle and the ambient temperature, such that $C_{i,e} = K_i \gamma_i m_i$, where γ_i is the activity coefficient for species i. For activity coefficients of order unity, we obtain

$$C_{i,e} \sim K_i m_i.$$

Combining these two expressions gives an equation describing the evolution of the gas-phase surface equilibrium concentrations

$$\frac{dC_{i,e}}{dt} \sim \frac{K_i}{m_W} N J_i,$$

and thus we find the characteristic time for the aqueous and gas phases to equilibrate due to changes in the gas-phase surface concentration is

$$\tau_p = \frac{m_W}{K_i} \tau_\infty.$$

In the derivation of this expression for τ_p, we assume the water content of the aerosol is not affected by condensation of the inorganics. If the water content increases with

condensation, the surface concentrations will not change as rapidly, and τ_p will be larger.

We can express both time constants in terms of the mass of aerosol per unit volume of air, $m_p = \frac{4}{3}\pi R_p^3 \rho_p N$, if we make the assumption that aqueous-phase particles are mostly water, that is $m_W \sim m_p$. This assumption is best for dilute aerosol particles that occur under conditions of high relative humidity and may be off by at most a factor of 5 for highly concentrated particles that occur under conditions of low relative humidity. Note that if the relative humidity drops so low that $NH_4X(s)$ condenses, τ_p is no longer a relevant time constant. The restated time constants are then

$$\tau_\infty = \frac{\rho_p R_p^2}{3 D_i m_p}(\beta_i + 1)$$

and

$$\tau_p = \frac{\rho_p R_p^2}{3 D_i K_i}(\beta_i + 1).$$

Notice that τ_∞ is not dependent on the thermodynamic parameter K_i, but only on the transport parameters R_p and D_i, whereas τ_p is dependent on the thermodynamic parameter K_i in addition to the transport parameters. Qualitatively, τ_∞ is the time scale for the gas and aerosol phases to equilibrate due to transport, whereas τ_p is the corresponding time scale due to thermodynamics. In the next section we will relate the relative magnitude of these time scales to whether transport or thermodynamics is the primary process that governs the distribution of ammonium salt condensate with respect to particle size. Let us now evaluate these time scales for some typical atmospheric conditions.

The ranges of these time constants are explored in Figures 3 and 4. The gas-phase time constant, τ_∞, is primarily a function of the mean particle radius and the aerosol mass concentration, and ranges from as little as a few seconds

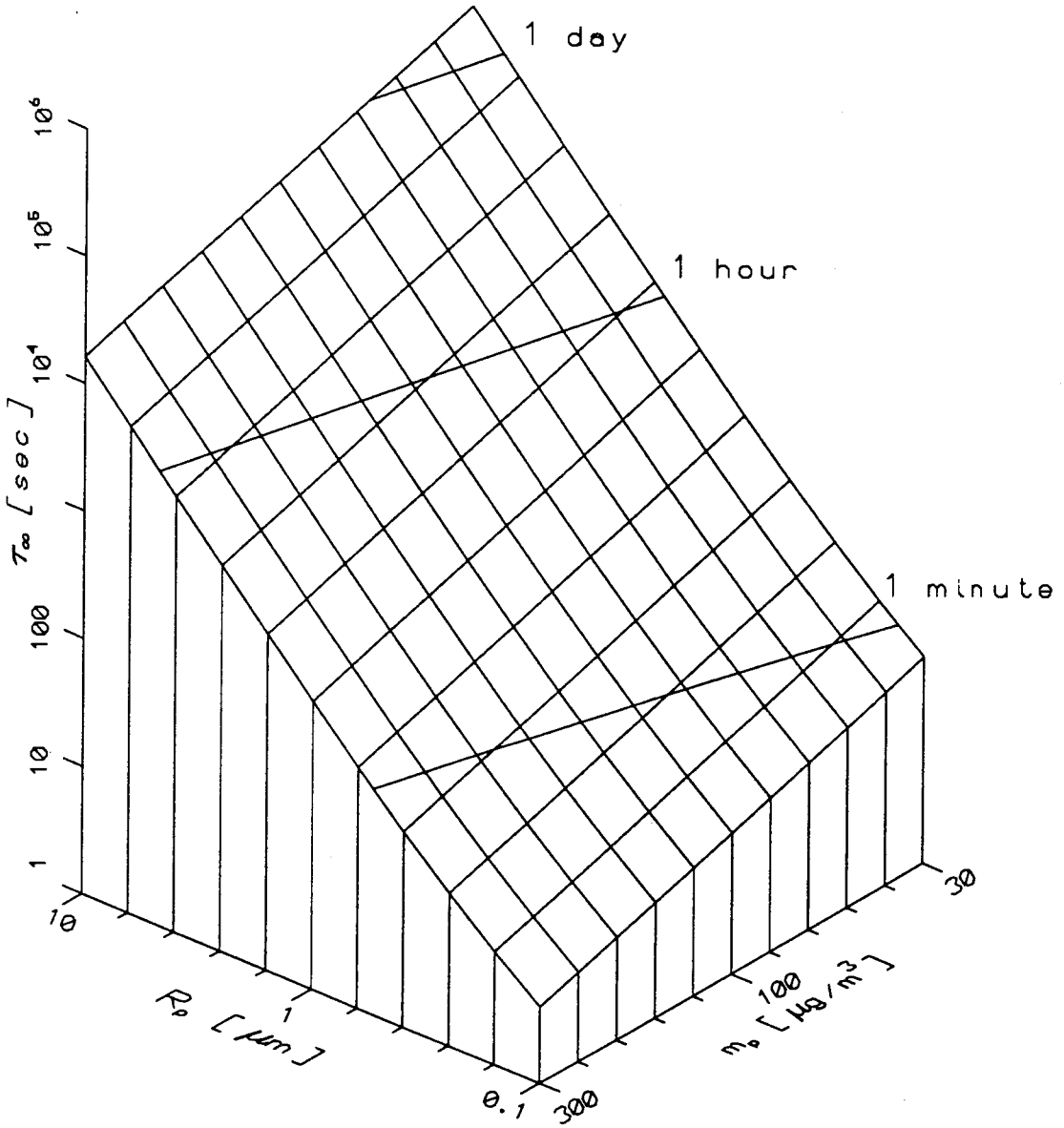

Figure 3. The vapor phase time constant as a function of aerosol mass concentration and mean radius for NH_3 at 298 K and $\alpha = 0.1$.

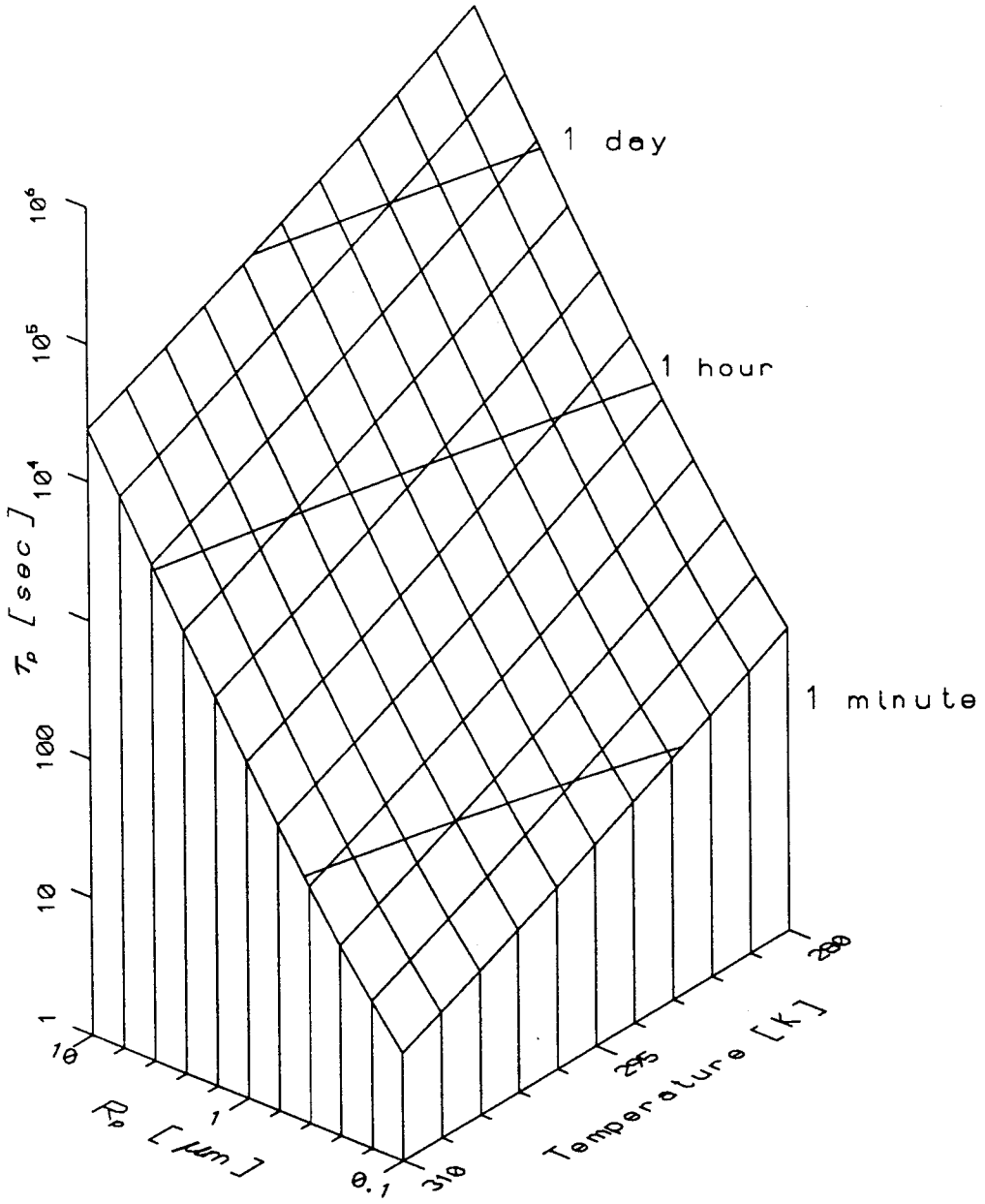

Figure 4. The particle surface concentration time constant as a function of ambient temperature and mean aerosol radius for NH_3 in aqueous phase particles and $\alpha = 0.1$.

under conditions of high aerosol mass concentration and small mean radius to more than one day for low mass concentration and large particle radius. The particle surface time constant, τ_p, is primarily a function of the mean particle radius and temperature, since for $NH_4Cl(aq)$ or $NH_4NO_3(aq)$ the equilibrium constant varies by many orders of magnitude over the range of typical atmospheric temperatures. The equilibrium constant used in Figure 4 is $\sqrt{K^*}$ of Stelson and Seinfeld (1982a) for $NH_4NO_3(aq)$, and from this figure we see that τ_p ranges from a few seconds for high ambient temperatures and small mean aerosol radius to over one day for low ambient temperatures and large mean radius. The ambient temperature and aerosol mass concentration govern how the magnitude of τ_∞ compares to that of τ_p. As will be discussed further in the next section, the relative size of these time scales is one factor that determines whether equilibrium or transport considerations govern the size distribution of ammonium salt condensate.

Two limiting cases may be identified from these figures for a location such as Los Angeles. Under *coastal* conditions (cool, low aerosol mass concentrations, and primary aerosol sizes), $\tau_\infty \sim \tau_p > 30$ hrs, and the aerosol surface concentrations are not necessarily in equilibrium with the gas phase. Under *inland* conditions (hot, high aerosol mass concentrations, and small aerosol sizes), $\tau_\infty \sim \tau_p \sim 4$ s, and equilibrium between the gas and aerosol phases is reached rather quickly. It is noteworthy that the data supporting thermodynamic equilibrium between the gas and aerosol phases were gathered at inland locations (Doyle et al., 1979 and Stelson et al., 1979). In fact, our estimate of these time constants generally supports and is supported by the calculations and data of Russell and Cass (1986) and others that have focused on the inland conditions just described. Even if the particle is coated by surface active organics that result in an accommodation coefficient of $\frac{1}{500}$, τ_∞ is still less than about 5 minutes.

For inland conditions, therefore, the assumption of equilibrium between the gas and aerosol phases is evidently valid. Under other conditions, and especially those in Los Angeles coastal regions, the two phases are predicted not to be in equilibrium, and transport considerations will govern the distribution of condensate over particle size. In the next section, we will demonstrate that even under conditions where equilibrium is attained rapidly, equilibrium considerations do not always uniquely determine the distribution of condensate with respect to particle size.

Thermodynamics is not enough

In this section we explore in more detail the question of when thermodynamic considerations determine the distribution of ammonium salt condensate over particle size. The conclusion that will be reached is that under some conditions thermodynamics dominates, under other conditions transport dominates, and there is a range of cases where both play a role. Thus, a full description of the thermodynamic and transport properties of the aerosol population must be used to determine the distribution of ammonium salt condensate over particle size.

A number of assumptions are useful in the analysis that follows. First, the water content of the aerosol is assumed to be in instantaneous thermodynamic equilibrium with the environment, such that the activity of the liquid water is always equal to the relative humidity. Second, the water content of the atmosphere is much larger than the water content of the aerosol, so that the ambient relative humidity is assumed to be unaffected by condensation of inorganics and water on the aerosol. Both of these assumptions can be justified by the fact that the mass concentration of water vapor is much larger than the mass concentration of inorganic species under even the most polluted conditions.

Third, of the five prevalent inorganic compounds—sodium, ammonia, nitrate, sulfate, and chlorine—sodium and sulfate are not volatile. Thus the primary concern

is with condensation and evaporation of NH_3, HCl, and HNO_3. And fourth, the Kelvin effect can be ignored, since in the range of particle radii of interest, 0.1 to 10μm, the Kelvin effect plays a small role (Seinfeld, 1986).

When the aerosol is in thermodynamic equilibrium with the environment, the concentrations of the volatile inorganics at the surface of the particle must be equal to the concentrations of these species in the atmosphere. By extension, two aerosol particles of different size or composition are in thermodynamic equilibrium with each other if the concentrations at their surfaces are equal. Condensation on aerosol particles is proportional to the difference between the particle surface equilibrium gas-phase concentrations and the background concentrations, as well as the molecular diffusivity of the condensing species, the size of the particles, and the surface reaction rate constant. If two particles have identical surface equilibrium concentrations, the partitioning of condensate between the particles is governed by transport considerations. However, if two particles have different equilibrium surface concentrations, thermodynamics may govern the partitioning of condensate between them. Let us examine the cases where thermodynamics does and does not play a role in this partitioning.

When the ambient relative humidity is sufficiently low, the aerosol is a solid, and the product of the surface concentrations, $C_{NH_3}C_{HCl}$ and $C_{NH_3}C_{HNO_3}$, is identical for all particles, independent of size. Thus, the driving force is identical for all solid particles, the distribution of condensate over particle size is determined solely by transport considerations, and thermodynamic equilibrium plays no role.

Under conditions of intermediate relative humidity, the aerosol may consist of both an aqueous phase and NH_4X(s) phase. If we assume these two phases to be in equilibrium, the product of the particle surface concentrations is governed by the existence of the solid. Thus, the presence of solid inclusions in an otherwise aqueous

phase is thermodynamically identical to a solid phase.

Under conditions of sufficiently high relative humidity, the aerosol is an aqueous solution. For simplicity, let us consider the dissolution of one species, NH_4X. Thermodynamics plays more or less of a role in the distribution of NH_4X over particle size depending on how *osmotically dominant* NH_4X is in the aerosol solution. NH_4X is termed osmotically dominant when the concentration of NH_4X in the aerosol is much greater than the concentration of the other species. In this case, the amount of NH_4X in the aerosol controls the amount of water in the aerosol. (This is only true for relative humidities less than 100%; we are not considering fogs or clouds in this analysis.) This concept can be clarified by considering the ZSR expression used to calculate the water content of aerosol (Pilinis and Seinfeld, 1987):

$$\sum_i \frac{m_i}{m_{0,i}(RH)} = 1$$

where m_i is the molality of electrolyte i and $m_{0,i}$ is the molality of electrolyte i such that the water activity is equal to RH in a solution whose only electrolyte is i. The molality can be expressed in terms of the moles of electrolyte i in the droplet divided by the mass of water in the droplet, $m_i = \hat{M}_i/W$, so that the expression above can be rewritten as

$$W = \frac{\hat{M}_{NH_4X}}{m_{0,NH_4X}(RH)} + \sum_{i \neq NH_4X} \frac{\hat{M}_i}{m_{0,i}(RH)}$$

where we have broken out the NH_4X term.

If $\hat{M}_{NH_4X}/m_{0,NH_4X}(RH) \gg \sum_{i \neq NH_4X} \hat{M}_i/m_{0,i}(RH)$, NH_4X is osmotically dominant, the particle water content is governed almost completely by the mass of NH_4X in the particle, and thus $m_{NH_4X} = m_{0,NH_4X}(RH)$. As NH_4X dissolves in the particle, water condenses in order to maintain the water activity identical to the atmospheric relative humidity, and thus the molality of NH_4X is constant and

equal to $m_{0,\mathrm{NH_4X}}(RH)$. Therefore, if a population of size-distributed particles, osmotically dominated by NH_4X and in thermodynamic equilibrium with each other and the gas phase, is exposed to new gas-phase concentrations of NH_3 and HX, the size distribution of the condensate (or evaporate) is governed only by transport considerations, since the thermodynamic driving force between the gas and aerosol phases is identical for all particles osmotically dominated by NH_4X. Note that a particle can have at most one osmotically dominant species.

In the opposite limit, the mass of NH_4X is low compared to other solutes—NH_4X is *osmotically benign*, $\hat{M}_{\mathrm{NH_4X}}/m_{0,\mathrm{NH_4X}}(RH) \ll \sum_{i\neq\mathrm{NH_4X}} M_i/m_{0,i}(RH)$—and the water content of the particle is not affected by small changes in the particle NH_4X mass content. Here we find that the molality of NH_4X is roughly proportional to the mass of NH_4X dissolved, and thus the surface concentrations of the components of NH_4X reflect the mass of NH_4X in the particle. When NH_4X is osmotically benign, thermodynamics *may* govern its distribution over particle size, since the mass of NH_4X in the aerosol is reflected in the equilibrium surface concentrations and thus affects the driving force.

Let us now relate the previous time scale analysis and the osmotic dominance of an ammonium salt to the salt's distribution with respect to particle size. If the salt is osmotically dominant, the surface concentrations do not change as condensation proceeds and, as with solid aerosol particles, the particle characteristic time, τ_p, is irrelevant. As we have shown, transport considerations govern the distribution of NH_4X with respect to particle size for 1) particles that contain NH_4X(s) and 2) aqueous-phase particles osmotically dominanted by NH_4X(aq).

For an osmotically benign ammonium salt, whether transport, thermodynamics, or a combination of the two governs the distribution of ammonium salt is dependent on the relative magnitudes of τ_∞ and τ_p. Imagine a population of aerosol

particles in equilibrium with the surrounding gas. At time $t = 0$, the gas-phase concentrations are suddenly increased in order to promote condensation. On the one hand, if $\tau_p \ll \tau_\infty$, the particle surface concentrations change until $t \sim \tau_p$, when they have come into equilibrium with the atmospheric concentrations and each other. During this equilibration, the gas-phase concentrations do not change significantly, because τ_∞ is large. Since the particles are in equilibrium, thermodynamic considerations govern the distribution with respect to particle size.

On the other hand, if $\tau_p \gg \tau_\infty$, the background concentrations adjust considerably faster than the particle concentrations until $t \sim \tau_\infty$, when the background concentrations come into equilibrium with the average gas-phase particle surface concentrations. Since τ_p is long compared to τ_∞, the particle surface concentrations do not have time to change, and we conclude that transport considerations alone have thus far governed the distribution of condensate. At this point, the particle surface concentrations averaged over the aerosol population are in equilibrium with the gas-phase concentrations, but particles of different size or composition may not be in equilibrium with each other. For $t > \tau_\infty$, these different aerosol particles tend to equilibrate, until $t \sim \tau_p$ when they reach a state of mutual equilibrium and thermodynamic considerations govern the distribution of condensate.

In conclusion, we find that transport considerations govern the distribution of condensate with respect to particle size for 1) solid particles, 2) an osmotically dominant ammonium salt in aqueous-phase particles, and 3) osmotically benign ammonium salts in aqueous-phase particles under the conditions just outlined. Otherwise, thermodynamic considerations or a combination of thermodynamic and transport considerations must be taken into account when distributing condensate over a size- and composition-dispersed aerosol population.

ACCURACY OF THE PREDICTED SIZE DISTRIBUTION

We have demonstrated that thermodynamics and transport both determine the distribution of ammonium salt condensate over a size-distributed aerosol. Furthermore, we have derived the governing equations for the flux of gas-phase species to a particle of a given composition. In this section, we examine the accuracy that we might expect to achieve in predicting the distribution of ammonium salt condensate over particle size.

There are three factors that determine the size distribution of condensing inorganics. First, the size and composition of the particles determine the magnitude of the Kelvin effect, which provides a thermodynamic driving force that moves NH_4X from smaller particles to larger ones.

Second, if particles of a given size have a uniform composition, the difference in composition between different size particles establishes a thermodynamic driving force between them. If, however, particles of a given size have very different compositions, there is also a thermodynamic driving force between particles of the same size. In either case, particle composition affects the distribution of condensate via changes in the surface equilibrium concentrations.

Third, the surface rate constants not only govern the rate at which condensation and evaporation occur, but also the moment of the size distribution that determines the placement of the ammonium salts in the size spectrum. These rate constants are not well known under atmospheric conditions due to the limited data on the effective accommodation coefficient of surface active chemical species and which of these species are adsorbed on aerosols under different atmospheric conditions.

Ultimately, the model of the condensation of ammonia, nitric acid, and hydrochloric acid on aerosols that we have developed here will need to be incorporated into trajectory (Pilinis et al., 1987) and Eulerian (Pilinis and Seinfeld, 1988) models

of urban and regional scale air pollution. In previous work, the assumption is made that the composition of aerosol particles of a given size is uniform (Pilinis and Seinfeld, 1988). In addition to this approximation, there are inherent uncertainties in how well we can determine thermodynamic and physical properties of the aerosol population. In light of these approximations and uncertainties, we expect some uncertainty in the predicted size distribution of ammonium salt condensate. We will now estimate the source and magnitude of these uncertainties.

The Kelvin effect

The chemical potential of a species in a spherical aerosol particle, μ_p, can be related to its chemical potential in the bulk phase, μ_b, by the Gibbs-Thompson equation

$$\mu_p = \mu_b + \frac{2\sigma v}{R_p}$$

where σ is the surface tension and v is the molar volume of the species. For a pure particle, the Kelvin effect serves to increase the equilibrium partial pressure over the particle by a factor of $\exp(2\sigma v/RTR_p)$. For a solution droplet, the Kelvin effect tends to decrease the equilibrium water activity below the atmospheric relative humidity by this factor while increasing the equilibrium solute vapor pressure by this factor. In this section we examine the magnitude of the Kelvin effect.

Uncertainties in the magnitude of the Kelvin effect arise primarily because of a lack of surface tension data. In general, surface tension data are available for aqueous solution droplets and solid NH_4Cl or NH_4NO_3 particles in a vacuum. We assume that these surface tension values are applicable under atmospheric conditions in spite of the fact that atmospheric constituents adsorbed onto the particle surface would tend to lower its surface tension (Gill et al., 1983).

Table 2 shows the value of $2\sigma v/RTR_p$ for various particle compositions and sizes. Since these values are all significantly less than unity, we can expand the expo-

Table 2

Kelvin effect at 300 K

Particle Compostion	Molality [mol/kg]	σ [ergs/cm^2]	v [ml/mol]	$R_p = 0.03$ μm $\frac{2\sigma v}{RTR_p}$	$R_p = 0.1$ μm $\frac{2\sigma v}{RTR_p}$
NH_4Cl(s)	–	80(a)	36(d)	0.07	0.03
NH_4NO_3(s)	–	120(b)	46(d)	0.15	0.05
Pure Water	–	73(c)	18(d)	0.04	0.01
NH_4Cl(aq)	0	73(c)	36(e)	0.07	0.02
NH_4Cl(aq)	6	80(c)	36(e)	0.08	0.02
NH_4NO_3(aq)	0	73(c)	48(e)	0.09	0.03
NH_4NO_3(aq)	6	78(c)	26(e)	0.05	0.02

a: Average of values in Henry et al. (1983), b: Extrapolated from Shah and Roberts (1985), c: Pruppacker and Klett (1980), d: Perry and Chilton (1973), e: Interpolated from Perry and Chilton (1973)

nential in a Taylor series and retain the first two terms to obtain $\exp(2\sigma v/RTR_p) \sim 1 + 2\sigma v/RTR_p$, so that $2\sigma v/RTR_p$ is approximately the change in surface partial pressures due to the Kelvin effect. If the Kelvin effect is taken into account, equilibrium is reached for solid particles when the volatile species have evaporated from the smaller particles and condensed on the largest ones. For aqueous solution particles, a volatile osmotically dominant species evaporates along with water until another species becomes osmotically dominant. This may substantially affect the size dis-

tribution of the aerosol, depending on the time scales involved. We expect that the surface tension may be uncertain by as much as 20%, so that from Table 2 we see that errors in surface equilibrium concentrations due to errors in the evaluation of the Kelvin effect may be as high as 3% but are usually less than 1%.

Surface Equilibrium Concentrations

Errors in the size distribution of condensate may result from the approximation that the volatile inorganic composition of the aerosol in a size range is uniform if in reality it is not. We might expect that non-volatile inorganics may not be uniformly distributed within a size range, but that the distribution of volatile species should be relatively uniform. We assume that this is the case and that errors in the surface equilibrium concentrations are due to inaccuracies in the calculation of the thermodynamic properties of the aerosol.

To assess the effect of these inaccuracies, let us examine the rate of NH_4X mass transfer between two arbitrary particle sizes. In the case of an aerosol containing solid NH_4X, the surface concentrations are determined by the equilibrium constant, which is independent of particle size or composition. When the particles are an aqueous solution and NH_4X is osmotically dominant, the surface concentrations are determined by the equilibrium constant and $m_{0,i}(RH)$ which again is independent of particle size. Thus, in both cases, the mass transfer and the resulting misplaced condensate are small. It is fortunate that the solid and osmotically dominant cases are not greatly affected by errors in the surface concentrations. Since the surface concentrations in these two cases are insensitive to the quantity of NH_4X in a particle, large amounts of material could be erroneously transferred from one particle size to another.

For an osmotically benign species, errors especially in the ZSR relation and in the Bromley model (Pilinis and Seinfeld, 1987) can lead to erroneous transfer of

NH_4X between different size particles. A 10% error is reasonable for the ZSR and Bromley methods, and we use this error estimate in conjunction with subsequent time scale analysis to estimate the effect on the predicted distribution of NH_4X with respect to particle size.

Surface kinetics

Although the accommodation coefficients and surface accommodation rate constants are not well known, they may not greatly affect the distribution of condensate. Under the coastal conditions that we described previously, the aerosol is most likely aqueous, coated with either a biogenic or anthropogenic surface active hydrocarbon. If all particle sizes have a similar coating of organic, their accommodation coefficients are similar and the condensation is proportional to the second moment of the size distribution. Under these conditions, condensation proceeds relatively slowly and thus absolute errors in the accommodation coefficients or relative errors between the accommodation coefficients of different size particles only affect the distribution of a small quantity of condensate.

Under inland conditions typical of Los Angeles, the condensation proceeds rapidly due to the shorter time scales. Here we expect the gas and aerosol phases to be in relative equilibrium and thermodynamic differences between the composition of particles to govern the distribution of condensate (rather than the surface rate coefficients).

Time scales for movement of condensate between particle sizes

Uncertainties in the surface tension or thermodynamic properties of aqueous-phase aerosols may result in uncertainties in the distribution of inorganic condensate. To quantify this latter uncertainty, we now examine the movement of conden-

sate between different size ranges of particles:

$$\frac{d\hat{m}_j}{dt} = N_j J_{i,j} f_W M_i$$

where $\hat{m}_j$ is the particle mass at size j, $J_{i,j}$ is the molar flux of species i to a particle of size j, M_i is the molecular weight of species i, N_j is the number density of particles of size j, and f_W is the change in total aerosol mass due to condensation of the volatile inorganic. f_W accounts for the condensation of water that results from the condensation of the ammonium salt. For solid particles or an osmotically benign species in aqueous particles, f_W is about one since the mass of water in these particles does not change significantly during condensation, however, for the osmotically dominant species,

$$f_W \sim 1 + \frac{1000}{m_{0,\mathrm{NH_4X}}(RH) M_{\mathrm{NH_4X}}}.$$

The molar flux can be expressed in terms of the concentration difference by $J_{i,j} \sim 4\pi D_i R_{p,j} \frac{\Delta C_i}{\beta_i + 1}$. If the uncertainty in surface concentration is the product of the background concentration and some factor, ϵ, then $\Delta C_i = \epsilon C_{i,\infty}$. The mass of aerosol in size range j can be expressed in terms of the particle radius, density, and number concentration by $m_j \sim \frac{4}{3}\pi R_{p,j}^3 \rho_p N_j$. Combining these expressions gives the characteristic time, τ_s, for movement of species i from one size particle to another

$$\tau_s \sim \frac{R_{p,j}^2 \rho_p (\beta + 1)}{3 D_{\mathrm{NH_4X}} M_{\mathrm{NH_4X}} \epsilon C_{\mathrm{NH_4X},\infty} f_W}.$$

Under coastal conditions, let us assume that $C_{i,\infty} \sim 1$ ppb and $f_W \sim 10$ since the aerosol is a dilute aqueous phase, which gives $\tau_s \sim 20$ days for $\epsilon = 0.1$. Thus, under coastal conditions, mass transfer between particles is so slow that a small error in surface concentrations has a small effect on the distribution of ammonium salt.

Under inland conditions, let us assume that $C_{i,\infty} \sim 50$ ppb and $f_W \sim 1$, which gives $\tau_s \sim 2$ minutes for $\epsilon = 0.1$. Errors in the surface tension or thermodynamics may be reflected in the predicted size distribution in only 2 minutes, whereas with $\epsilon = 0.01$, the error would take 20 minutes to be reflected in the distribution. Uncertainties in the surface tension do not seem to be reflected in significant uncertainties in the size distribution of ammonium salt condensate, since they are generally in the range of 1% or less. If under inland conditions the aerosol is in the solid phase, the surface partial pressures are well characterized and a 1% uncertainty is reasonable.

If the aerosol is a highly concentrated aqueous solution, the surface partial pressures of the osmotically dominant species are predicted fairly accurately, but we would not expect 1% accuracy for an osmotically benign species or a species of intermediate osmotic impact. Fortunately, these species do not comprise a large fraction of the total aerosol mass (since they are not osmotically dominant), and, although we expect some error, this error will not have a large impact on the total mass in a given size range. The largest uncertainties in the distribution probably occur under conditions of moderate humidity such that the aerosol is a highly concentrated solution, but such that there are a substantial fraction of the smaller size particles. Under these circumstances, τ_s is small and the surface concentrations of all but the osmotically dominant species are poorly defined.

CONCLUSIONS

Over the past decade, a number of investigators have estimated the quantity of ammonium salt in atmospheric aerosol by assuming that chemical equilibrium exists between NH_4Cl and NH_4NO_3 in the aerosol phase and NH_3, HCl, and HNO_3 in the gas phase. We have undertaken a theoretical analysis of the chemical and physical processes that govern the formation of these aerosol ammonium salts and find that the time scales for the gas and aerosol phases to equilibrate depend crucially on

the ambient conditions and the composition and state of the aerosol. In particular, these characteristic times are too long to justify the equilibrium assumption under cool ambient conditions or when the aerosol particles are large. Allen et al. (1989) find departures from equilibrium under cool conditions or under conditions of higher relative humidity (when the particles are expected to be large due to increased water content) in agreement with our predictions.

Whether there is a thermodynamic preference for ammonium salt condensate to appear in one size particle over another depends on the state of the condensed ammonium salt (aqueous or solid), the osmotic dominance of the ammonium salt if it exists in the aqueous phase, and the relative magnitude of the time scales for the aerosol and the gas phase to equilibrate if the ammonium salt is not osmotically dominant. Thus an accurate prediction of the quantity of ammonium salt in atmospheric aerosol and its distribution with respect to particle size can only be obtained by explicitly modeling the transport of NH_3, HNO_3, and HCl between the gas and aerosol phases.

ACKNOWLEDGEMENT

This work was supported by the State of California Air Resources Board under Agreement No. A932-054.

REFERENCES

Adamson A. W. (1979) *A textbook of physical chemistry, Page 70.* Academic, New York.

Allen A. G., Harrison R. M. and Erisman J. (1989) Field measurements of the dissociation of ammonium nitrate and ammonium chloride aerosols. *Atmos. Environ.* **23** 1591-1599.

Andersen W. H., Bills K. W., Dekker A. O., Mishuck E., Moe G. and Schultz R. D. (1958) The gasification of solid ammonium nitrate. *Jet Propul.* **28** 831-832.

Bassett M. and Seinfeld J. H. (1983) Atmospheric equilibrium model of sulfate and nitrate aerosols. *Atmos. Environ.* **17** 2237-2252.

Bassett M. and Seinfeld J. H. (1984) Atmospheric equilibrium model of sulfate and nitrate aerosols – II. Particle size analysis. *Atmos. Environ.* **18** 1163-1170.

Chaiken R. F., Sibbett D. J., Sutherland J. E., Van de Mark D. K. and Wheeler A. (1962) Rate of sublimation of ammonium halides. *J. Chem. Phys.* **37** 2311-2318.

Clementi E. and Gayles J. N. (1967) Study of the electronic structure of molecules. VII. Inner and outer complex in the NH_4Cl formation from NH_3 and HCl. *J. Chem. Phys.* **47** 3837-3841.

Countess R. J. and Heicklen J. (1973) Kinetics of particle growth. II. Kinetics of the reaction of ammonia with hydrogen chloride and the growth of particulate ammonium chloride. *J. Phys. Chem.* **77** 444-447.

Dahlin R. S., Su J. and Peters L. K. (1981) Aerosol formation in reacting gases: Theory and application to the anhydrous $NH_3 - HCl$ system. *AIChE J.* **27** 404-418.

de Kruif C. G. (1982) The vapor phase dissociation of ammonium salts: Ammonium halides, ammonium rhodanide, ammonium nitrate, and ammonium bicarbonate. *J. Chem. Phys.* **77** 6247-6250.

Doyle G. J., Tuazon E. C., Graham R. A., Mischke T. M., Winer A. M. and Pitts J. N. (1979) Simultaneous concentrations of ammonia and nitric acid in a polluted atmosphere and their equilibrium relationship to particulate ammonium nitrate. *Environ. Sci. Technol.* **13** 1416-1419.

Flagan R. C. and Seinfeld J. H. (1988) *Fundamentals of air pollution engineering.* Prentice Hall, Englewood Cliffs, NJ.

Gelbard F., Tambour Y. and Seinfeld J. H. (1980) Sectional representation for simulating aerosol dynamics. *J. Colloid Interface Sci.* **76** 541-556.

Gill P. S., Graedel T. E. and Weschler C. J. (1983) Organic films on atmo-

spheric aerosol particles, fog droplets, cloud droplets, raindrops, and snowflakes. *Rev. Geophys. Space Phys.* **21** 903-920.

Graedel T. E., Gill P. S. and Weschler C. J. (1983) Effects of organic surface films on the scavenging of atmospheric gases by raindrops and aerosol particles. In: *Precipitation scavenging, dry deposition, and resuspension.* Edited by H. R. Pruppacher, R. G. Semonin and W. G. N. Slinn. Pages 417-430 Elsevier Science, New York

Gray H. A., Cass G. R., Huntziger J. J., Heyerdahl E. K. and Rau J. A. (1986) Characteristics of atmospheric organic and elemental carbon particle concentrations in Los Angeles. *Environ. Sci. Technol.* **20** 580-589.

Grosjean D. (1982) The stability of particulate nitrate in the Los Angeles atmosphere. *Sci. Total Environ.* **25** 263-275.

Heintzenberg J. (1989) Fine particles in the global troposphere. A review. *Tellus* **41B** 149-160.

Henry J. F., Gonzalez A. and Peters L. K. (1983) Dynamics of NH_4Cl particle nucleation and growth at 253 – 296 K. *Aerosol Sci. Technol.* **2** 321-339.

Hightower R. L. and Richardson C. B. (1988) Evaporation of ammonium nitrate particles containing ammonium sulfate. *Atmos. Environ.* **22** 2587-2591.

Hildemann L. M., Russell A. G. and Cass G. R. (1984) Ammonia and nitric acid concentrations in equilibrium with atmospheric aerosols: experiment vs theory. *Atmos. Environ.* **18** 1737-1750.

Hill C. G. (1977) *An Introduction to chemical engineering kinetics and reactor design.* Wiley, New York.

Moore W. J. (1972) *Physical Chemistry.* Prentice-Hall, Englewood Cliffs, New Jersey.

Perry R. H. and Chilton C. H. (1973) *Chemical engineers' handbook.* McGraw-

Hill, New York.

Pilinis C. and Seinfeld J. H. (1987) Continued development of a general equilibrium model for inorganic multicomponent atmospheric aerosols. *Atmos. Environ.* **21** 2453-2466.

Pilinis C., Seinfeld J. H. and Seigneur C. (1987) Mathematical modeling of the dynamics of multicomponent atmospheric aerosols. *Atmos. Environ.* **21** 943-955.

Pilinis C. and Seinfeld J. H. (1988) Development and evaluation of an Eulerian photochemical gas-aerosol model. *Atmos. Environ.* **22** 1985-2001.

Pio C. A. and Harrison R. M. (1987) Vapour pressure of ammonium chloride aerosol: effect of temperature and humidity. *Atmos. Environ.* **21** 2711-2715.

Pruppacher H. R. and Klett J. D. (1980) *Microphysics of clouds and precipitation.* Reidel, Holland.

Ramsay and Young (1886) On evaporation and dissociation. *Phil. Trans. R. Soc. London* **177** 71-122.

Richardson C. B. and Hightower R. L. (1987) Evaporation of ammonium nitrate particles. *Atmos. Environ.* **21** 971-975.

Rodebush W. H. and Michelak J. C. (1929) The vapor pressure and vapor density of intensively dried ammonium chloride. *J. Am. Chem. Soc.* **51** 748-759.

Russell A. G., McRae G. J. and Cass G. R. (1983) Mathematical modeling of the formation and transport of ammonium nitrate aerosol. *Atmos. Environ.* **17** 949-964.

Russell A. G. and Cass G. R. (1986) Verification of a mathematical model for aerosol nitrate and nitric acid formation and its use for control measure evaluation. *Atmos. Environ.* **20** 2011-2025.

Russell A. G., McCue K. F. and Cass G. R. (1988) Mathematical modeling of the formation of nitrogen-containing air pollutants. 1. Evaluation of an Eulerian

photochemical model. *Environ. Sci. Technol.* **22** 263-271.

Saxena P., Seigneur C. and Peterson T. W. (1983) Modeling of multiphase atmospheric aerosols. *Atmos. Environ.* **17** 1315-1329.

Saxena P., Hudischewskyj A. B., Seigneur C. and Seinfeld J. H. (1986) A comparative study of equilibrium approaches to the chemical characterization of secondary aerosols. *Atmos. Environ.* **20** 1471-1483.

Schultz J. S., Goddard J. D. and Suchdeo S. R. (1974) Facilitated transport via carrier-mediated diffusion in membranes. *AIChE J.* **20** 417-444.

Schultz R. D. and Dekker A. O. (1956) The effect of physical adsorption on the absolute decomposition rates of crystalline ammonium chloride and cupric sulfate trihydrate. *J. Phys. Chem* **60** 1095-1100.

Seinfeld J. H. (1986) *Atmospheric chemistry and physics of air pollution.* Wiley, New York.

Shah K. D. and Roberts A. G. (1985) Properties of ammonium nitrate. *Fert. Sci. Technol. Ser.* **4** 171-197.

Shibata S. (1970) Structure of gaseous ammonium chloride. *ACTA Chem. Scand.* **24** 705-706.

Smith A. and Lombard R. H. (1915) The densities and degrees of dissociation of the saturated vapors of the ammonium halides, and the related thermal data. *J. Am. Chem. Soc.* **37** 38-70.

Stelson A. W., Friedlander S. K. and Seinfeld J. H. (1979) A note on the equilibrium relationship between ammonia and nitric acid and particulate ammonium nitrate. *Atmos. Environ.* **13** 369-371.

Stelson A. W. and Seinfeld J. H. (1982a) Relative humidity and temperature dependence of the ammonium nitrate dissociation constant. *Atmos. Environ.* **16** 983-992.

Stelson S. W. and Seinfeld J. H. (1982b) Relative humidity and pH dependence of the vapor pressure of ammonium nitrate-nitric acid solutions at 25 C. *Atmos. Environ.* **16** 993-1000.

Stephenson C. C. (1944) The dissociation of ammonium chloride. *J. Chem. Phys.* **12** 318-319.

Sturges W. T. and Harrison R. M. (1988) The evaporation of ammonium chloride aerosol. In: *Aerosols. Their generation, behaviour, and applications. Proc. of the Second Conference of the Aerosol Society*, U. K., pp. 7-12.

Tang S. P. and Fenn J. B. (1973) Vacuum sublimation of ammonium perchlorate. *J. Phys. Chem.* **77** 940-944.

Tanner R. L. (1982) An ambient experimental study of phase equilibrium in the atmospheric system: aerosol H^+, NH_4^+, SO_2^{2-}, NO_3^- – NH_3(g), HNO_3(g). *Atmos. Environ.* **16** 2935-2942.

SECTION 4

SECOND-GENERATION INORGANIC AEROSOL MODEL

ABSTRACT

Accurate prediction of the mass and size distribution of the inorganic components of atmospheric aerosols must account for both the thermodynamic properties of the aerosol particles and transport between the gas and aerosol phases. For volatile inorganic species the transport rate is governed by the particle surface partial pressures which, in turn, is determined by the phase state and composition of the aerosol. We develop a model of the temporal composition of atmospheric aerosol particles based on their transport and thermodynamic properties. Included in the model is an improved theory of the temperature and composition dependence of deliquescence. Components of the model are tested against measurements of activity coefficients in single- and multicomponent aqueous solutions and general agreement is found. Aerosol water predictions are significantly higher under conditions of low relative humidity due to the improved theory of deliquescence.

Key word index: Deliquescence, efflorescence, water activity, atmospheric aerosols, thermodynamic equilibrium.

INTRODUCTION

Traditionally the mass, composition, and size distribution of the volatile inorganics in atmospheric aerosol have been predicted assuming local thermodynamic equilibrium between the aerosol and gas phases (Russell et al., 1983, 1986, 1987; Bassett and Seinfeld, 1983, 1984; Pilinis and Seinfeld, 1987, 1988). Atmospheric measurements by Allen et al. (1989) demonstrate that under certain ambient conditions the volatile inorganics are not in equilibrium with the aerosol, and in a recent paper, we show that 1) the characteristic time scales for equilibration between the gas and aerosol phases are often too long for the equilibrium assumption to hold, in agreement with the observations of Allen, and 2) under typical atmospheric conditions both transport and thermodynamic considerations determine the size distribution of volatile inorganics (Wexler and Seinfeld, 1990).

Inorganic salts comprise 25-50% of atmospheric fine aerosol mass (Gray et al., 1986; Heintzenberg, 1989). The concentration of the aerosol inorganics, together with the ambient relative humidity, determine the aerosol water content, which, in turn, is a significant portion of the total aerosol mass under conditions of higher ambient relative humidity. The remaining aerosol mass is generally composed of primary and secondary condensed organics and primary elemental carbon.

Since mass transport influences the total aerosol mass and its size distribution, a model has been developed that simulates both the thermodynamics of the aerosol and the transport between the gas and aerosol phases. It will be referred to as the aerosol inorganics model (AIM). Ultimately AIM will be coupled to trajectory and grid based air quality models. In this paper we describe the model, test components of the model by comparing predictions with fundamental thermodynamic data, and compare the equilibrium predictions of AIM to those of other models. In the first section of this paper, we present the fundamental relationships that govern

the transport and aerosol thermodynamics and in the second section we describe the numerical methods and algorithms used to solve these governing equations. In the third section we derive some useful relationships that describe the deliquescence properties of atmospheric aerosols. We then compare the thermodynamic predictions of the model to fundamental thermodynamic data and finally we compare the equilibrium predictions of AIM to those of equilibrium models.

TRANSPORT TO AND THERMODYNAMICS OF AEROSOL PARTICLES

In this section we present the equations that govern transport between the gas and aerosol phases and the phase state and composition of the aerosol. The predominant inorganic components of atmospheric aerosol in the 1μm size range and smaller are sodium, ammonium, chloride, nitrate, and sulfate. Sodium chloride is found close to the ocean in aerosol particles that are formed from sea spray, and all sodium can be assumed to remain in the aerosol phase. The chloride initially associated with NaCl can be displaced by strong acids and may evaporate or condense as HCl. Ammonia is present in virtually all terrestrial air masses and condenses on aerosol particles where it neutralizes aerosol acidity. HNO_3 is formed by gas-phase oxidation of primary NO_x emissions and moves to the aerosol phase to equilibrate the gas and aerosol phases. Sulfate is formed by gas-phase oxidation of sulfite and is transported to the aerosol phase, where it remains due to its low vapor pressure. Given this list of constituents the aerosol may be comprised of an aqueous solution of Na^+, NH_4^+, NO_3^-, Cl^-, and SO_4^{2-} and solid salt phases of pure NaCl, $NaNO_3$, Na_2SO_4, $NaHSO_4$, NH_4Cl, NH_4NO_3, $(NH_4)_2SO_4$, NH_4HSO_4, and $(NH_4)_3H(SO_4)_2$.

The rate of change of the mass, M_i, of species i in aerosol particles of radius R_p at time t due to diffusion and surface accomodation of the corresponding vapor

phase species is given by

$$\frac{dM_i}{dt} = \frac{4\pi N D_i R_p}{\beta + 1}(C_{i,\infty} - C_{i,e}) \tag{1}$$

where D_i is the gas-phase molecular diffusivity of species i, N is the number concentration of particles, $C_{i,\infty}$ is the ambient gas-phase concentration of species i, and $C_{i,e}$ is the equilibrium gas-phase concentration at the particle surface (Wexler and Seinfeld, 1990). Imperfect accommodation on the particle surface is accounted for by $\beta = D_i/\alpha_i c_i R_p$, where α_i is the surface accommodation coefficient of species i and c_i is the molecular velocity of species i.

The surface equilibrium concentration, $C_{i,e}$, depends on the composition and phase state of the aerosol. The particles consist of an aqueous phase at high relative humidities, one or more solid phases at low relative humidities, and both aqueous and solid phases at intermediate relative humidities. We will assume that if the aerosol consists of more than one phase, these phases are in thermodynamic equilibrium; the system is closed with respect to the total quantity of available inorganic components; and the Gibbs free energy is at the global minimum. Furthermore, one can assume that water is in equilibrium between the aerosol and gas phases, such that the activity of water in the aerosol phase is equal to the relative humidity. Once the equilibrium composition of the aerosol is determined, the surface equilibrium gas-phase concentrations of the volatile species can be deduced from appropriate equilibrium constants.

The phase composition of the aerosol is determined by minimizing the Gibbs free energy of the aerosol system. The change in Gibbs free energy, dG, due to changes in composition of the solid, $dn_{s,i}$, and aqueous, $dn_{I,i}$, phases is given by

$$dG = \sum_i \mu_{s,i} dn_{s,i} + \sum_i \mu_{I,i} dn_{I,i}, \tag{2}$$

where $\mu_{s,i}$ and $\mu_{I,i}$ are the chemical potentials of the species in these phases. The chemical potential of the solid phases is the standard free energy of formation, $\mu^{\circ}_{s,i}$. The chemical potential of the ionic species is

$$\mu_{I,i} = \mu^{\circ}_{I,i} + RT \ln a_i \tag{3}$$

where $\mu^{\circ}_{I,i}$ is the standard free energy of formation of ion i in solution, R is the gas constant, T is the ambient temperature, and a_i is the activity of ion i. This activity is a function of the composition of the aerosol aqueous phase. The free energies of formation of the solid, ionic, and gaseous species are calculated from (Bassett and Seinfeld, 1983)

$$\frac{\mu^{\circ}}{RT} = \frac{\Delta G^{\circ}_f}{RT_o} + \frac{\Delta H^{\circ}_f}{RT_o}\left(\frac{T_o}{T} - 1\right) - \frac{\Delta C_p}{R}\left(\frac{T_o}{T} - 1 - \ln \frac{T_o}{T}\right) \tag{4}$$

where the values of the standard free energy of formation, ΔG°_f, enthalpy, ΔH°_f, and heat capacity, C°_p, for the species of interest here are given in Tables 1, 2, and 3.

What remains in the evaluation of Equation (3) is calculation of the activity, a_i. The current literature does not provide an exact means for calculating the thermodynamic properties of the concentrated aqueous solutions, so empirical or semi-empirical methods must be employed. In polluted urban environments, ammonium nitrate is frequently the dominant inorganic electrolyte and at STP ammonium nitrate is in equilibrium with its solid phase at a concentration of over 25 M. Models of multicomponent electrolyte solutions of, for instance, Pitzer (1979) or Chen et al. (1982, 1986) are limited to ionic strengths below 6 M. Due to the exponential variation of these correlations with ionic strength, above 6 M the predictions of these models often do not agree well with experimental data (Zematis et al., 1986). More recently, relations have been developed that hold at higher ionic

Table 1

Thermodynamic Properties of Solids

Relevant to Atmospheric Aerosols

Solid	ΔH_f° kJ/mol	ΔG_f° kJ/mol	C_p° J/mol K
NaCl	−411.153	−384.138	50.50
$NaNO_3$	−467.85	−367.00	92.88
$NaHSO_4$	−1125.5	−992.8	85.[d]
Na_2SO_4	−1387.08	−1270.16	128.20
NH_4Cl	−314.43	−202.87	84.1
NH_4NO_3	−365.57	−183.87	139.3
NH_4HSO_4	−1026.96	−823.[a]	127.5[b]
$(NH_4)_2SO_4$	−1180.85	−901.67	187.49
$(NH_4)_3H(SO_4)_2$	−1730.[a]	−2207.[a]	315.[c]

Source: Wagman et al. (1982) unless otherwise indicated: (a) Bassett and Seinfeld (1983); (b) Karapet'yants and Karapet'yants (1970); (c) Sum of C_p° for $(NH_4)_2SO_4$ and NH_4HSO_4; (d) Estimated from $C_p^\circ(NH_4HSO_4)C_p^\circ(Na_2SO_4)/C_p^\circ((NH_4)_2SO_4)$.

strengths (Pitzer, 1986; Haghtalab and Vera, 1988; Liu et al., 1989), but correlations for multicomponent systems of the type that occur in atmospheric aerosols have yet to be developed. The empirical correlations of Kusik and Meissner (1978)

Table 2

Thermodynamic Properties of Ions in Solutions

Relevant to Atmospheric Aerosols

Ion	ΔH_f° kJ/mol	ΔG_f° kJ/mol	C_p° J/mol K
H^+	0	0	0
Na^+	−240.12	−261.905	46.4
NH_4^+	−132.51	−79.31	79.9
NO_3^-	−205.0	−108.74	−86.6
Cl^-	−167.159	−131.228	−136.4
SO_4^{2-}	−909.27	−744.53	−293.0
HSO_4^-	−887.34	−755.91	−84.0

Source: Wagman et al. (1982) except NO_3^- which is in error in this source. The equivalent HNO_3(aq) data was used instead.

have been chosen for use here since these relations are well behaved at high ionic strengths, correlations for most of the individual components of atmospheric aerosol are available in the literature, and the model does not require correlations for multicomponent solutions. The notable exception here is sulfuric acid, which is poorly dealt with by all of these electrolyte models (Zematis et al., 1986). In a subsequent section, the ability of the Kusik and Meissner model to predict the activity coefficients of multicomponent electrolyte solutions will be compared with experimental

Table 3

Thermodynamic Properties of the Gas-Phase Components of Atmospheric Aerosols

Gas	ΔH_f° kJ/mol	ΔG_f° kJ/mol	C_p° J/mol K
HCl	−92.307	−95.299	29.12
HNO_3	−135.06	−74.72	53.35
NH_3	−46.11	−16.45	35.06

Source: Wagman et al. (1982).

data for systems relevant to atmospheric aerosols.

The mass of water in the aerosol aqueous phase is dependent on the composition of this phase and the ambient relative humidity, such that the activity of water in the aerosol phase is equal to the relative humidity. The ZSR relationship (Zdanovskii, 1948; Stokes and Robinson, 1966) has been used to predict the water content of atmospheric aerosols (Hanel and Zankl, 1979; Cohen et al., 1987; Pilinis and Seinfeld, 1987),

$$W = \sum_i \frac{\hat{M}_i}{m_{i,0}(r.h.)} \tag{5}$$

where W is the mass of water in the aerosol in kg of water per m^3 of air, $\hat{M}_i$ is the number of moles of electrolyte i per m^3 of air, and $m_{0,i}$ is the molality (moles/kg) of a single-component aqueous solution of electrolyte i that has a water activity $r.h.$

Equations (1-5) form a system of equations that describe the time evolution

of the mass of inorganic species in the aerosol phase. In the following section we describe a method for solving these equations.

INTEGRATING TRANSPORT AND MINIMIZING GIBBS FREE ENERGY

Transport

Since Equation (1) will ultimately be included in a grid-based model of urban atmospheric aerosols, its integration must be done economically. A number of numerical integrators have been considered for use in predicting the temporal concentrations of atmospheric pollutants and the hybrid integrator has been determined to be economical and accurate (McRae et al., 1982). The hybrid integrator (Young and Boris, 1977) was developed for integrating chemical kinetics in reacting flows. AIM employs a recent update of this code, available in Young (1980) and Young (1983), to integrate Equation (1). Under typical urban atmospheric conditions, the code conserves mass and maintains positivity, but under conditions of low relative humidity, when the aerosol water content is small, a large number of evaluations of the right hand side of Equation (1) may be required. This occurs because the surface partial pressures of NH_3, HCl, and HNO_3 are governed by the pH of the aerosol and at low relative humidity, the solute concentrations are high, so that small changes in hydrogen ion content result in large changes in pH and consequently difficult integration conditions.

Thermodynamics

The equilibrium composition of the aerosol is calculated by directly minimizing the Gibbs free energy, subject to the constraints that the water activity is fixed at the relative humidity and the total inorganic aerosol mass is conserved. The minimization algorithm is described in this section.

In the minimization procedure employed in AIM, the independent variables are the number of moles of each of the solid phases and the dependent variable is the

Gibbs free energy. Initially, the aerosol is assumed to be completely aqueous. If one or more of the ions listed previously do not appear in the solution in significant quantities, the corresponding solid phases of these salts cannot exist and are therefore eliminated from consideration. In addition, if the relative humidity is above the deliquescence point for a solid phase, this solid phase cannot exist. (This is proved in the next section.) If both of these criteria eliminate all solid phases from consideration, the aerosol exists as an aqueous solution and the water content is simply calculated from Equation (5).

If one or more solid phases may exist, the number of moles of these phases that minimizes the Gibbs free energy is calculated as follows. The number of moles in each of the solid phases, **s**, is initially zero. The gradient of the Gibbs free energy, $\nabla G(\mathbf{s})$, with respect to the number of moles of each solid is evaluated at the current phase composition and the negative of this gradient is followed until a minimum is found. The gradient direction comes from Equation (2) by taking the differential with respect to $n_{s,j}$:

$$\begin{aligned} \frac{\partial G}{\partial n_{s,j}} &= \mu_{s,j} - \sum_i \nu_{i,j}\mu_{I,i} \\ &= \mu^\circ_{s,j} - \sum_i \nu_{i,j}(\mu^\circ_{I,i} + RT \ln a_i) \end{aligned} \tag{6}$$

where the values of $\nu_{i,j} = \partial n_{I,i}/\partial n_{s,j}$, the stoichiometry of the solid phases in terms of their ionic components, are given in Table 4.

The mass of water, obtained from Equation (5), is used to calculate the molalities of the aqueous phase components, which are then used in the Kusik and Meissner model to calculate the activities, a_i.

This minimization is subject to two classes of linear constraints: both the number of moles of each solid phase and the number of moles of each ion in the aqueous phase must be non-negative. The constrained gradient direction, $\nabla_c G(\mathbf{s})$,

Table 4

Solid Stoichiometry in Terms of the Ionic Components

Solids	Na^+	NH_4^+	H^+	Cl^-	NO_3^-	SO_4^{2-}
NaCl	1	0	0	1	0	0
$NaNO_3$	1	0	0	0	1	0
$NaHSO_4$	1	0	1	0	0	1
Na_2SO_4	2	0	0	0	0	1
NH_4Cl	0	1	0	1	0	0
NH_4NO_3	0	1	0	0	1	0
NH_4HSO_4	0	1	1	0	0	1
$(NH_4)_2SO_4$	0	2	0	0	0	1
$(NH_4)_3H(SO_4)_2$	0	3	1	0	0	2

is calculated by the method of Russell (1970).

Changing the phase composition of the aerosol by moving in the $-\nabla_c G$ direction will eventually encounter one of the constraints. The line segment from the current value of $\mathbf{s}$ to the constraint is given by $\mathbf{s} - \eta \nabla_c G(\mathbf{s})$, where $0 \leq \eta \leq \eta_{max}$, and η_{max} is the value of η where the first constraint is encountered. A binary search is performed along this line segment to find the zero of

$$\nabla_c G(\mathbf{s}) \cdot \nabla G(\mathbf{s} - \eta \nabla_c G(\mathbf{s})).$$

The value of η at this zero, η_0, defines a new estimate of the phase composition, $\mathbf{s} \leftarrow \mathbf{s} - \eta_0 \nabla_c G(\mathbf{s})$.

Under conditions of low ambient relative humidity many if not all of the salts may precipitate. If reciprocal salt pairs form, such as NaCl and NH_4NO_3, and NH_4Cl and $NaNO_3$, the Gibbs free energy of the solid phases can be further minimized, without altering the composition of the aqueous phase, by shifting the composition from one salt pair to the other. Typically the Gibbs free energy of the solid phases is minimized when one of the reciprocal salts is no longer present. Minimizing the Gibbs free energy of the solid phases is a linear programming problem with two kinds of constraints, inequality constraints such that the moles in each solid phase are non-negative and equality constraints such that the total number of moles of each ion is conserved in the solid phases.

Thus the Gibbs free energy minimization involves two steps. The first is a nonlinear constrained minimization that moves material between the aqueous phase and one or more solid phases. The second step is a linear constrained minimization that moves material between reciprocal solid phases. These two minimization steps result in a new estimate of **s**. If this new estimate is sufficiently close to the previous value of **s**, convergence is assumed. Otherwise, a new gradient is calculated at the current value of **s** and the procedure is repeated until convergence is acheived.

The algorithm described here assumes that salt precipitates can be eliminated from consideration if the ambient relative humidity is above the deliquescence relative humidity (DRH) of the salt. In the following section we prove that this is a valid assumption and then derive an expression for the temperature dependence of the deliquescence point.

DELIQUESCENCE AND EFFLORESCENCE

The Gibbs free energy minimization algorithm employs the assumption that a salt will not precipitate at relative humidities above its deliquescence point, where here the deliquescence point (DRH) at a given temperature is defined as the water

activity of a single electrolyte solution that is in equilibrium with its salt precipitate. In general, the water activity at which a precipitate is in equilibrium with an electrolyte solution is dependent on its temperature and composition. In this section we will prove that the deliquescence point of a salt in equilibrium with a multicomponent solution always occurs at a relative humidity lower than its deliquescence point in a single-component solution. We will then derive an expression for the temperature dependence of the deliquescence point of a single electrolyte solution.

Variation of DRH with Composition

Let us consider two electrolytes in a solution exposed to the atmosphere. The solution and the atmosphere are in equilibrium with respect to water when the ambient relative humidity is equal to the water activity in solution. Under conditions of sufficiently low relative humidity, one of the electrolytes may form a salt precipitate that is in equilibrium with its ions in solution. At still lower relative humidities, both electrolytes will exist in the solid phase. Let us define the relative humidity where one of the electrolytes is in equilibrium with its solid phase as the DRH for this electrolyte. This DRH is a function of the relative mole fractions of the two electrolytes.

That the DRH of one electrolyte is lowered by the addition of another electrolyte is a conclusion of the Gibbs-Duhem equation, which for a solution of two electrolytes (1 and 2) in water (w) at constant temperature and pressure is

$$n_1 d\mu_1 + n_2 d\mu_2 + n_w d\mu_w = 0. \tag{7}$$

Let us assume that initially electrolyte 1 is in equilibrium with solid salt 1 in a solution that does not yet contain electrolyte 2. As electrolyte 2 is added to the solution, the chemical potential of electrolyte 1 does not change, because it is in

equilibrium with its solid phase. Thus $d\mu_1 \equiv 0$ and Equation (7) becomes

$$n_2 d\mu_2 + n_w d\mu_w = 0. \tag{8}$$

The chemical potentials of electrolyte 2 and water can be expressed in terms of their activities by

$$\mu_i = \mu_i^\circ + RT \ln a_i \tag{9}$$

where μ_i° is the chemical potential of species i under standard conditions and a_i is the activity of species i in the solution. By combining Equations (8) and (9) and noting that $n_2/n_w = M_w m_2/1000$ and $d\mu_i^\circ \equiv 0$ gives

$$m_2 d\ln a_2 + \frac{1000}{M_w} d\ln a_w = 0 \tag{10}$$

where m_2 is the molality of species 2 and M_w is the molecular weight of water. Integrating this expression from $m_2' = 0$ to $m_2' = m_2$ gives

$$\ln \frac{a_w(m_2)}{a_w(0)} = -\frac{M_w}{1000} \int_0^{m_2} \frac{m_2'}{a_2} \frac{da_2}{dm_2'} dm_2'. \tag{11}$$

Although the integrand of Equation (11) is difficult to evaluate for these highly concentrated solutions, it is sufficient to show that the integrand is greater than zero to demonstrate that the DRH of one electrolyte is lowered by the addition of a second electrolyte. The solutes that are being considered here behave like most strong electrolytes. At low ionic strengths their activity coefficient, γ, decreases with increasing concentration according to Debye-Huckel theory. At intermediate ionic strengths their activity coefficient levels-out, and at high ionic strengths it increases with concentration. Solutions that are in equilibrium with the solid phases typical of atmospheric aerosols have high ionic strength, so $d\gamma_2/dm_2 > 0$ and thus $da_2/dm_2 > 0$. Even at low ionic strength where Debye-Huckel theory applies the

decrease in γ_2 with increasing concentration is not enough to cause a_2 to decrease with increasing concentration. That the water activity is at a minimum at the mutual solubility point has been stated without proof in previous work (Kirgintsev and Trushnikova, 1968).

Since the integrand is greater than zero, the activity of water (which is equivalent to the DRH of solute 1 since the solution is in equilibrium with the solid phase of electroltye 1) decreases as electrolyte 2 is added to the system until the solid phase of salt 2 forms. Adding more electrolyte 2 to the solution beyond this point increases the amount of salt in the solid phase, but does not change the composition of the solution. For solutions with more than two electrolytes, a similar analysis can be used to prove that the DRH of a salt in a multicomponent solution is always lower than its DRH in solution alone.

Evaluation of Equation (11) is complicated because there is no rigorous theory for the activity of an electrolyte in a solution saturated with another electrolyte, so we will assume that the electrolyte activities obey a generalized Harned's rule (Harned and Owen, 1958, p. 600)

$$\gamma_2(m_2) = \gamma_2(0)\exp(\alpha_2 m_2) \tag{12}$$

where γ_2 is the activity coefficient of electrolyte 2 at molality m_2 and α_2 is an arbitrary constant determined from data.

For a simple binary mixture of two uni-univalent electrolytes $a = \gamma^2 m_{cation} m_{anion}$. If we consider, for example, the system NH_4NO_3 – NH_4Cl – H_2O, then $a_{NH_4NO_3} = \gamma^2_{NH_4NO_3} m_{NH_4^+} m_{NO_3^-}$ and $a_{NH_4Cl} = \gamma^2_{NH_4Cl} m_{NH_4^+} m_{Cl^-}$, which for this system is $a_{NH_4NO_3} = \gamma^2_{NH_4NO_3}(m_{NH_4NO_3} + m_{NH_4Cl}) m_{NH_4NO_3}$ and $a_{NH_4Cl} = \gamma^2_{NH_4Cl}(m_{NH_4NO_3} + m_{NH_4Cl}) m_{NH_4Cl}$. Using these expressions and Equation (12) we can integrate Equation (11) and evaluate the constants $\alpha_{NH_4NO_3} = -0.028$ and

Table 5

Deliquescence Relative Humidity at Mutual Solubility Point at 303 K

Compounds	MDRH	DRH1	DRH2
$NH_4NO_3 + NaCl$	42.2*	59.4	75.2
$NH_4NO_3 + NaNO_3$	46.3	59.4	72.4
$NH_4NO_3 + NH_4Cl$	51.4	59.4	77.4
$NaNO_3 + NH_4Cl$	51.9*	72.4	77.2
$NH_4NO_3 + (NH_4)_2SO_4$	62.3	59.4	79.2
$NaNO_3 + NaCl$	67.6	72.4	75.2
$NaCl + NH_4Cl$	68.8	75.2	77.2
$NH_4Cl + (NH_4)_2SO_4$	71.3	77.2	79.2

Note: DRH1 corresponds to the first salt in the compound; DRH2 corresponds to the second.

Source: Adams and Merz (1929) for all single and mutual DRH values except for the MDRH values indicated.

(*) The stable solids are $NaNO_3$ and NH_4Cl at this temperature. Source: Merz et al. (1933).

$\alpha_{NH_4Cl} = 0.051$ from the solubility data of Prutton et al. (1935) and the water activity data at saturation of Adams and Merz (1929) (see Table 5). The resulting approximate solution to Equation (11) for the system saturated with NH_4Cl is

$$\frac{a_w(m_{NH_4NO_3})}{0.774} = \tag{13}$$
$$= \exp[-\frac{18}{1000}(2m_{NH_4NO_3} - 0.028m^2_{NH_4NO_3} + m_{NH_4Cl}\ln(1 - X_{NH_4NO_3}))]$$

and for the system saturated with NH_4NO_3 it is

$$\frac{a_w(m_{NH_4Cl})}{0.594} = \exp[-\frac{18}{1000}(2m_{NH_4Cl} + 0.051m^2_{NH_4Cl} + m_{NH_4NO_3}\ln X_{NH_4NO_3})] \tag{14}$$

where $X_{NH_4NO_3} \equiv \frac{m_{NH_4NO_3}}{m_{NH_4NO_3}+m_{NH_4Cl}}$ is the solute relative mole fraction. By evaluating Equations (13) and (14) at the molalities determined by Prutton et al. (1935) we can plot the water activity at saturation as a function of $X_{NH_4NO_3}$. This curve is displayed in Figure 1.

When $X_{NH_4NO_3}$ is 0, the aerosol contains NH_4Cl and water, and the solution deliquesces at 77.4% relative humidity. If NH_4NO_3 is added to the solution, the DRH decreases along curve 1 until a precipitate of NH_4NO_3 forms at $X_{NH_4NO_3} = 0.811$. The solution in equilibrium with precipitates of both NH_4Cl and NH_4NO_3 has the mutual deliquescence relative humidity, MDRH, of 51.4%. Likewise, when $X_{NH_4NO_3}$ is 1, the aerosol contains NH_4NO_3 and water, and the solution deliquesces at 59.4%. If NH_4Cl is added to the solution, the DRH follows curve 2 until the precipitate of NH_4Cl forms at $X_{NH_4NO_3} = 0.811$.

In region a of Figure 1, the ambient relative humidity is above both deliquescence points, and the salts are completely dissolved. In region b, the ambient relative humidity is between the deliquescence points of the two electrolytes. The mixture is in solution for combinations of composition and relative humdity to the right of line 1, whereas the mixture exists as solid NH_4Cl in equilibrium with a solution of both electrolytes to the left of line 1. In region c, the ambient relative humidity is below the deliquescence points for both electrolytes, but the Gibbs free energy of

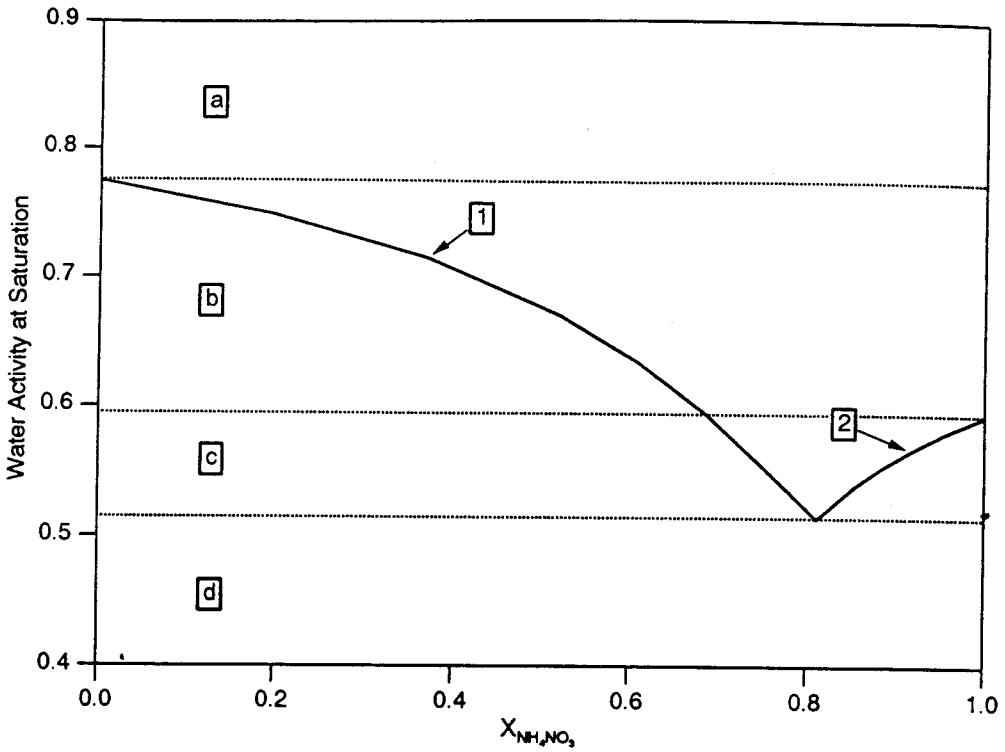

Figure 1. Water activity at saturation of an aqueous solution of NH_4NO_3 and NH_4Cl.

the system is not necessarily minimized by the aerosol particle becoming a solid. Instead the mixture exists as a solution between lines 1 and 2. To the left of line 1 the mixture exists as $NH_4Cl(s)$ in equilibrium with a solution of both electrolytes, whereas to the right of line 2 the mixture exists as $NH_4NO_3(s)$ in equilibrium with a solution of both electrolytes. Finally, in region d the ambient relative humidity is below the MDRH and the mixture is composed of $NH_4NO_3(s)$ and $NH_4Cl(s)$.

Let us now examine what transpires as a particle of given composition is exposed to decreasing relative humidities. Starting at say 80% relative humidity and $X_{NH_4NO_3} = 0.4$, the particle is aqueous. As the relative humidity drops the solution becomes more concentrated until at about 70% relative humidity $NH_4Cl(s)$ forms. Further decreases in relative humidity result in precipitation of additional $NH_4Cl(s)$ such that $X_{NH_4NO_3}$ in the aqueous phase follows curve 1. Finally at a relative humidity of 51.4% the aqueous phase reaches $X_{NH_4NO_3} = 0.811$ and $NH_4NO_3(s)$ forms. Further decreases in relative humidity cause the aerosol to abruptly effloresce.

It has been assumed that as an aerosol particle is dissolved during exposure to steadily increasing relative humidity, the H_2O mass of the aerosol will experience step increases at each of the single-component deliquescence points (e.g., Rood et al., 1987; Pilinis et al., 1989). A consequence of deliquescence point lowering in multicomponent solutions is that the theory does not allow step changes in aerosol H_2O mass as the ambient relative humidity is raised or lowered; there is at most one step and this step corresponds to the mutual deliquescence point of the solution. For relative humidities below the MDRH, the aerosol is dry. Just above the MDRH, the aerosol consists of one or more solids in equilibrium with a highly concentrated solution that contains the dissolved components of these solids. This is the only step change. Further increases in relative humidity cause more of the solid phases to dissolve until finally one by one the solid phases each disappear.

The relative humidity where a given solid completely dissolves corresponds to its DRH in the multicomponent solution, but does not correspond to a step change in the aerosol mass. Instead a plot of aerosol mass versus relative humidity would exhibit abrupt changes in slope at these DRH points (Winkler, 1973, 1988). Abrupt changes in aerosol mass may occur due to nucleation events or hysteresis effects, but equilibrium thermodynamics does not predict them.

Thus, the assumption that a salt will not precipitate at relative humidities above its single electrolyte deliquescence point is valid for electrolytes that do not precipitate as double salts or solid solutions. In the next section we will explore how these single electrolyte deliquescence points vary with temperature.

Variation of DRH with Temperature

The DRH for a single electrolyte in solution can increase, decrease, or remain constant as the temperature of the solution and the surrounding gas is varied (O'Brien, 1948). The temperature dependence of DRH has been explored for NH_4NO_3 (Stelson and Seinfeld, 1982) and NH_4Cl (Pio and Harrison, 1987), who both showed a significant decrease in DRH with increasing temperature. In this section we will derive an expression for the variation of DRH with temperature and, for atmospherically relevant electrolytes, compare this variation to the existing experimental evidence.

Consider a single-component aqueous electrolyte solution in equilibrium with both water vapor and the crystalline form of the electrolyte. Denbigh (1981, eqn. 7-11, p. 218) derives an expression for the variation of water vapor pressure with temperature for such a system,

$$\frac{d \ln p_s}{dT} = \frac{\Delta H}{RT^2} \tag{15}$$

where p_s is the water vapor pressure over the solution, $\Delta H = L_{w,s} + \frac{M_w}{1000} m_s L_s$

is the change in enthalpy of the system when 1 mole of water is evaporated and a corresponding $\frac{M_w}{1000} m_s$ moles of solute are fused, m_s is the molality of the solute at saturation, $L_{w,s}$ is the latent heat of vaporization of water at molality m_s, and L_s is the latent heat of fusion of the electrolyte from saturated solution at molality m_s.

The variation of water vapor pressure over pure water with temperature is given by the Clausius-Clapeyron equation (Denbigh 1981, eqn. 6-11, p. 200)

$$\frac{d \ln p_p}{dT} = \frac{L_{w,p}}{RT^2} \tag{16}$$

where p_p is is the water vapor pressure over pure water and $L_{w,p}$ is the latent heat of vaporization of pure water. For sufficiently low vapor pressures such as exist under typical atmospheric conditions, the water activity, a_w, can be expressed in terms of the water vapor pressure over solution, p_s, and the water vapor pressure over pure water, p_p by $a_w = p_s/p_p$. Differentiating the logarithm of this expression with respect to temperature gives

$$\frac{d \ln a_w}{dT} = \frac{d \ln p_s}{dT} - \frac{d \ln p_p}{dT}. \tag{17}$$

Combining Equations (15) through (17) yields an expression for the variation in water activity with temperature in an electrolyte solution in equilibrium with the crystalline phase of the salt:

$$\frac{d \ln a_w}{dT} = \frac{L_{w,s} - L_{w,p} + \frac{M_w}{1000} m_s L_s}{RT^2}. \tag{18}$$

If we now assume that the molality and latent heats are relatively constant over small excursions in ambient temperature, this equation can be integrated to yield

$$\ln \frac{a_w(T)}{a_w(T_o)} = -\frac{L_{w,s} - L_{w,p} + \frac{M_w}{1000} m_s L_s}{R} \left(\frac{1}{T} - \frac{1}{T_o}\right) \tag{19}$$

where T_o is the temperature at which the water activity is known and is typically 298.15 K. If we further assume that the latent heat of vaporization of water is not significantly affected by the presence of the solute then $L_{w,s} - L_{w,p} \ll (M_w/1000)m_s L_s$ and

$$\ln \frac{a_w(T)}{a_w(T_o)} = -\frac{M_w}{1000} m_s \frac{L_s}{R}\left(\frac{1}{T} - \frac{1}{T_o}\right) \tag{20}$$

Robinson and Stokes (1959) have measured the water activity in saturated solutions of NaCl, $NaNO_3$, NH_4Cl, NH_4NO_3, and $(NH_4)_2SO_4$ at 298.15 K. Using the activity and thermodynamic data of Table 6, Equation (20) can be evaluated for each electrolyte:

$$(\mathrm{NaCl}) \qquad \ln \frac{a_w(T)}{0.7528} = 25\left(\frac{1}{T} - \frac{1}{298.15}\right) \tag{21}$$

$$(\mathrm{NaNO_3}) \qquad \ln \frac{a_w(T)}{0.7379} = 304\left(\frac{1}{T} - \frac{1}{298.15}\right) \tag{22}$$

$$(\mathrm{NH_4Cl}) \qquad \ln \frac{a_w(T)}{0.7710} = 239\left(\frac{1}{T} - \frac{1}{298.15}\right) \tag{23}$$

$$(\mathrm{NH_4NO_3}) \qquad \ln \frac{a_w(T)}{0.6183} = 852\left(\frac{1}{T} - \frac{1}{298.15}\right) \tag{24}$$

$$((\mathrm{NH_4})_2\mathrm{SO_4}) \qquad \ln \frac{a_w(T)}{0.7997} = 80\left(\frac{1}{T} - \frac{1}{298.15}\right) \tag{25}$$

Stelson and Seinfeld (1982), using a least squares regression, obtained 856 for the slope in Equation (24) from data in Dingemans (1941). With lack of other information, their hypothesis for the temperature dependence of the DRH for NH_4NO_3 implied that this dependence was the same for all electrolytes, which we now see is not the case as evidenced by Equations (21) to (25). Pio and Harrison (1987) present data that imply a linear relationship between DRH and temperature for NH_4Cl, but the slope of their curve ($da_w/dT = 2.02 \times 10^{-3}$ K^{-1}) is in excellent agreement with the slope of Equation (23) at 298 K ($da_w/dT = 2.09 \times 10^{-3}$ K^{-1}).

Table 6

Data at 298.16 K for Calculating Temperature Dependence of Deliquescence Relative Humidity

Species	DRH[a]	ΔH^b_{cr} kJ/mol	ΔH^c_{aq} kJ/mol	m_s mol/kg	$\frac{M_w}{1000} m_s \frac{L_s}{R}$ K
NaCl	0.7528	−411.153	−409.3	6.144[d]	−25
$NaNO_3$	0.7379	−467.85	−454.9	10.830[d]	−304
NH_4Cl	0.7710	−314.43	−299.5	7.405[d]	−239
NH_4NO_3	0.6183	−365.56	−350.4	25.954[d]	−852
$(NH_4)_2SO_4$	0.7997	−1180.85	−1174.5	5.843[e]	−80

Symbols: ΔH_{cr} is the standard heat of formation of the crystalline phase and ΔH_{aq} is the standard heat of formation of the species in aqueous solution at molality m_s. $L_s = \Delta H_{cr} - \Delta H_{aq}$ is the latent heat of fusion for the salt from a saturated solution, R is the gas constant, and M_w is the molecular weight of water.

Sources: (a) Robinson and Stokes (1959); (b) Wagman et al. (1982); (c) extrapolated from Wagman et al. (1982); (d) Hamer and Wu (1972); (e) Wishaw and Stokes (1954).

A few important assumptions were used to derive Equations (20) to (25). First we assumed that the latent heat of vaporization of water is not changed significantly by the presence of the solute. Second, we extrapolated the enthalpy data of Wagman et al., (1982) to saturation molalities. Third, we assumed that the

molality at saturation, m_s, does not change significantly over the range of temperatures of atmospheric relevance. And finally we assumed that over this range of temperature and molality the latent heat of fusion of the salt, L_s, does not change significantly. To investigate the validity of Equations (21)–(25), they are compared to experimental data in Figures 2–6. The data are from measurements of water vapor pressure or relative humidity over saturated salt solutions. Since the solution and the vapor are in equilibrium, the relative humidity and water activity are identical. The agreement between the data and the equations is generally within $\pm 1\%$ relative humidity. Thus Equations (20)–(25) accurately represent the temperature dependence of DRH in the range $283 - 313$ K and the available enthalpy data (Wagman et al., 1982) can be extrapolated to obtain enthalpy data at saturation without introducing substantial error.

Sodium Sulfate

Sodium sulfate, a constituent of atmospheric aerosols, is not included here because the data in Wagman et al. (1982) are not as accurate as for the electrolytes listed above (see Wagman et al., 1982, p. 2–16) and the predicted temperature dependence does not agree with the available data. Enough information is available about sodium sulfate at least to give a semi-quantitative picture of its deliquescence behaviour. At 298 K and relative humidities below about 81% (Baxter and Lansing, 1920; Wilson, 1921), sodium sulfate exists as Na_2SO_4(s). At 81% relative humidity, Na_2SO_4 and $Na_2SO_4 \cdot 10H_2O$ are in equilibrium. Between 81% and a higher relative humidity (e.g., 86%, Leopold and Johnston, 1927; 97%, Csontos, 1956) that we will call DRH_{10}, $Na_2SO_4 \cdot 10H_2O$(s) is the stable species although metastable Na_2SO_4(s) has often been observed (e.g., Leopold and Johnston, 1927). At DRH_{10}, $Na_2SO_4 \cdot 10H_2O$(s) is in equilibrium with its aqueous solution and above DRH_{10} only the aqueous solution exists.

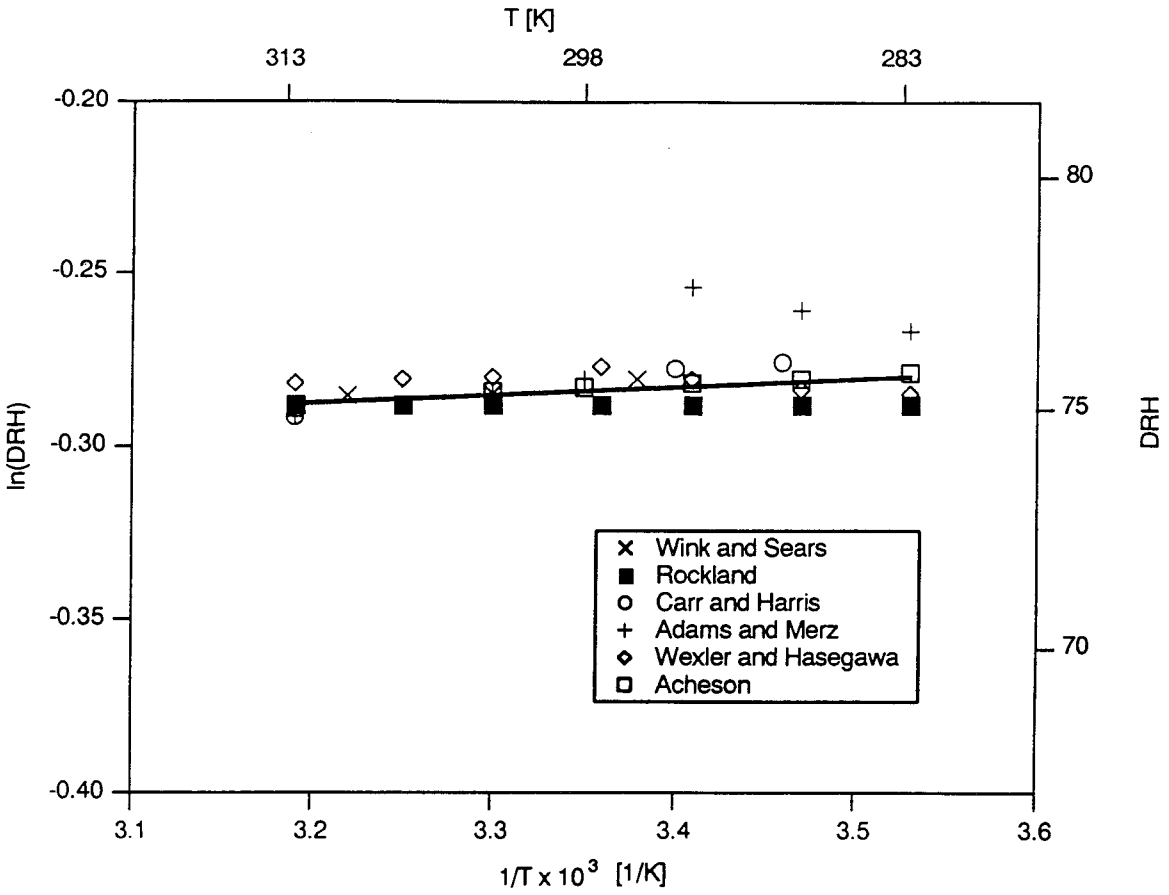

Figure 2. Temperature dependence of DRH for NaCl.

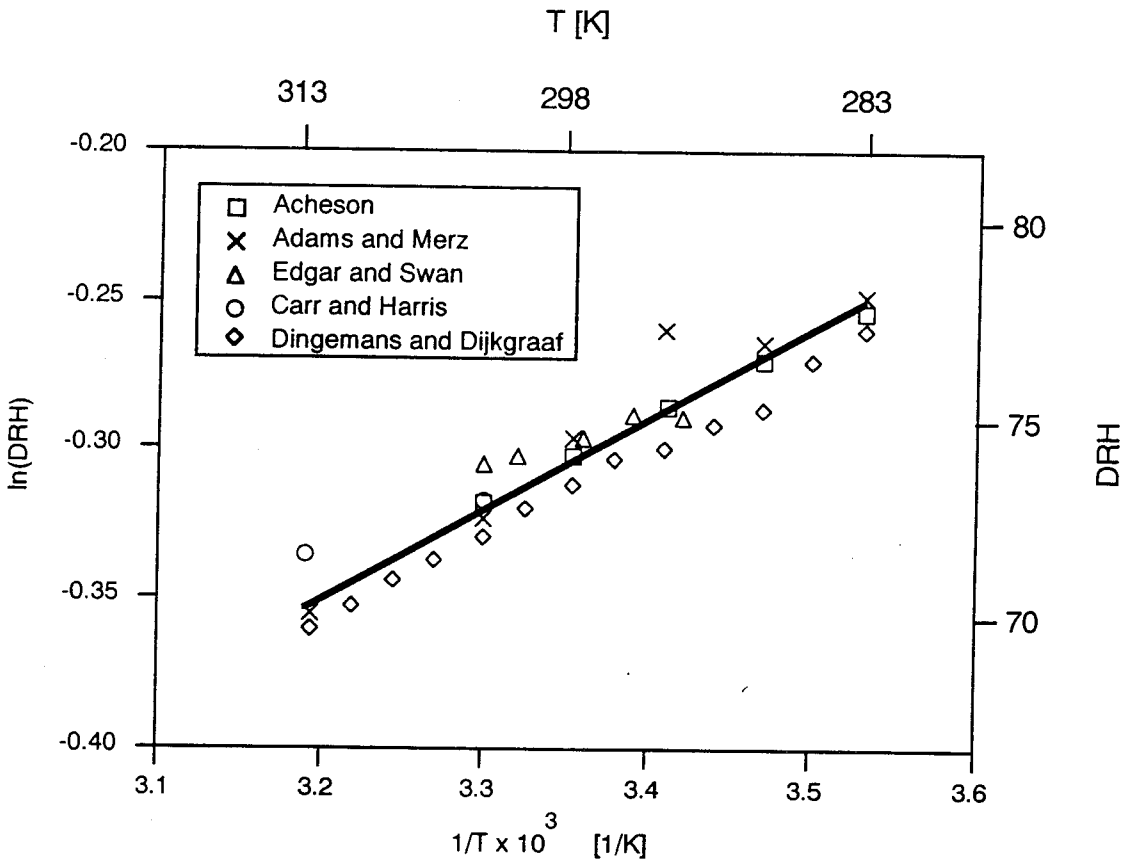

Figure 3. Temperature dependence of DRH for $NaNO_3$.

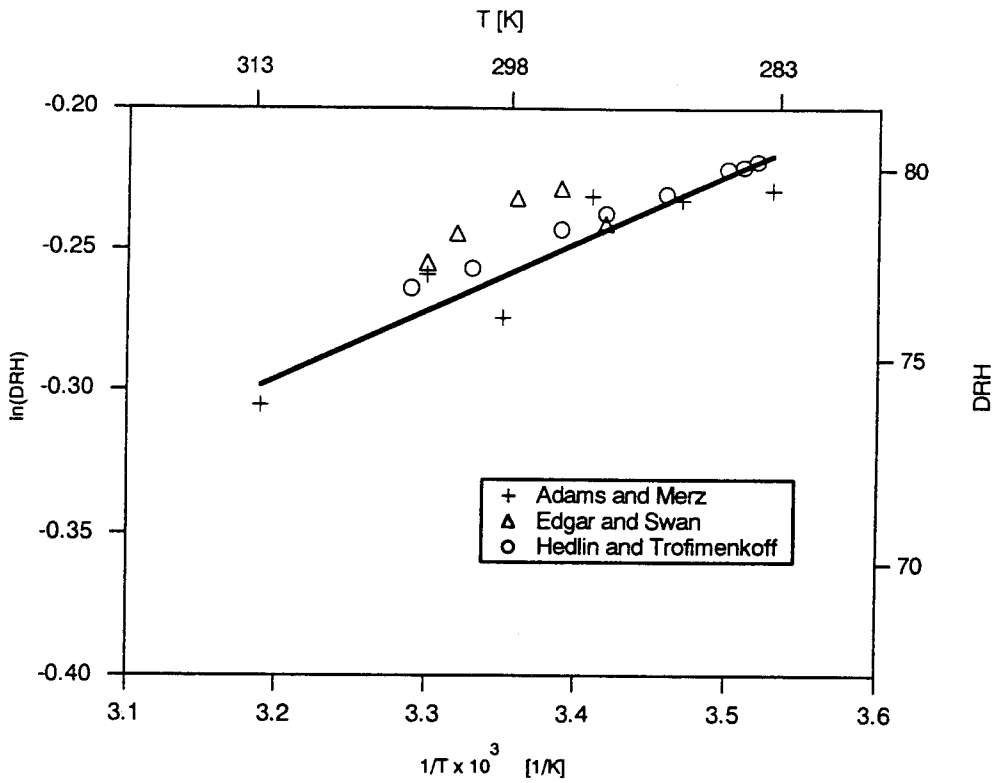

Figure 4. Temperature dependence of DRH for NH_4Cl.

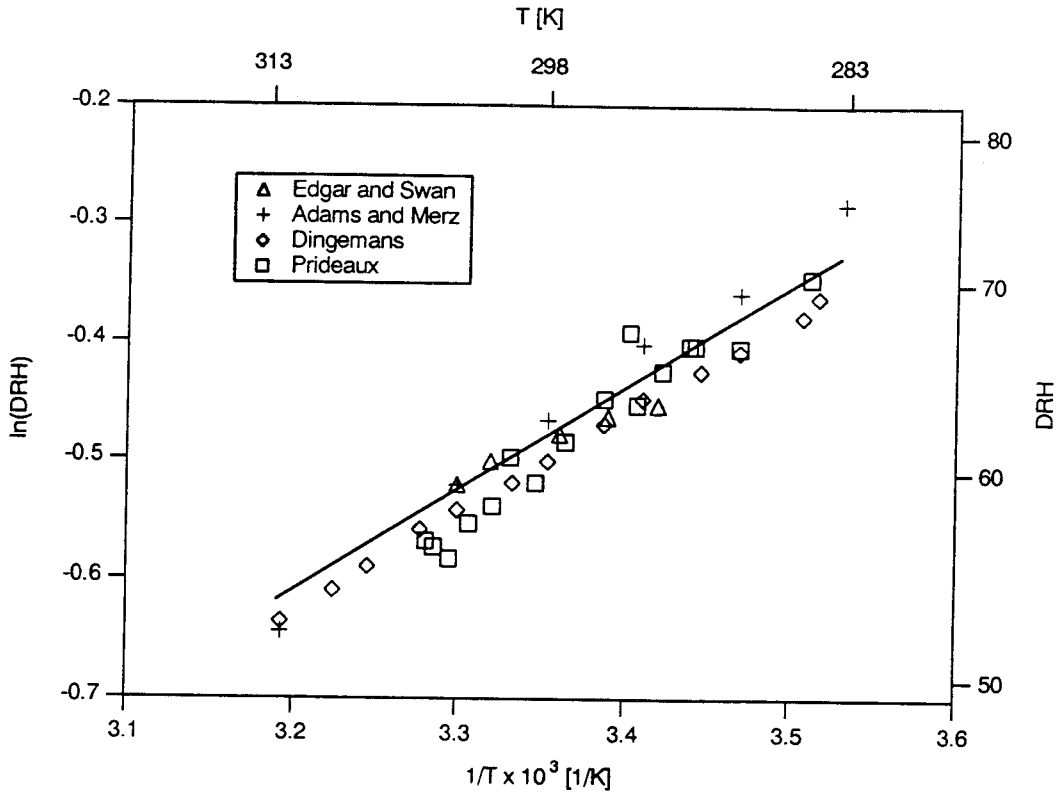

Figure 5. Temperature dependence of DRH for NH_4NO_3.

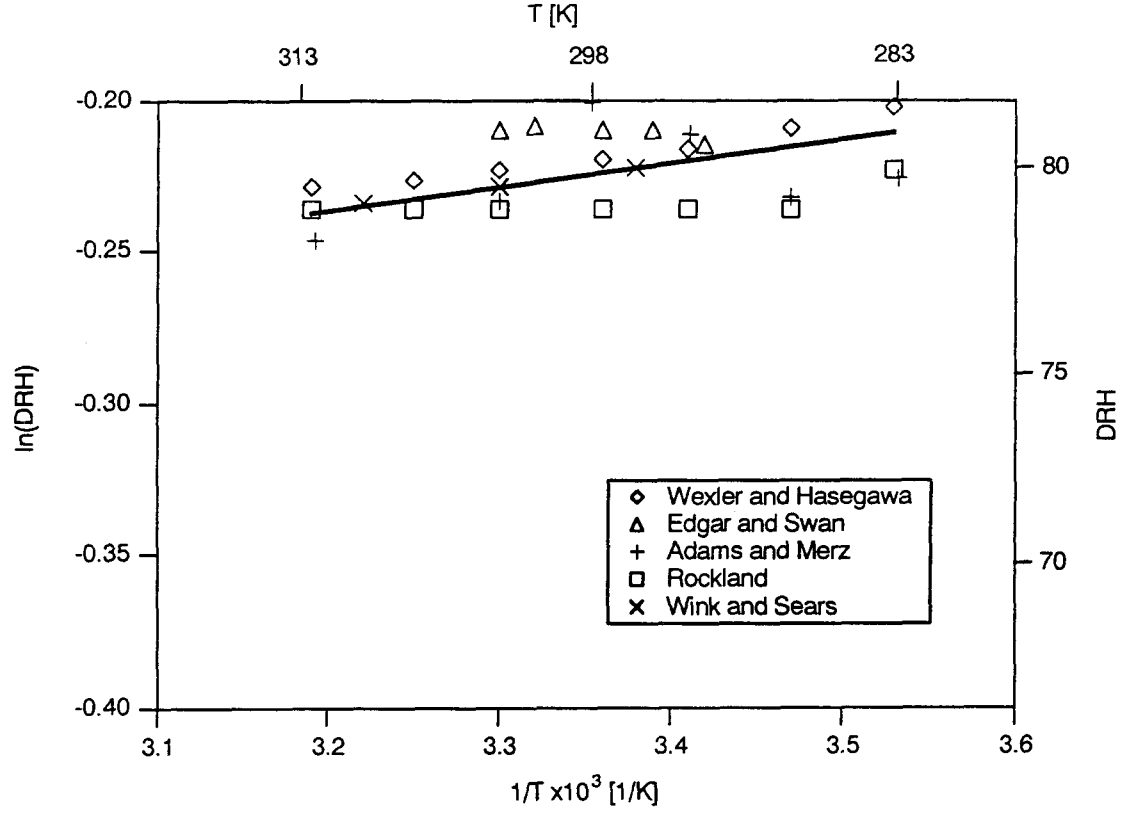

Figure 6. Temperature dependence of DRH for $(NH_4)_2SO_4$.

Below about 305 K, sodium sulfate has, in effect, two deliquescence points. The first occurs where the anhydrous and decahydrate salts are in equilibrium. The second occurs where the decahydrate salt and aqueous solution are in equilibrium. A triple point occurs at about 305 K where all three stable forms, anhydrous, decahydrate, and aqueous solution, exist in mutual equilibrium. Above the triple point temperature, there is one deliquescence point where the anhydrous salt and aqueous solutions are in equilibrium and the decahydrate form is no longer stable.

Other sulfates of ammonium and sodium have been observed in the atmosphere, but due to lack of sufficient data, analysis of their deliquescence properties as a function temperature will not be attempted. The solubility diagram for the ammonium sulfates at 303 K is available in Tang, et al. (1978) and the corresponding diagram for sodium sulfates and their hydrates at 298 K is available in Gmelin, supplement 3 (1966).

Modelling Implications

Previous models of the inorganic components of atmospheric aerosol (MARS: Saxena et al., 1986; SEQUILIB: Pilinis and Seinfeld, 1987) have assumed, first, that the deliquescence point does not significantly vary with temperature, and second, that the aerosol is a solid below the lowest DRH of the aerosol electrolytes. The first assumption may result in serious over- or underprediction of the water content of the aerosol at temperatures other than 298 K. This is especially important for common aerosol species such as NH_4NO_3, NH_4Cl, and $NaNO_3$, each of whose DRH has a significant temperature dependence. In this section, we have presented a consistent theory that accurately predicts the temperature variation of five salts of atmospheric relevance as evidenced by a large body of independent experimental data. AIM employs Equations (21)–(25) to assess the temperature dependence of each of these deliquescence points. The deliquescence points of other salts are

assumed to be constant.

As a result of the second assumption noted above, the computer codes SEQUILIB and MARS predict a dry aerosol at relative humidities significantly above the actual deliquescence point of the mixture. In a subsequent section we compare the predictions of AIM and SEQUILIB under typical atmospheric conditions.

COMPARISON OF PREDICTED AND MEASURED ACTIVITIES

In AIM, the activity coefficients of the solutes are predicted by the method of Kusik and Meissner (1978) and the aerosol water content is predicted by the ZSR method (Zdanovskii, 1948; Stokes and Robinson, 1966). Both of these methods are empirical in nature and their accuracy has not been established for the mix of solutes found in atmospheric aerosol particles. In this section, the components of the model that predict the thermodynamic properties of aerosol aqueous solutions will be compared to fundamental data.

Single-Solute Activity Coefficients

The Meissner electrolyte activity model is a so-called single parameter model and Kusik and Meissner (1978) report recommended values for this parameter that agree with the available activity data ($NaNO_3$: Wu and Hamer, 1980; $(NH_4)_2SO_4$: Wishaw and Stokes, 1954; Na_2SO_4: Goldberg, 1981; NaCl, NH_4Cl, and NH_4NO_3: Hamer and Wu, 1972) to within about 10% over the range of 1 M to saturation. For HCl and HNO_3 we use parameter values of 6.0 and 2.6 respectively, so that the model fits the data over a wider range of ionic strengths, 1 to 16 M. For H_2SO_4, no parameter value is supplied and we chose 0.7 as a best fit. For these acids, Figures 7-9 compare the activity coefficients predicted by the model and the reported data (HCl and HNO_3: Hamer and Wu, 1972; H_2SO_4: Staples, 1981). The agreement between predictions and measurements is good except for H_2SO_4, as has been previously addressed (Meissner and Peppas, 1973; Zemaitis et al., 1986).

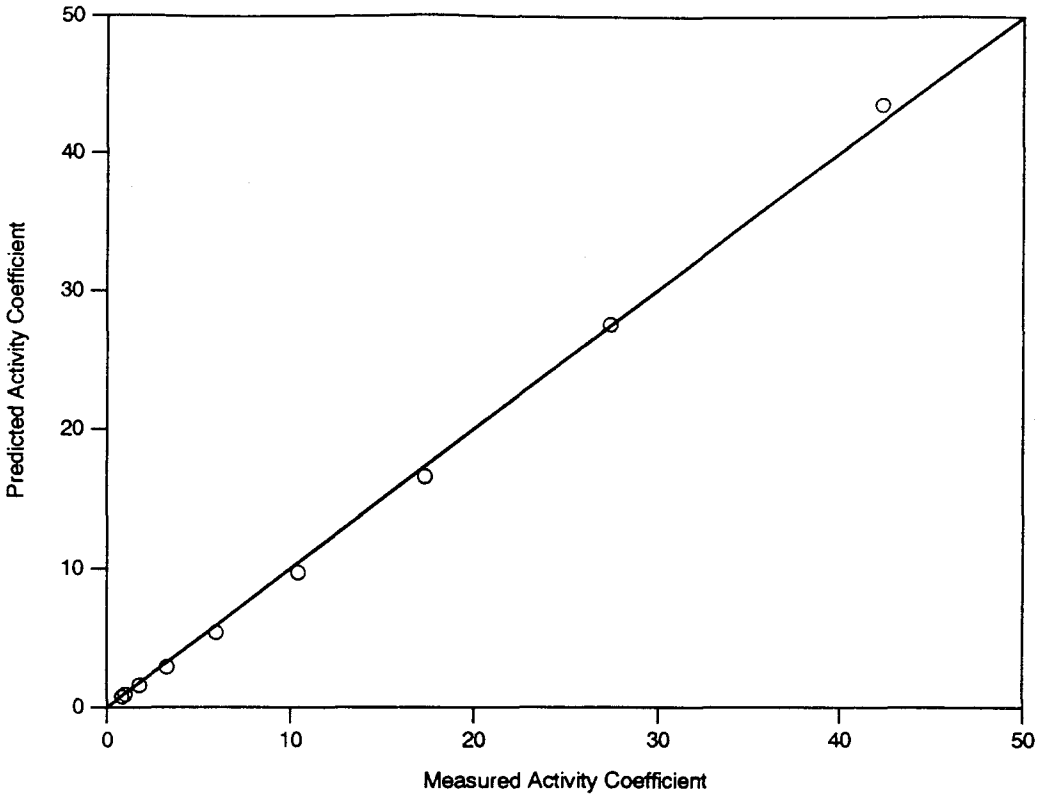

Figure 7. Predicted versus measured activity coefficient for HCl.

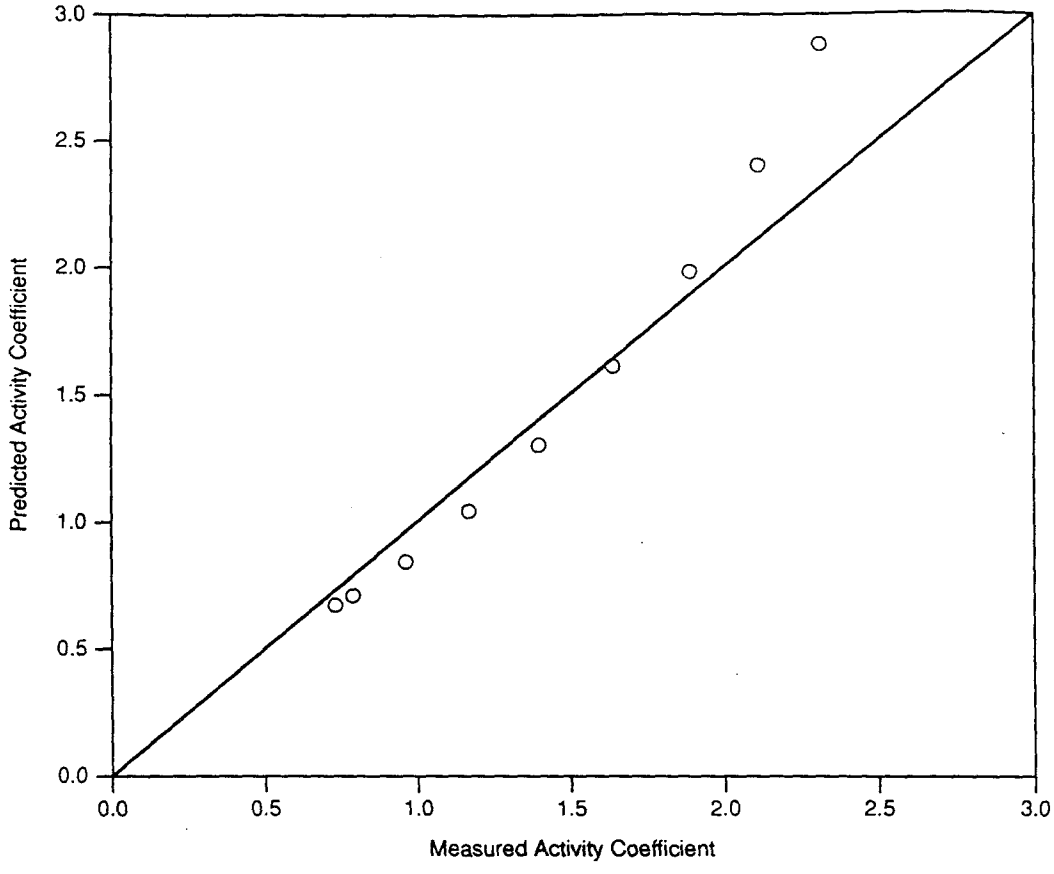

Figure 8. Predicted versus measured activity coefficient for HNO_3.

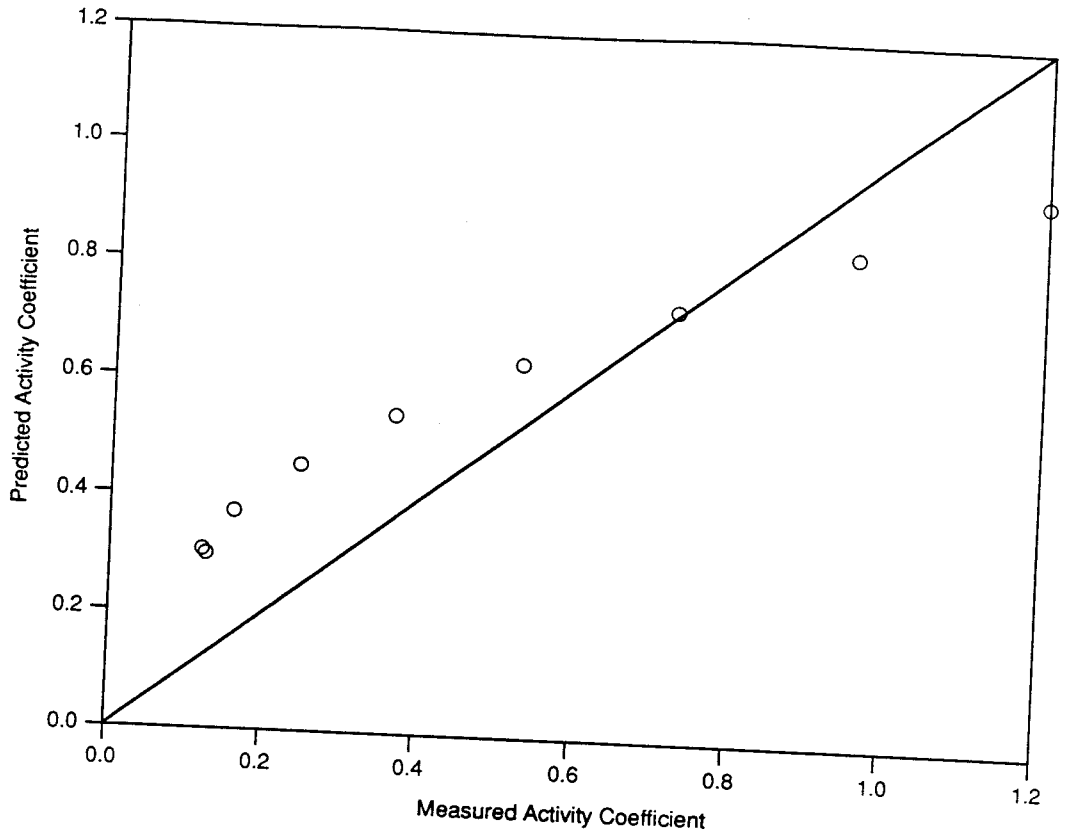

Figure 9. Predicted versus measured activity coefficient for H_2SO_4.

What is the impact of errors in the prediction of the H_2SO_4 activity coefficient? The activity coefficient of H_2SO_4 is used to calculate the activity coefficients of $NaHSO_4$, NH_4HSO_4, and $(NH_4)_3H(SO_4)_2$:

$$\gamma_{NaHSO_4} = \sqrt{\gamma_{Na_2SO_4}\gamma_{H_2SO_4}}$$

$$\gamma_{NH_4HSO_4} = \sqrt{\gamma_{(NH_4)_2SO_4}\gamma_{H_2SO_4}}$$

$$\gamma_{(NH_4)_3H(SO_4)_2} = (\gamma^3_{(NH_4)_2SO_4}\gamma_{H_2SO_4})^{1/4}$$

which are then used to establish equilibrium between the aqueous phase and these three solid phases. Inaccuracies in the activity coefficients result in a maldistribution of these species between the solid and aqueous phases. For NH_4HSO_4 and $(NH_4)_3H(SO_4)_2$ this maldistribution will result in altered NH_4^+ concentrations in the aqueous phase and therefore altered predictions of the surface gas-phase concentrations or gas-aerosol phase distribution of ammonia. The ability of any of the existing strong electrolyte activity models to predict the activity of complexing electrolytes, such as H_2SO_4, is limited (Zemaitis et al., 1986). Since the square root or fourth root of $\gamma_{H_2SO_4}$ are used in the calculation of the activities of $NaHSO_4$, NH_4HSO_4, and $(NH_4)_3H(SO_4)_2$, the impact of any inaccuracy is substantially reduced.

Multiple-Solute Activity Coefficients

There is a large body of experimental data on the activity coefficients of multicomponent aqueous solutions (Harned and Robinson, 1968), but unfortunately, there are limited data on the systems of relevance here. Data are available for aqueous solutions of NaCl–$NaNO_3$ (Lanier, 1965; Bezboruah et al., 1970), NaCl–HCl (Lietzke et al., 1965), NaCl–Na_2SO_4 (Wu et al., 1968; Lanier, 1965; Butler et al., 1967), HCl–NH_4Cl (Robinson et al., 1974), and Na_2SO_4–H_2SO_4 (Akerlof,

1926). For the first four systems the predicted and measured activity coefficients agree to within 6%. For the fifth system the values differ by a nearly constant factor of two, not an unexpected result considering the poor fit for single component sulfate solutions.

The ZSR relationship, given in Equation (5), requires single component water activity data as a function of molality. These data are entered into AIM and SEQUILIB in tabular form for each electrolyte (Pilinis and Seinfeld, 1987) and so for single electrolyte solutions, the model and data agree by definition. For multicomponent solutions, water activity has been measured in aqueous solutions of NaCl–NH_4Cl (Kirgintsev and Luk'yanov, 1963), NaCl–$NaNO_3$ (Kirgintsev and Luk'yanov, 1964; Bezboruah et al.,1970), $NaNO_3$–NH_4NO_3 (Kirgintsev and Luk'yanov, 1965), NaCl–$(NH_4)_2SO_4$ (Cohen et al., 1987), and NaCl–Na_2SO_4 (Wu et al., 1968). All of these data are predicted to within a few percent by the ZSR model, even for the supersaturated solutions of Cohen et al. (1987). Stokes (1948) has measured the water activity of $NaHSO_4$ solutions, which are equivalent to the equimolar solution Na_2SO_4–H_2SO_4. Figure 10 shows the predicted and measured molalities as a function of water activity. At high water activities corresponding to dilute solutions, the molalities are in agreement. As the water activity decreases, the predictions and measurements deviate. At $a_w = 0.765$, the deviation in the two values has reached about 25%. This deviation is due to the formation of the bisulfate ion at the higher concentrations.

With the exception of solutions that contain H_2SO_4, the Kusik and Meissner and ZSR models accurately predict the activity of the solutes and the mass of water. In typical urban aerosols, sulfate is mostly neutralized by sodium and ammonium, and under these conditions the sulfate activities will be accurately predicted. Aerosol pH is usually lowest immediately after a fog. In Los Angeles post-fog con-

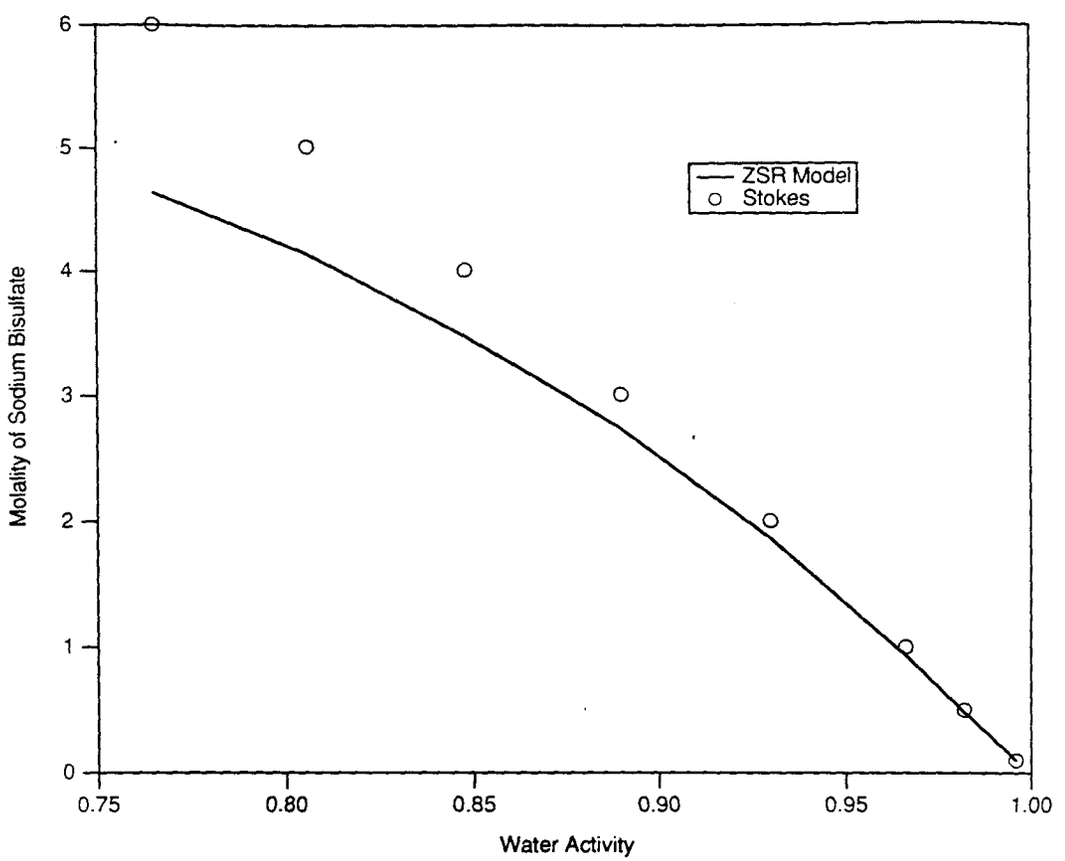

Figure 10. Predicted and measured $NaHSO_4$ concentration as a function of water activity.

ditions (Jacob et al., 1985), aerosols are composed primarily of ammonium, nitrate, and sulfate. The low pH results in rapid evaporation of nitric acid and neutralization of the sulfate by ammonia. Thus we expect that any large H_2SO_4 concentrations will be rapidly neutralized by ammonium and that inaccuracies in sulfate activity will have only a transient effect on the overall predictions of aerosol composition. The model is least accurate under atmospheric conditions with a large generation of sulfate and insufficient aerosol sodium or ammonium to neutralize this sulfate.

COMPARISON OF EQUILIBRIUM MODELS

AIM consists of two components: the thermodynamic portion and the transport portion. In this section the thermodynamic portion of the code is tested by running AIM until equilibrium is attained between the aerosol and gas phases. Pilinis and Seinfeld (1987) compared their SEQUILIB model to the predictions of EQUIL (Bassett and Seinfeld, 1983) and MARS (Saxena et al., 1986) and found general agreement. EQUIL is an early aerosol equilibrium model that only includes ammonium, nitrate, and sulfate. MARS considers these same components, but is faster than EQUIL because it divides the composition and relative humidity space up into regions. In each region, fewer phases need to be considered so less computing is performed to minimize the Gibbs free energy. SEQUILIB uses the same approach as MARS, but in addition, sodium and chloride are considered. In this section the SEQUILIB model will be compared to AIM.

Table 7 reproduces the results of the conditions examined in Table 7 of Pilinis and Seinfeld (1987). At the lowest relative humidities there is substantial disagreement between the two models. At 46% relative humidity both models predict the aerosol to be composed of $NH_4NO_3(s)$ and $(NH_4)_2SO_4(s)$. The disagreement between the models is due to a difference in the equilibrium constant for the reaction $NH_4NO_3(s) \rightleftharpoons NH_3(g) + HNO_3(g)$. SEQUILIB uses the free energy of formation

Table 7

Aerosol Model Predictions of NO_3^-, NH_4^+, and H_2O for
$T = 298$ K, $10\mu g/m^3$ H_2SO_4, $10\mu g/m^3$ NH_3, and $30\mu g/m^3$ HNO_3

	AIM			SEQUILIB		
RH	NH_4^+	NO_3^-	H_2O	NH_4^+	NO_3^-	H_2O
46	5.9	7.6	0	7.4	12.9	0
51	6.0	7.9	8	7.4	12.9	0
56	6.5	9.7	11	7.4	12.9	0
61	7.0	11.4	15	7.4	12.9	0
66	7.4	13.0	20	7.8	14.0	19
71	7.8	14.3	25	8.2	15.5	26
76	8.2	15.6	34	8.6	16.8	35
81	8.5	17.5	47	9.0	18.3	49
86	8.9	19.4	71	9.4	19.7	73
91	9.6	20.6	129	9.8	21.2	124

data from Parker et al. (1976), JANAF (1971), and Wagman et al. (1968) to obtain an equilibrium constant of 30 ppb^2. AIM uses the more recent and self-consistent data contained in Tables 1–3 (Wagman et al., 1982) to obtain an equilibrium constant of 58 ppb^2. This factor of two difference in equilibrium constants results in AIM predicting much higher gas-phase concentrations of NH_3 and HNO_3 and

correspondingly lower aerosol phase concentrations of NH_4NO_3.

At 298 K, the deliquescence point of NH_4NO_3 occurs at 62% relative humidity. For ambient relative humidities of 51%, 56% and 61%, SEQUILIB assumes that the aerosol is composed of NH_4NO_3(s) and $(NH_4)_2SO_4$(s), but as we have shown, the relative humidity of deliquescence of a salt is lowered in multicomponent solutions. At 51% relative humidity AIM predicts that the aerosol is composed of a solid phase, $(NH_4)_2SO_4$(s), in equilibrium with an aqueous phase containing NH_4^+, NO_3^-, and SO_4^{2-}, whereas at 56% and 61% AIM predicts the aerosol to be composed of a single aqueous phase. That the two models differ in their prediction of the aerosol mass of ammonium and nitrate is primarily due to differences in the free energies of formation used by each model, but the difference in water mass is due to the incorrect assumption in SEQUILIB that each salt deliquesces at its individual DRH. At these three relative humidities, SEQUILIB predicts a dry aerosol, whereas AIM predicts a water content of 8, 11, and 15 $\mu g/m^3$, a significant portion of the total aerosol mass.

At relative humidities above 61% both models predict the aerosol to be composed of a single aqueous phase. Both models use similar thermodynamic properties to represent the aqueous phase so the agreement is excellent.

SEQUILIB employs two classes of assumption that we improve upon in AIM. The first is that the aerosol is composed solely of solid phases at relative humidities below the lowest single-solute deliquescence point of the species in the aerosol. As we have proven previously and shown here, the deliquescence point is lowered for multicomponent solutions. Table 5 lists values of MDRH at 303 K for a number of salt pairs of atmospheric interest and all MDRH values, except that for NH_4NO_3–$(NH_4)_2SO_4$, are significantly below each single electrolyte value.

When two electrolytes combine to precipitate a double salt, there are two mu-

tual deliquescence relative humidities—one when the double salt and the first single salt are in equilibrium with solution, and the other when the double salt and the second single salt are in equilibrium with solution. This seemingly more complicated picture reduces to Figure 1 if one of the electrolytes is considered to be the double salt and the other electrolyte is the single salt that exists in solid form. In the experiments of Adams and Merz (1929), some amount of $(NH_4)_2SO_4$(s) and NH_4NO_3(s) were combined with a small portion of water. This mixture was allowed to equilibrate and the resulting vapor pressure of water was measured. Adams and Merz hypothesized that the double salt $(NH_4)_2SO_4 - 2NH_4NO_3$ is formed by this mixture. The DRH for $(NH_4)_2SO_4 - 2NH_4NO_3$ is 56.4% (Tang 1980), which is significantly below the relative humidity measured by Adams and Merz.

There are a number of possible explanations for this anomaly. That the system may not have reached equilibrium seems to be the most likely since solid-solid phase changes can be extremely slow. Another possibility is that a double salt such as $(NH_4)_2SO_4 - 3NH_4NO_3$ was formed (Tani et al., 1983) which may have a higher DRH than that measured over the mixture. In this case, the NH_4NO_3(s) would have to have been completely transformed into the double salt to not violate Equation (11).

As can be seen in Table 5 for binary solutions, the MDRH values may be substantially lower than the single electrolyte DRH values. For solutions containing more components, the MDRH values are predicted to be even lower. For AIM to predict the MDRH values accurately, the ZSR water content model and Meissner solute activity model must be accurate for multicomponent solutions at ionic strengths exceeding 25 M (the solubility of NH_4NO_3). At these high ionic strengths, uncertainties in both models do not permit the accurate prediction of MDRH values. Nevertheless, there is a range of relative humidities where AIM correctly predicts

an aqueous aerosol and the previous equilibrium models erroneously predict a dry one.

CONCLUSIONS

We have developed a model of the inorganic components of atmospheric aerosols, AIM. This model assumes that the components of the aerosol are in internal phase equilibrium and that the water activity of the aerosol is in equilibrium with the ambient relative humidity. Since the time constants for equilibration of the gas and aerosol phases may be large, equilibrium is not assumed between the gas and aerosol phase for the volatile inorganics, instead transport is explicitly modeled. Comparison between the model predictions and experimentally determined electrolyte activities show satisfactory agreement except for H_2SO_4, but since most H_2SO_4 is neutralized by NH_3 in atmospheric aerosols H_2SO_4 usually comprises a small portion of total aerosol mass.

Predictions of AIM have been improved over those of previous equilibrium models. First the distribution of NH_4NO_3 between the gas and aerosol phases is based on more up-to-date thermodynamic data in AIM. Second, water may comprise a significant fraction of aerosol mass even under conditions of low relative humidity, so accurate prediction of aerosol water content is important. We have derived expressions for the temperature dependence of the single-component deliquescence point and proven that the deliquescence point in a multicomponent aerosol is lower than the single-component points. A common misconception is that multicomponent aerosols deliquesce at the lowest single-component deliquescence point. Pilinis et al. (1989) attempt to explain the non-zero water content that has been observed in aerosols below the lowest single-component deliquescence point by suggesting that the aerosol is composed of a supersaturated metastable solution instead of a stable one in equilibrium. That this assumption is not necessary follows from the work

presented here.

Urban airshed models that predict total aerosol mass or aerosol size distribution have assumed thermodynamic equilibrium between the gas and aerosol phase for the volatile inorganic components (Russell et al., 1983; Hogo et al., 1985; Pilinis and Seinfeld, 1988). We have shown in previous work (Wexler and Seinfeld, 1990) that thermodynamic equilibrium is not sufficient for determining the aerosol mass of volatile inorganics. In this paper we describe the development and testing of an aerosol inorganics model that assumes 1) thermodynamic equilibrium within the aerosol and between water in the gas and aerosol phases and 2) transport of inorganics between the gas and aerosol phases. In subsequent work this aerosol model will be included in an urban airshed model and its predictions compared with gas and aerosol phase measurements taken during SCAQS.

ACKNOWLEDGEMENT

This work was supported by the State of California Air Resources Board Agreement A932-054.

REFERENCES

Acheson D. T. (1965) Vapor pressure of saturated aqueous salt solutions. In: *Humidity and Moisture, vol. 3.* Edited by A. Wexler. Pages 521-530 Reinhold Publishing Co., New York.

Adams J. R. and Merz A. R. (1929) Hygroscopicity of fertilizer materials and mixtures. *Indust. Eng. Chem.* **21** 305-310.

Akerlof G. (1926) Investigations of sulfate solutions. Experimental methods and results on cells without liquid junction. *J. Am. Chem. Soc.* **48** 1160-1177.

Allen A. G., Harrison R. M. and Erisman J. (1989) Field measurements of the dissociation of ammonium nitrate and ammonium chloride aerosols. *Atmos. Environ.* **23** 1591-1599.

Bassett M. and Seinfeld J. H. (1983) Atmospheric equilibrium model of sulfate and nitrate aerosols. *Atmos. Environ.* **17** 2237-2252.

Bassett M. E. and Seinfeld J. H. (1984) Atmospheric equilibrium model of sulfate and nitrate aerosols – II. Particle size analysis. *Atmos. Environ.* **18** 1163-1170.

Baxter G. P. and Lansing J. E. (1920) The aqueous pressure of some hydrated crystals. Oxalic acid, strontium chloride and sodium sulfate. *J. Am. Chem. Soc.* **42** 419-426.

Bezboruah C. P., Covington A. K. and Robinson R. A. (1970) Excess gibbs energies of aqueous mixtures of alkali metal chlorides and nitrates. *J. Chem. Thermodynamics* **2** 431-437.

Butler J. N., Hsu P. T. and Synnott J. C. (1967) Activity coefficient measurements in aqueous sodium chloride-sodium sulfate electrolytes using sodium amalgam electrodes. *J. phys. Chem.* **71** 910-913.

Carr D. S. and Harris B. L. (1949) Solutions for maintaining constant relative humidity. *Indust. Eng. Chem.* **41** 2014-2015.

Chen C.-C., Britt H. I., Boston J. F. and Evans L. B. (1982) Local composition model for excess gibbs energy of electrolyte systems. *AIChE J.* **28** 588-596.

Chen C.-C. and Evans L. B. (1986) A local composition model for the excess gibbs energy of aqueous electrolyte systems. *AIChE J.* **32** 444-454.

Cohen M. D., Flagan R. C. and Seinfeld J. H. (1987) Studies of concentrated electrolyte solutions using the electrodynamic balance. 2. Water activities for mixed-electrolyte solutions. *J. phys. Chem.* **91** 4575-4582.

Csontos E. (1956) Equilibrium relative humidity of saturated solutions of some crystalline compounds. *Agrokema Talajtan* **5** 425-432.

Denbigh K. (1981) *The principles of chemical equilibrium.* Cambridge Univer-

sity Press, Cambridge.

Dingemans P. (1941) Die dampfspannung von gestattigten NH_4NO_3-losungen. *Rec. Trav. Chim.* **60** 317-321.

Dingemans P. and Dijkgraaf L. L. (1948) The vapour pressure of saturated solutions of sodium nitrate in water. *Rec. Trav. Chim.* **67** 231-234.

Edgar G. and Swan W. O. (1922) The factors determining the hygroscopic properties of soluble substances. I. The vapor pressures of saturated solutions. *J. Am. Chem. Soc.* **44** 570-577.

Gmelins (1966) *Gmelins Handbuch der Anorganischen Chemie, Natrium Erganzungsband Lieferung 3.* Verlag Chemie, Weinheim.

Goldberg R. N. (1981) Evaluated activity and osmotic coefficients for aqueous solutions: Thirty-six uni-bivalent electrolytes. *J. Phys. Chem. Ref. Data* **10** 671-764.

Gray H. A., Cass G. R., Huntzicker J. J., Heyerdahl E. K. and Rau J. A. (1986) Characteristics of atmospheric organic and elemental carbon particle concentrations in Los Angeles. *Environ. Sci. Technol.* **20** 580-589.

Haghtalab A. and Vera J. H. (1988) A nonrandom factor model for the excess gibbs energy of electrolyte solutions. *AIChE J.* **34** 803-813.

Hamer W. J. and Wu Y.-C. (1972) Osmotic coefficients and mean activity coefficients of uni-univalent electrolytes in water at 25 C. *J. Phys. Chem. Ref. Data* **1** 1047-1099.

Hanel G. and Zankl B. (1979) Aerosol size and relative humidity: Water uptake by mixtures of salts. *Tellus* **31** 478-486.

Harned H. S. and Robinson R. A. (1968) Multicomponent electrolyte solutions. In: *The international encyclopedia of physical chemistry and chemical physics Topic 15. Equilibrium properties of electrolyte solutions.* Edited by R. A. Robinson.

Volume 2, Pergamon Press, Oxford.

Hedlin C. P. and Trofimenkoff F. N. (1965) Relative humidities over saturated solutions of nine salts in the temperature range from 0 to 90 F. In: *Humidity and Moisture, vol. 3.* Edited by A. Wexler. pp. 519-520 Reinhold Publishing Co., New York.

Heintzenberg J. (1989) Fine particles in the global troposphere. *Tellus* **41B** 149-160.

Hogo H., Seigneur C. and Yocke M. A. (1985) Technical description of a photochemical air quality model with extensions to calculate aerosol dynamics and visibility. *Draft SCAQMD STAR Project, Working Paper 1.*

Jacob D. J., Waldman J. M., Munger J. W. and Hoffman M. R. (1985) Chemical composition of fogwater collected along the California coast. *Environ. Sci. Technol.* **19** 730-736.

JANAF (1971) Thermochemical tables. *NSRDS-NBS* **37** .

Karapet'yants M. Kh. and Karapet'yants M. L. (1970) *Thermodynamic constants of inorganic and organic compounds.* Humphrey Science Publishers, Ann Arbor.

Kirgintsev A. N. and Luk'yanov A. V. (1963) Isopiestic investigation of ternary solutions. I. *Russ. J. phys. Chem.* **37** 1501-1502.

Kirgintsev A. N. and Luk'yanov A. V. (1964) Isopiestic investigation of ternary solutions. III. Sodium chloride–sodium nitrate–water, sodium chloride–sodium bromide–water, and ammonium chloride–ammonium bromide–water. *Russ. J. phys. Chem.* **38** 867-869.

Kirgintsev A. N. and Luk'yanov A. V. (1965) Isopiestic investigation of ternary solutions. VI. Aqueous ternary solutions containing sodium nitrate with the nitrates of lithium, potassium, ammonium, rubidium, and caesium respectively. *Russ. J.*

phys. Chem. **39** 653-655.

Kirgintsev A. N. and Trushnikova L. N. (1968) Isopiestic method of determining the composition of solid phases in three-component systems. *Russ. J. Inorg. Chem.* **13** 600-601.

Kusik C. L. and Meissner H. P. (1978) Electrolyte activity coefficients in inorganic processing. *AIChe Symp. Series* **173,74** 14-20.

Lanier R. D. (1965) Activity coefficients of sodium chloride in aqueous three-component solutions by cation-sensitive glass electrodes. *J. phys. Chem.* **69** 3992-3998.

Leopold H. G. and Johnston J. (1927) The vapor pressure of the saturated aqueous solution of certain salts. *J. Am. Chem. Soc.* **49** 1974-1988.

Lietzke M. H., Hupf H. B. and Stroughton R. W. (1965) Electromotive force studies in aqueous solutions at elevated temperatures. VI. The thermodynamic properties of HCl–NaCl mixtures. *J. phys. Chem* **69** 2395-2399.

Liu Y., Harvey A. H. and Prausnitz J. M. (1989) Thermodynamics of concentrated electrolyte solutions. *Chem. Eng. Comm.* **77** 43-66.

McRae G. J., Goodin W. R. and Seinfeld J. H. (1982) Numerical solution of the atmospheric diffusion equation for chemically reacting flows. *J. Comp. Physics* **45** 1-42.

Meissner H. P. and Peppas N. A. (1973) Activity coefficients–aqueous solutions of polybasic acids and their salts. *AIChE J.* **19** 806-809.

Merz A. R., Fry W. H., Hardesty J. O. and Adams J. R. (1933) Hygroscopicity of fertilizer salts. *Indust. Eng. Chem.* **25** 136-137.

O'Brien F. E. M. (1948) The control of humidity by saturated salt solutions. *J. Sci. Instruments* **25** 73-76.

Parker V. B., Wagman D. D. and Garvin D. (1976) Selected thermochemical

data compatible with the CODATA recommendations. *NBSIR 75-968.*

Pilinis C. and Seinfeld J. H. (1987) Continued development of a general equilibrium model for inorganic multicomponent atmospheric aerosols. *Atmos. Environ.* **21** 2453-2466.

Pilinis C. and Seinfeld J. H. (1988) Development and evaluation of an Eulerian photochemical gas-aerosol model. *Atmos. Environ.* **22** 1985-2001.

Pilinis C., Seinfeld J. H. and Grosjean D. (1989) Water content of atmospheric aerosols. *Atmos. Environ.* **23** 1601-1606.

Pio C. A. and Harrison R. M. (1987) The equlibrium of ammonium chloride aerosol with gaseous hydrochloric acid and ammonia under tropospheric conditions. *Atmos. Environ.* **21** 1243-1246.

Pitzer K. S. (1979) Theory: ion interaction approach. In: *Activity coefficients in electrolyte solutions, vol. 1.* Edited by R. M. Pytkowicz. pp. 157-208 CRC Press, Boca Raton, Florida

Pitzer K. S. (1986) Theoretical considerations of solubility with emphasis on mixed aqueous electrolytes. *Pure Appl. Chem.* **58** 1599-1610.

Prideaux E. B. R. (1920) The deliquescence and drying of ammonium and alkali nitrates and a theory of the absorption of water vapour by mixed salts. *J. Soc. Chem. Ind.* **39** 182T-185T.

Prutton C. F., Brosheer J. C. and Maron S. H. (1935) The system $NH_4Cl - NH_4NO_3 - H_2O$ at 0.4, 25, and 50°. *J. Am. Chem. Soc.* **57** 1656-1657.

Robinson R. A. and Stokes R. H. (1959) *Electrolyte Solutions.* Butterworths, London.

Robinson R. A., Roy R. N. and Bates R. G. (1974) The system $H_2O - HCl - NH_4Cl$ at 25°*C*: A study of Harned's rule. *J. Sol. Chem.* **3** 837-846.

Rockland L. B. (1960) Saturated salt solutions for static control of relative

humidity between 5 and 40 C. *Anal. Chem.* **32** 1375-1376.

Rood M. J., Covert D. S. and Larson T. V. (1987) Hygroscopic properties of atmospheric aerosol in Riverside, California. *Tellus* **39B** 383-397.

Russell A. G., McRae G. J. and Cass G. R. (1983) Mathematical modeling of the formation and transport of ammonium nitrate aerosol. *Atmos. Environ.* **17** 949-964.

Russell A. G. and Cass G. R. (1986) Verification of a mathematical model for aerosol nitrate and nitric acid formation and its use for control measure evaluation. *Atmos. Environ.* **20** 2011-2025.

Russell A. G., McCue K. F. and Cass G. R. (1988) Mathematical modeling of the formation of nitrogen-containing air pollutants. 1. Evaluation of an Eulerian photochemical model. *Environ. Sci. Technol.* **22** 263-271.

Russell D. L. (1970) *Optimization Theory.* W. A. Benjamin, New York.

Saxena P., Hudischewskyj A. B., Seignur C. and Seinfeld J. H. (1986) A comparative study of equilibrium approaches to the chemical characterization of secondary aerosols. *Atmos. Environ.* **20** 1471-1483.

Staples B. R. (1981) Activity and osmotic coefficients of aqueous sulfuric acid at 298.15 K. *J. Phys. Chem. Ref. Data* **10** 779-798.

Stelson A. W. and Seinfeld J. H. (1982) Relative humidity and temperature dependence of the ammonium nitrate dissociation constant. *Atmos. Environ.* **16** 983-992.

Stokes R. H. (1948) The vapor pressures of solutions of sodium and potassium bisulfates at 25°. *J. Am. Chem. Soc.* **70** 874.

Stokes R. H. and Robinson R. A. (1966) Interactions in aqueous nonelectrolyte solutions. I. Solute-solvent equilibria. *J. phys. Chem.* **70** 2126-2130.

Tang I. N., Munkelwitz H. R. and Davis J. G. (1978) Aerosol growth studies–

IV. Phase transformation of mixed salt aerosols in a moist atmosphere. *J. Aerosol Sci.* **9** 505-511.

Tang I. N. (1980) Deliquescence properties and particle size change of hygroscopic aerosols. In: *Generation of aerosols.* Edited by K. Willeke. pp. 153-167 Ann Arbor Science Publishers, Ann Arbor, MI

Tani B., Siegel S., Johnson S. A. and Kumar R. (1983) X-ray diffraction investigation of atmospheric aerosols in the $0.3-1.0$ μm aerodynamic size range. *Atmos. Environ.* **17** 2277-2283.

Wagman D. D., Evans W. H., Parker V. B., Harlow I., Baily S. M. and Schumm R. H. (1968) Selected values of chemical thermodynamic properties; tables for the first thirty-four elements in the standard order of arrangement. *NBS technical note* **270-3** .

Wagman D. D., Evans W. H., Parker V. B., Schumm R. H., Halow I., Bailey S. M., Churney K. L. and Nuttall R. L. (1982) The NBS tables of chemical thermodynamic properties: Selected values for inorganic and C_1 and C_2 organic substances in SI units. *J. Phys. Chem. Ref. Data* **11** Suppl. 2.

Wexler A. and Hasegawa S. (1954) Relative humidity-temperature relationships of some saturated salt solutions in the temperature range 0 to 50 C. *J. Res. Natl. Bur. Std.* **53** 19-26.

Wexler A. S. and Seinfeld J. H. (1990) The distribution of ammonium salts among a size and composition dispersed aerosol. *Atmos. Environ.* **24A** 1231-1246.

Wilson R. E. (1921) Some new methods for the determination of the vapor pressure of salt-hydrates. *J. Am. Chem. Soc.* **43** 704-725.

Wink W. A. and Sears G. R. (1950) Instrumentation Studies LVII. Equilibrium relative humidities above saturated salt solutions at various temperatures. *TAPPI* **33** 96A-99A.

Winkler P. (1973) The growth of atmospheric aerosol particles as a function of the relative humidity – II. An improved concept of mixed nucleii. *Aerosol Sci.* **4** 373-387.

Winkler P. (1988) The growth of atmospheric aerosol particles with relative humidity. *Physica Scripta* **37** 223-230.

Wishaw B. F. and Stokes R. H. (1954) Activities of aqueous ammonium sulphate solutions at 25°*C*. *Trans. Faraday Soc.* **50** 952-954.

Wu Y. C., Rush R. M. and Scatchard G. (1969) Osmotic and activity coefficients for binary mixtures of sodium chloride, sodium sulfate, magnesium sulfate, and magnesium chloride in water at 25°*C*. I. Isopiestic measurements on the four systems with common ions. *J. phys. Chem.* **72** 4048-4053.

Wu Y. C. and Hamer W. J. (1980) Revised values of the osmotic coefficients and mean activity coefficients of sodium nitrate in water at 25°*C*. *J. Phys. Chem. Ref. Data* **9** 513-518.

Young T. R. and Boris J. P. (1977) A numerical technique for solving stiff ordinary differential equations associated with the chemical kinetics of reactiv-flow problems. *J. phys. Chem.* **81** 2424-2427.

Young T. R. (1980) CHEMEQ - A subroutine for solving stiff ordinary differential equations. *Naval Research Laboratory Memorandum Report 4091.*

Young T. R. (1983) CHEMEQ - VAX version update to Appendix B of T. R. Young (1980).

Zdanovskii A. B. (1948) New methods of calculating solubilities of electrolytes in multicomponent systems. *Zhur. Fiz. Khim.* **22** 1475-1485.

Zemaitis J. F., Clark D. M., Rafal M. and Scrivner N. C. (1986) *Handbook of aqueous electrolyte thermodynamics.* AIChE, New York.

SECTION 5

AEROSOL AMMONIUM NITRATE DURING SCAQS

ABSTRACT

Inorganic composition and size distribution of atmospheric aerosols measured during the 1987 Southern California Air Quality Study (SCAQS) are used to investigate the degree to which ammonia and nitric acid in the gas phase and ammonium nitrate in the aerosol phase are in equilibrium. The data exhibit significant scatter around the equilibrium prediction. Attempts to correlate the departure from equilibrium with the estimated values of the equilibration time constants do not support a departure from equilibrium that results from transport limitations between the gas and aerosol phases. When measured size distributions of ammonium and nitrate are compared as another indication of transport-limited departure from equilibrium, it is concluded that often different size aerosol particles are not in mutual equilibrium, which supports our earlier hypothesis that both thermodynamics and mass transport must be considered to accurately predict the size distribution of the volatile inorganics in atmospheric aerosol.

Key word index: SCAQS, ammonium nitrate, atmospheric aerosols, thermodynamic equilibrium.

INTRODUCTION

One of the most intriguing aspects of atmospheric aerosols concerns the behavior of ammonium nitrate. Stelson et al. (1979) first suggested that aerosol ammonium nitrate levels could be determined from the equilibrium among ammonia, nitric acid, and aerosol ammonium nitrate. The assumption of thermodynamic equilibrium has been employed to partition the volatile compounds between the gas and aerosol phases (Bassett and Seinfeld, 1983; Russell et al., 1983; Saxena et al., 1983, 1986; Russell and Cass, 1986; Russell et al., 1988) and to predict their aerosol size distribution (Bassett and Seinfeld, 1984; Pilinis et al., 1987; Pilinis and Seinfeld, 1987, 1988). Although the equilibrium assumption has been supported by some ambient data (Doyle et al., 1979; Grosjean, 1982; Hildemann et al., 1984), other data indicate that it may not always hold (Cadle et al., 1982; Tanner, 1982; Allen et al., 1989).

The South Coast Air Basin (SoCAB) of southern California experiences some of the highest aerosol concentrations in the United States. These aerosols are primarily composed of elemental carbon, and organic and inorganic compounds. The inorganic compounds are primarily ammonium, sodium, nitrate, sulfate, and chloride, which typically comprise 25-50% of the mass of the aerosol (Gray et al., 1986). During the summer and fall of 1987, extensive measurements were made in the SoCAB of the gas-phase concentrations of ammonia and nitric acid, the aerosol phase concentrations of sodium, ammonium, nitrate, sulfate, and chloride and their size distributions (Hering and Blumenthal, 1989; Lawson, 1990) as part of the Southern California Air Quality Study (SCAQS). This study contained the first simultaneous measurement of these quantities and the first carried out at multiple sites concurrently. Briefly, at nine B sites in the SoCAB, the gas- and aerosol-phase concentrations of ammonium and nitric acid were measured with annular denuders contained

in the SCAQS sampler (Hering and Blumenthal, 1989). SCAQS sampler data were collected by Aerovironment (Fitz and Zwicker, 1988; Chan and Durkee, 1989) and meteorological data were collected by the California Air Resources Board and the South Coast Air Quality Management District (Chan and Durkee, 1989). At four of these sites, Claremont, downtown Los Angeles, Riverside, and Long Beach, called the B+ sites, size distributions were measured using Berner impactors (Wall et al., 1988). These data were collected by the Air and Industrial Hygiene Laboratory of the California Department of Health Services (John et al., 1989ab, 1990). In this paper we explore the evidence for thermodynamic equilibrium among ammonia, nitric acid, and aerosol ammonium nitrate for the B+ sites during SCAQS.

In previous work we have predicted that under certain atmospheric conditions, the volatile inorganic components of atmospheric aerosol may not be in equilibrium with their gas-phase counterparts due to transport limitations, so that under such conditions mass transport between the gas and aerosol phases may have to be modeled, explicitly. We also predicted that even if the aerosol is in equilibrium with the gas phase, the size distribution of the volatile inorganic components of atmospheric aerosols often cannot be uniquely determined from thermodynamic considerations alone, and thus mass transport usually has to be included to determine the size distribution of the volatile inorganic components of atmospheric aerosols (Wexler and Seinfeld, 1990). In a subsequent work, we developed a transport model of atmospheric aerosols that assumes the aerosol particles are in internal equilibrium to predict their surface partial pressures of ammonia and nitric acid, and explicitly models transport between the gas and aerosol phases. In that work we compared the predictions of the model to 1) laboratory measurements and 2) the predictions of other aerosol equilibrium models (Wexler and Seinfeld, 1991). The dynamics of the departure from equilibrium has also been examined by Harrison and MacKenzie

(1990), who tested their hypothesis of a kinetically-limited departure from equilibrium with a model of gas-to-particle transport and surface reaction processes.

The purpose of the present study is to analyze the data from the four SCAQS B+ sites, identify departures from equilibrium, and examine possible physical and chemical causes for these departures. We first discuss the meteorological data and how they affect the equilibrium calculation. Then we proceed to the calculation of the time constant that governs equilibration due to transport between the gas and aerosol phases. Next we explore the departure from equilibrium between the gas and aerosol phases by examining gas-phase and PM2.5 aerosol-phase data. Then we explore how particles of different size and composition depart from equilibrium with each other. Finally we discuss the implications of our findings to the behavior of atmospheric aerosols.

DEPENDENCE OF AMMONIUM NITRATE EQUILIBRIUM ON METEOROLOGICAL CONDITIONS

In this section we first discuss the dependence of the ammonium nitrate equilibrium constant on ambient meteorological conditions, and then we select temperature and relative humidity values representative of the ambient conditions during the gas and aerosol measurements. Atmospheric aerosols may exist in either the solid or aqueous phases. At relative humidities below the deliquescence point, the particles exist in the solid phase, and above this point the particles exist in a mixed solid-aqueous or purely aqueous form. This deliquescence point is dependent on the temperature of the aerosol particles (Wexler and Seinfeld, 1991). The ammonium nitrate equilibrium constant between the solid and gas phases is dependent on the ambient temperature, such that at higher temperatures, the equilibrium ammonium nitrate gas-phase concentration is increased over that at lower temperatures. The ammonium nitrate equilibrium constant between the aqueous and gas phase

is dependent on both the ambient temperature and relative humidity. Increases in temperature increase the equilibrium gas-phase ammonium nitrate concentration, just as in the case of a solid-phase aerosol. Increases in relative humidity increase the water content of the aerosol, thereby decreasing the ammonium nitrate molality and the equilibrium gas-phase concentration. Since the ammonium nitrate equilibrium is dependent on both the ambient temperature and relative humidity, care must be taken when selecting the appropriate values of these parameters for analysis of aerosol data.

The values of temperature and relative humidity for the data we will consider are given in columns 3 and 4 of Tables 1-5. These values are those reported by the California Air Resources Board for the times and dates indicated in columns 1 and 2. The times were chosen to lie in the middle of the sampling periods (Hering and Blumenthal, 1989; John et al., 1990). Although the meteorological data sets for downtown Los Angeles and Claremont were complete, there were missing relative humidity data for Long Beach and missing relative humidity and temperature data for Riverside. Data obtained from the National Oceanic and Atmospheric Administration for Long Beach airport (NOAA, 1987) were used to complete the Long Beach data, whereas data from the South Coast Air Quality Management District were used to complete the Riverside data.

During sampling periods with constant temperature and relative humidity, the values in Tables 1-5 are representative of the ambient conditions, but during sampling periods when the temperature or relative humidity changes, these values may not be representative of the ambient conditions. Since the equilibrium between ammonia and nitric acid in the gas phase and ammonium nitrate in the aerosol phase is dependent on the ambient temperature and relative humidity, any inherent uncertainty in these measurements, combined with any uncertainty due to changes

Table 1
Indicators of Ammonium Nitrate Equilibrium for Claremont, CA

Date (1987)	Hour	Temp. [C]	R.H. [%]	PPP_m [ppb^2]	PPP_p [ppb^2]	τ_∞ [hours]	C_{an}
6/19	04	13.0	77	0.57	1.13	--	--
6/19	08	19.1	59	1.57	12.7	0.04	0.76
6/19	12	25.7	36	13.8	68.3	0.05	0.74
6/19	16	23.9	44	11.4	43.6	0.07	0.54
6/19	21	15.9	71	3.77	3.27	0.05	0.63
6/24	04	13.9	84	0.39	0.94	--	--
6/24	08	20.3	65	0.28	12.8	0.03	0.85
6/24	12	27.6	44	6.72	109	0.05	0.76
6/24	16	27.2	46	21.2	109	0.05	0.53
6/24	21	16.9	80	1.73	2.20	0.06	0.75
6/25	04	15.8	82	0.12	1.62	--	--
6/25	08	22.9	60	2.50	32.1	0.04	0.83
6/25	12	29.2	41	23.7	161	0.03	0.84
6/25	16	26.9	46	34.6	92.0	0.07	0.61
6/25	21	19.0	72	3.43	5.63	0.07	0.67
7/13	04	15.5	63	0.53	2.09	--	--
7/13	08	22.9	52	1.07	33.8	0.05	0.78
7/13	12	29.1	35	28.6	157	0.05	0.78
7/13	16	27.4	40	34.2	104	0.07	0.57
7/13	21	18.5	68	1.90	5.67	0.16	0.53
7/14	04	14.8	83	0.27	1.00	--	--
7/14	08	21.4	63	3.55	16.3	0.05	0.80
7/14	12	28.7	41	--	142	0.06	0.79
7/14	16	28.9	42	46.0	142	0.06	0.53
7/14	21	17.1	80	3.20	2.03	0.07	0.73
7/15	04	15.7	84	0.43	1.08	--	--
7/15	08	19.1	73	1.59	5.26	0.05	0.81
7/15	12	24.3	57	3.79	38.9	0.07	0.76
7/15	16	25.7	53	5.77	68.3	0.06	0.77
7/15	21	17.2	80	2.08	2.32	0.06	0.87

Table 1 (continued)
Indicators of Ammonium Nitrate Equilibrium for Claremont, CA

Date (1987)	Hour	Temp. [C]	R.H. [%]	PPP_m [ppb^2]	PPP_p [ppb^2]	τ_∞ [hours]	C_{an}
8/27	04	14.9	80	0.03	1.44	--	--
8/27	08	22.5	58	--	30.6	0.05	0.76
8/27	12	31.7	32	17.6	294	0.03	0.84
8/27	16	27.3	45	46.0	101	0.07	0.63
8/27	21	19.0	67	3.07	6.69	0.09	0.57
8/28	04	18.1	67	1.08	5.92	--	--
8/28	08	25.3	49	--	61.9	0.05	0.74
8/28	12	31.9	35	56.1	308	0.04	0.80
8/28	16	28.8	45	77.2	146	0.04	0.58
8/28	21	19.0	74	4.33	5.06	0.05	0.67
8/29	04	17.1	80	1.46	2.49	--	--
8/29	08	19.7	74	3.45	7.10	0.02	0.84
8/29	12	27.7	48	22.4	111	0.03	0.85
8/29	16	26.9	51	35.4	83.3	0.04	0.73
8/29	21	20.0	73	6.91	5.50	0.04	0.75
9/02	04	27.3	28	--	101	--	--
9/02	08	29.6	31	16.8	177	0.15	0.25
9/02	12	38.1	16	214.	1308	0.06	0.70
9/02	16	34.1	29	225.	518	0.15	0.24
9/02	21	23.3	51	29.4	37.3	0.11	0.48
9/03	04	19.5	63	2.16	9.68	--	--
9/03	08	25.3	51	--	61.9	0.05	0.73
9/03	12	31.5	37	54.9	280	0.03	0.81
9/03	16	25.4	55	24.2	51.0	0.10	0.44
9/03	21	17.2	83	0.22	1.70	0.11	0.58

Table 2
Indicators of Ammonium Nitrate Equilibrium for Long Beach, CA in the Summer

Date (1987)	Hour	Temp. [C]	R.H. [%]	PPP_m [ppb^2]	PPP_p [ppb^2]	τ_∞ [hours]	C_{an}
6/19	04	15.0	89	0.84	0.48	--	--
6/19	08	17.0	78	0.21	1.45	0.05	0.27
6/19	12	20.0	59	3.23	10.8	0.14	0.22
6/19	16	21.0	55	5.42	19.8	0.11	0.15
6/19	21	16.0	73	0.73	2.19	0.11	0.29
6/24	04	17.0	90	--	0.43	--	--
6/24	08	18.0	81	--	1.61	0.07	0.38
6/24	12	22.0	64	--	9.61	0.14	0.24
6/24	16	23.0	66	--	13.4	0.11	0.39
6/24	21	17.0	87	1.18	0.84	0.06	0.48
6/25	04	17.0	90	--	0.45	--	--
6/25	08	19.0	84	--	1.35	0.12	0.20
6/25	12	22.0	66	2.46	9.10	0.18	0.25
6/25	16	23.0	69	3.20	5.82	0.32	0.30
6/25	21	17.0	84	0.61	1.32	0.14	0.77
7/13	04	15.0	89	0.38	0.40	--	--
7/13	08	21.0	76	1.24	7.88	0.05	0.75
7/13	12	24.0	49	11.3	44.7	0.08	0.57
7/13	16	23.0	51	7.40	34.7	0.10	0.22
7/13	21	17.0	87	--	--	0.15	0.25
7/14	04	17.0	88	0.11	0.43	--	--
7/14	08	18.0	84	--	0.76	0.11	0.20
7/14	12	23.0	66	4.47	7.59	0.08	0.28
7/14	16	22.0	56	7.71	19.0	0.08	0.22
7/14	21	18.0	81	0.19	1.25	0.15	0.36
7/15	04	17.0	98	--	--	--	--
7/15	08	18.0	87	--	0.54	0.08	0.36
7/15	12	19.0	78	--	0.12	0.24	0.18
7/15	16	20.0	73	0.38	0.72	0.24	0.49
7/15	21	18.0	87	--	0.24	0.24	0.22

Table 2 (continued)
Indicators of Ammonium Nitrate Equilibrium for Long Beach, CA in the Summer

Date (1987)	Hour	Temp. [C]	R.H. [%]	PPP_m [ppb^2]	PPP_p [ppb^2]	τ_∞ [hours]	C_{an}
8/27	04	16.0	92	0.32	0.37	--	--
8/27	08	20.0	81	0.78	4.26	0.05	0.66
8/27	12	25.0	47	--	57.4	0.07	0.49
8/27	16	21.0	58	6.59	13.1	0.15	0.28
8/27	21	18.0	81	0.29	1.70	0.10	0.40
8/28	04	17.0	96	--	0.16	--	--
8/28	08	19.0	84	3.08	2.25	0.03	0.64
8/28	12	24.0	62	2.96	19.7	0.04	0.43
8/28	16	23.0	56	5.47	23.6	0.09	0.19
8/28	21	18.0	87	1.08	0.97	0.09	0.31
8/29	04	18.0	90	0.07	0.59	--	--
8/29	08	18.0	90	0.69	0.75	0.04	0.46
8/29	12	21.0	69	--	1.74	0.09	0.12
8/29	16	22.0	71	4.63	6.74	0.13	0.05
8/29	21	18.0	81	2.07	1.39	0.14	0.39
9/02	04	20.0	99	0.24	0.02	--	--
9/02	08	27.0	99	4.27	0.16	0.01	0.49
9/02	12	33.0	68	109.	169.	0.02	0.67
9/02	16	28.0	68	34.0	32.7	0.07	0.18
9/02	21	20.0	97	4.98	0.15	0.06	0.29
9/03	04	19.0	97	0.66	0.12	--	--
9/03	08	22.0	92	--	2.20	0.09	0.24
9/03	12	22.0	61	2.24	10.8	0.12	0.09
9/03	16	21.0	69	4.12	3.66	0.18	0.03
9/03	21	19.0	88	2.94	0.95	0.20	0.06

Table 3
Indicators of Ammonium Nitrate Equilibrium for Riverside, CA

Date (1987)	Hour	Temp. [C]	R.H. [%]	PPP_m [ppb^2]	PPP_p [ppb^2]	τ_∞ [hours]	C_{an}
6/19	04	13.3	82	4.40	0.97	--	--
6/19	08	20.0	58	4.41	12.8	0.03	0.76
6/19	12	27.7	35	--	--	0.02	0.85
6/19	16	25.6	36	42.9	66.7	0.04	0.73
6/19	21	16.7	70	22.3	4.51	0.04	0.56
6/24	04	15.0	85	15.7	1.23	--	--
6/24	08	20.0	70	--	9.24	0.02	0.78
6/24	12	30.6	38	108.	226.	0.01	0.93
6/24	16	28.3	42	--	129.	0.03	0.77
6/24	21	18.3	79	29.9	4.01	0.02	0.77
6/25	04	16.1	85	4.76	1.56	--	--
6/25	08	25.0	58	27.5	57.4	0.02	0.87
6/25	12	31.7	35	229.	294.	0.01	0.92
6/25	16	28.3	36	141.	129.	0.05	0.82
6/25	21	20.6	67	8.97	12.4	0.03	0.78
7/13	04	15.0	81	20.4	1.59	--	--
7/13	08	25.0	46	121.	57.4	0.02	0.87
7/13	12	32.2	30	136.	331.	0.02	0.92
7/13	16	29.4	38	113.	169.	0.02	0.89
7/13	21	21.1	57	43.5	21.4	0.06	0.75
7/14	04	15.0	83	10.0	1.16	--	--
7/14	08	23.3	56	61.8	37.5	0.04	0.83
7/14	12	32.2	34	117.	331.	0.02	0.92
7/14	16	30.6	39	44.5	226.	0.03	0.88
7/14	21	18.3	76	20.7	4.28	0.03	0.86
7/15	04	16.1	86	0.60	1.26	--	--
7/15	08	19.4	77	6.45	5.35	0.02	0.88
7/15	12	27.8	47	7.04	114.	0.02	0.91
7/15	16	27.8	47	15.6	114.	0.03	0.93
7/15	21	18.3	76	0.64	4.29	0.03	0.89

Table 3 (continued)
Indicators of Ammonium Nitrate Equilibrium for Riverside, CA

Date (1987)	Hour	Temp. [C]	R.H. [%]	PPP_m [ppb^2]	PPP_p [ppb^2]	τ_∞ [hours]	C_{an}
8/27	04	14.4	89	31.1	0.66	--	--
8/27	08	22.2	64	14.2	22.2	0.01	0.81
8/27	12	34.4	27	300.	556.	0.01	0.94
8/27	16	28.9	40	243.	150.	0.02	0.89
8/27	21	20.0	68	9.72	10.5	0.02	0.78
8/28	04	15.6	84	2.03	1.51	--	--
8/28	08	23.9	58	34.4	43.6	0.02	0.79
8/28	12	35.6	27	45.7	736.	0.01	0.93
8/28	16	29.4	44	38.5	169.	0.02	0.89
8/28	21	20.0	76	25.2	7.01	0.01	0.88
8/29	04	16.1	88	0.04	1.14	--	--
8/29	08	22.2	71	--	16.0	0.01	0.89
8/29	12	29.4	44	47.6	169.	0.02	0.93
8/29	16	28.3	41	91.4	129.	0.02	0.90
8/29	21	21.7	71	13.1	13.2	0.02	0.79
9/02	04	22.2	46	7.75	--	--	--
9/02	08	33.3	31	13.0	182.	0.12	0.22
9/02	12	38.3	16	20.3	2034	0.26	0.08
9/02	16	36.1	29	9.71	826.	0.22	0.32
9/02	21	25.6	51	7.68	66.7	0.03	0.79
9/03	04	18.3	81	--	3.31	--	--
9/03	08	26.7	51	6.38	87.5	0.04	0.63
9/03	12	34.4	37	110.	556.	0.02	0.86
9/03	16	26.7	53	74.0	87.5	0.04	0.81
9/03	21	18.9	81	6.13	3.48	0.05	0.70

Table 4
Indicators of Ammonium Nitrate Equilibrium for downtown Los Angeles, CA

Date (1987)	Hour	Temp. [C]	R.H. [%]	PPP_m [ppb^2]	PPP_p [ppb^2]	τ_∞ [hours]	C_{an}
11/11	04	15.6	39	1.88	5.08	--	--
11/11	08	20.6	32	7.02	18.8	0.17	--
11/11	12	27.8	20	39.3	114.	0.12	0.26
11/11	16	23.3	28	24.8	37.5	0.05	0.73
11/11	21	17.2	40	11.1	7.77	0.11	0.72
11/12	04	13.9	47	0.66	3.22	--	--
11/12	08	19.4	35	11.5	13.8	0.07	0.70
11/12	12	26.1	27	27.6	75.5	0.02	0.95
11/12	16	20.0	41	15.8	16.1	0.02	0.89
11/12	21	15.6	55	--	5.08	0.05	0.87
11/13	04	13.9	64	6.05	2.94	--	--
11/13	08	15.6	58	--	5.08	0.02	0.95
11/13	12	17.8	51	6.96	9.10	0.02	0.91
11/13	16	16.7	56	4.92	6.81	0.04	0.74
11/13	21	15.0	64	1.07	3.63	0.10	0.74
12/03	04	10.0	54	0.75	1.10	--	--
12/03	08	13.9	47	--	3.22	0.02	0.96
12/03	12	21.7	27	32.5	24.9	0.02	0.95
12/03	16	16.1	54	11.7	5.80	0.01	0.92
12/03	21	12.8	59	0.20	2.39	0.03	0.92
12/10	04	12.2	48	--	2.03	--	--
12/10	08	16.1	42	0.85	5.80	0.06	0.87
12/10	12	24.4	30	50.1	47.8	0.03	0.93
12/10	16	18.9	40	18.0	12.1	0.03	0.87
12/10	21	15.0	49	6.31	4.33	0.04	0.89
12/11	04	10.6	57	--	1.30	--	--
12/11	08	15.0	47	5.72	4.33	0.03	0.93
12/11	12	22.8	33	30.4	33.0	0.01	0.93
12/11	16	17.8	49	5.30	9.10	0.01	0.93
12/11	21	14.4	53	1.91	3.68	0.02	0.93

Table 5
Indicators of Ammonium Nitrate Equilibrium for Long Beach, CA in the Winter

Date (1987)	Hour	Temp. [C]	R.H. [%]	PPP_m [ppb^2]	PPP_g [ppb^2]	τ_∞ [hours]	C_{an}
11/11	04	15.0	62	2.97	4.11	--	--
11/11	08	20.0	47	5.77	16.1	0.07	0.77
11/11	12	29.0	25	29.2	153.	0.05	0.89
11/11	16	24.0	35	25.2	44.7	0.04	0.83
11/11	21	18.0	64	4.93	7.87	0.05	0.80
11/12	04	13.0	75	1.40	--	--	--
11/12	08	18.0	61	3.54	9.59	0.03	0.90
11/12	12	25.0	46	30.7	57.4	0.02	0.89
11/12	16	21.0	63	10.2	17.9	0.02	0.84
11/12	21	17.0	85	1.68	1.72	0.03	0.87
11/13	04	17.0	90	4.07	1.04	--	--
11/13	08	17.0	80	--	3.02	0.01	0.89
11/13	12	19.0	61	3.97	10.1	0.08	0.48
11/13	16	18.0	70	2.00	4.06	0.13	0.32
11/13	21	18.0	76	0.97	2.89	0.12	0.47
12/03	04	9.0	95	--	--	--	--
12/03	08	11.0	90	3.55	0.27	0.00	0.94
12/03	12	19.0	50	2.77	12.4	0.01	0.92
12/03	16	16.0	79	3.17	2.57	0.00	0.91
12/03	21	13.0	88	1.06	0.56	0.01	0.89
12/10	04	10.0	83	0.97	0.47	--	--
12/10	08	13.0	67	11.0	2.42	0.01	0.91
12/10	12	23.0	35	35.3	34.7	0.01	0.94
12/10	16	19.0	53	17.7	12.4	0.02	0.81
12/10	21	13.0	83	1.02	0.89	0.05	0.84
12/11	04	16.0	92	--	0.59	--	--
12/11	08	14.0	90	1.92	0.53	0.02	0.97
12/11	12	19.0	64	10.8	11.0	0.01	0.93
12/11	16	17.0	69	4.22	5.40	0.01	0.94
12/11	21	12.0	88	1.00	0.39	0.01	0.94

in these quantities during the sampling period, will lead to uncertainties in our assessment of the departure from equilibrium. The degree of uncertainty in our determination of the departure from equilibrium that is due to the uncertainty in the meteorological data will be discussed in more detail in a subsequent section.

TIME CONSTANT FOR EQUILIBRATION OF NH_4NO_3

For ammonium nitrate equilibrium to hold, transport between the gas and aerosol phases must be fast compared to the time scales that characterize changes in the ambient temperature, relative humidity and gas-phase concentrations of ammonia and nitric acid (Wexler and Seinfeld, 1990). There are two distinct physical processes that lead to equilibration between the gas and aerosol phases, and these processes have different time scales. In this section we describe the time scales that govern equilibration between the gas and aerosol phases and evaluate them from data collected during SCAQS.

Let us consider an atmosphere containing gas-phase ammonia and nitric acid and aqueous or solid aerosol particles that contain ammonium nitrate and possibly other salts. If the ambient gas-phase ammonia and nitric acid concentrations exceed those at the particle surface, ammonia and nitric acid diffuse towards and condense on the particles. This diffusive transport between the two phases eventually leads to their equilibration because of depletion of ammonia and nitric acid from the gas phase, and resulting decreases in their gas-phase concentrations.

Transport from the gas to the aerosol phase also increases the amount of aerosol ammonia and nitric acid. These increases in the aerosol mass of ammonium nitrate lead to equilibration if the particle-surface gas-phase concentrations of these species also increase. For instance, if the aerosol mass of water remains constant during condensation of ammonia and nitric acid on an aqueous phase particle, the aerosol phase ammonium nitrate molality increases during condensation, which is reflected

by an increase in the surface partial pressures. This change in surface partial pressures then hastens the process of equilibration. However, increases in the aerosol mass of ammonium nitrate do not always lead to increases in the surface partial pressures. For instance, if the aerosol particles are solid, their surface partial pressures of ammonium nitrate are constant, in which case equilibration cannot take place simply as a result of changes in the aerosol mass of ammonium nitrate.

Thus diffusive transport between the gas and aerosol phases eventually leads to their equilibration, and two time scales govern the approach to equilibrium. One time scale, τ_∞, characterizes the approach due to changes in the gas-phase concentrations, and the other time scale, τ_p, characterizes the approach due to changes in the aerosol-phase concentrations. These equilibration time scales are not necessarily the same because during condensation the partial pressures at the particle surface may change slower or faster than the ambient partial pressures.

What is the overall time scale for equilibration between the gas and aerosol phases? Consider the gas phase and the aerosol phase to be two compartments that may exchange ammonium nitrate. For two coupled compartments, the overall time scale for equilibration, τ, is the harmonic mean of the individual time scales, which for the current case is $\tau = (1/\tau_\infty + 1/\tau_p)^{-1}$. Thus the shorter time scale governs the equilibration process. If one of the time scales is infinitely long, such as τ_p in the case of a solid aerosol, the overall time scale is equal to the finite one, in this case τ_∞.

For aerosol particles containing solid ammonium nitrate, τ_p is infinitely long and thus irrelevant to the equilibration process, since a change in the mass of solid aerosol ammonium nitrate does not lead to a change in the surface equilibrium concentration of the vapor-phase species. For aqueous aerosol particles, τ_p is also not relevant if ammonium nitrate is osmotically dominant, that is, if the ammonium

nitrate concentration greatly exceeds those of the other electrolytes. When a particle is osmotically dominated by ammonium nitrate, condensation of ammonium nitrate on the particle is accompanied by condensation of water to maintain the water activity in the particle equal to the ambient relative humidity. This condensation of water causes the ammonium nitrate molality to remain relatively constant as condensation ensues. Since the molality does not change substantially for these particles, neither does the surface gas-phase concentration. Thus τ_p is large or irrelevant for particles osmotically dominated by ammonium nitrate, because the surface concentrations cannot change and equilibrate with the ambient concentrations, and equilibration only takes place when the gas-phase concentrations decline to the point where they are equal to those at the particle surface.

When the ammonium nitrate is osmotically benign, that is, when its aerosol concentration is much less than that of other electrolytes, transport of ammonium nitrate to the particle does not affect the aerosol water content. In this case, changes in aerosol ammonium nitrate concentration are directly reflected as changes in molality, which are then directly reflected as changes in surface partial pressure. Particles osmotically benign with respect to ammonium nitrate, therefore, have shorter equilibration time scales than those whose water content increases significantly during condensation. For osmotically benign particles, the time scale changes with the aerosol mass of water. If the aerosol mass of water is large, the aerosol compartment is large, and a significant gas-to-particle conversion is needed to alter the particle ammonium nitrate molality and the surface partial pressures. Thus for osmotically benign particles, a large aerosol water content leads to a long time scale, and a small aerosol water content is characterized by a short time scale.

In summary, two time scales exist for equilibration. Diffusive transport between the gas and aerosol phases changes the amount of ammonia and nitric acid in

each phase with the resulting change in ambient concentrations giving the gas-phase equilibration time scale τ_∞. Change in particle surface concentrations due to changes in aerosol mass of ammonium nitrate from the transport of ammonia and nitric acid between the phases leads to the particle-phase equilibration time scale τ_p.

In general, atmospheric aerosol particles have different sizes and compositions. Consider n kinds of particles each of uniform size and composition. In this case there are n time scales $\tau_{p,i}$, $i = 1, n$, associated with equilibration of each kind of aerosol particle due to changes in its surface partial pressures, along with the single time scale τ_∞ associated with equilibration due to changes in the ambient gas-phase concentrations. Just as before, the time scale τ_∞ characterizes the change in ambient concentrations due to the overall transport between the gas and aerosol phases. But in this case there is no single τ_p. Instead there are n different $\tau_{p,i}$ values which cannot be combined into an appropriate single τ_p value.

Since there are numerous time scales, $\tau_{p,i}$, and under typical conditions in the SoCAB, 1) the relative humidity is often low enough to result in solid aerosol particles and 2) there is considerably more aerosol nitrate than sulfate, so the time constants $\tau_{p,i}$ are usually large compared to τ_∞, we will concentrate our analysis here on the time constant τ_∞. We wish to evaluate τ_∞ for the conditions during SCAQS, but to do so we must first express it in terms of the measured quantities. The rate of change of the ambient gas-phase concentration, C_∞, of a single species due to its transport between the gas and aerosol phases can be written as

$$\frac{dC_\infty}{dt} = \int_0^\infty n(R_p) J(R_p) dR_p, \tag{1}$$

where $n(R_p)$ is the number distribution of particles [m^{-4}] and $J(R_p)$ is the flux [mol s^{-1}] of the gas-phase species to or from a single particle of radius R_p [m]. An

expression for the single-particle flux is

$$J(R_p) = \frac{4\pi R_p D(C_p - C_\infty)}{(1 + D/\alpha\bar{c}R_p)}, \tag{2}$$

where C_p is the particle-surface gas-phase concentration, D is the molecular diffusivity, $\bar{c}$ is the mean molecular speed, and α is the particle-surface accommodation coefficient of the condensing species (Wexler and Seinfeld, 1990). We have shown in previous work that, for ammonia and nitric acid condensing on atmospheric particles, the quantity $D/\bar{c}$ can be approximated by λ, the mean free path of air molecules in air (Wexler and Seinfeld, 1990). Since the time constant τ_∞ is defined by $\tau_\infty^{-1} = \frac{1}{C_\infty}\frac{dC_\infty}{dt}$, we can combine this relation with Equations (1) and (2) to obtain

$$\tau_\infty^{-1} = 4\pi D \int_0^\infty \frac{n(R_p)R_p dR_p}{1 + \frac{\lambda}{\alpha R_p}}. \tag{3}$$

If the particle number distribution is available, τ_∞ may be estimated using Equation (3). If the particle mass distribution is available, the number distribution, $n(R_p)$, can be related to the mass distribution, $m(R_p)$, by $m(R_p) = 4/3\pi R_p^3 \rho_p n(R_p)$, where ρ_p is the particle density, to get

$$\tau_\infty^{-1} = 3D \int_0^\infty \frac{m(R_p)dR_p}{(1 + \frac{\lambda}{\alpha R_p})R_p^2 \rho_p}, \tag{4}$$

but since the mass distributions are provided in logarithmic form (John et al., 1989b), the identity $m(R_p)dR_p = m(\log_{10} R_p)d\log_{10} R_p = m(\log_{10} R_p)dR_p/2.303R_p$ yields the desired relation

$$\tau_\infty^{-1} = \frac{3D}{2.303} \int_0^\infty \frac{m(\log_{10} R_p)dR_p}{(1 + \frac{\lambda}{\alpha R_p})R_p^3 \rho_p}. \tag{5}$$

Either Equation (3) or (5) can be used to estimate τ_∞, since both number distributions (Chan and Durkee, 1989) and mass distributions of the inorganic species

(John et al., 1990) were measured during SCAQS. But both of these size distributions introduce different uncertainties into the estimate of τ_∞. Let us now examine the likely uncertainties caused by using each of these distributions.

As has been shown during SCAQS (McMurry and Stolzenburg, 1989), the aerosol is hygroscopically externally mixed, that is, a fraction of the particles of a given size are hydrophilic and the rest are hydrophobic. Since ammonium nitrate is very hygroscopic, we conclude that ammonium nitrate is not transported to a hydrophobic fraction of the particles and use of the overall number distributions to estimate τ_∞ tends to overestimate the surface area available for transport, which results in an underestimate of τ_∞ by at most a factor of 2 (McMurry and Stolzenburg, 1989).

Another consideration is that the hygroscopic aerosol particles contain non-ionic components such as elemental carbon and organics. The size distributions reported by John and co-workers (John et al., 1989b) do not include the non-ionic components, so use of these size distributions tend to underestimate m, thereby overestimating the value of τ_∞. Since both forms of size distribution data are difficult to relate to the calculation of τ_∞, we chose to use the data of John and co-workers (John et al., 1989a, 1989b, 1990) in Equation (5), since it will be used in other calculations in this work. Since the inorganics typically comprise about 1/3 of the total aerosol mass, this choice tends to result in overpredictions of τ_∞ by roughly a factor of 3.

To complete the evaluation of Equation (5), we must estimate values for the rest of the parameters on the right-hand side. Of these parameters, the most difficult one to estimate is the accommodation coefficient, α. The range of accommodation coefficient values for ammonia and nitric acid is probably $0.001 < \alpha < 1$ depending on the phase state of the particle and on the presence of organic surface-active

agents (Gill et al., 1983; Wexler and Seinfeld, 1990), and since the λ/R_p values for these particles are not much less than unity, uncertainties in α are reflected as uncertainties in τ_∞. For the calculations here, we have assumed $\alpha = 0.1$ which may tend to underpredict the value of τ_∞, since α may be one or two orders of magnitude smaller than 0.1. Due to the large uncertainty in α, it is not appropriate to compare the calculated values of τ_∞ to the values of other time scales of atmospheric relevance. Instead we will seek correlations between the values of τ_∞ and the values of other indicators of equilibrium. As long as the value of the accommodation coefficient α is constant, such correlations represent a valid approach to analyzing atmospheric data. In subsequent sections we will be concerned only with the relative values of τ_∞.

Column 7 of Tables 1–5 shows the values of the time constant, τ_∞, calculated with Equation (5) and assuming $D = 0.1$ cm^{2}s^{-1}, $\lambda = 0.065$ μm, $\rho_p = 1.3$ gm cm^{-3}, and $\alpha = 0.1$. The values of τ_∞ are generally in the range of 1 to 15 min. and since the inorganic aerosol measurements during SCAQS had sampling times in excess of three hours, it would appear that a departure from equilibrium may not be discernable. But if our estimates of the time constants are too short due to our choice of an accommodation coefficient of 0.1, we may be able to observe a departure from equilibrium. The values of τ_∞ in Tables 1–5 will be compared to various indicators of equilibrium in subsequent sections.

EQUILIBRIUM BETWEEN THE GAS AND AEROSOL PHASES

In this section we compare the measured gas-phase ammonium nitrate partial pressure product (PPP) to that calculated from SCAQS PM2.5 aerosol composition measurements at the B+ sites. For aerosol ammonium nitrate to be in equilibrium with gas-phase ammonia and nitric acid, the partial pressure product of the gas-phase species must be the same as that calculated at the particle surface from the

particle composition and the appropriate phase equilibrium relations. Columns 5 and 6 of Tables 1–5 list, respectively, PPP_m, the measured partial pressure product of ambient gas-phase ammonium nitrate, and PPP_p, the partial pressure product predicted using a state-of-the-art aerosol equilibrium program, AIM (Wexler and Seinfeld, 1991). Figure 1 is a scatter plot of these partial pressure product data. Missing PM2.5 aerosol composition data were completed using the data of John et al.(1990). The solid line signifies perfect agreement between the two values, and the dashed lines signify disagreement by a factor of 10 in each direction. The majority of the data lie within these bounds and the data are biased so that, on average, the partial pressure product predicted from the aerosol composition data is higher than observed.

The data span over 4 orders of magnitude and, although there is significant scatter, the data tend to cluster around the solid line that indicates equilibrium. Under ambient conditions when the aerosol is predicted to be a solid (designated by + and solid triangles) generally higher partial pressures are observed, whereas under ambient conditions when an aqueous phase aerosol is predicted (× and open triangles) generally lower partial pressures are observed, in agreement with expectations. The large scatter in this type of data has been observed by others (Doyle et al., 1979; Stelson et al., 1979; Cadle et al., 1982; Tanner, 1982; Hildeman et al., 1984; Allen et al., 1989). One possible explanation for the scatter is lack of equilibrium between the aerosol and gas phases. This and other physical and chemical causes for the scatter and bias in Figure 1 are examined qualitatively in subsequent sections.

Aerosol-Phase Measurements

In the SCAQS sampler, PM2.5 concentrations of ammonium and nitrate were

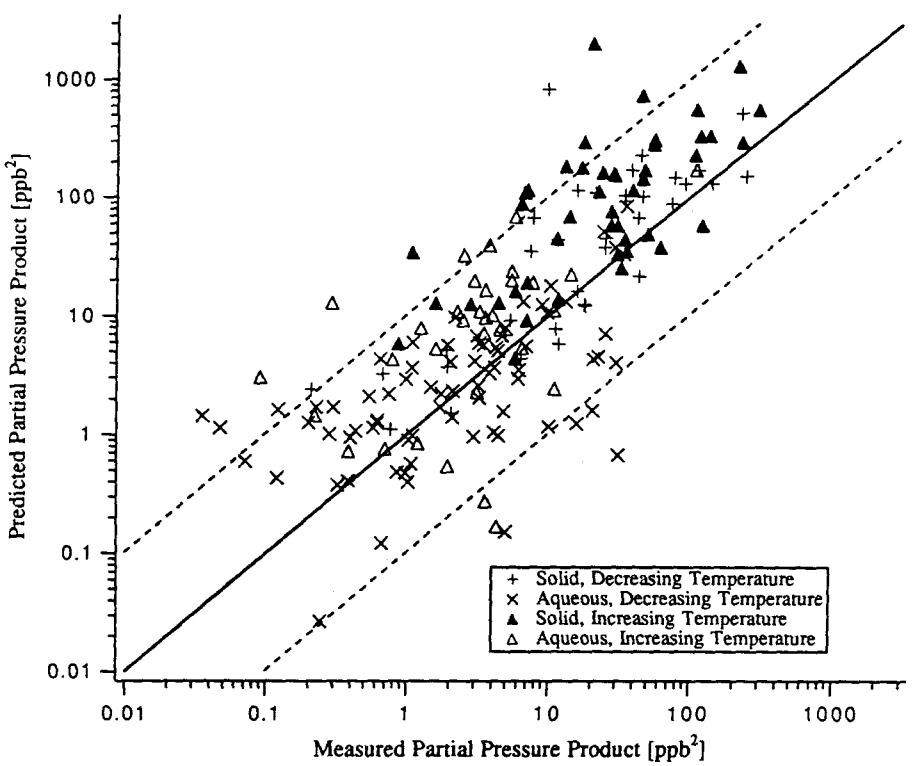

Figure 1. Comparison of the measured partial pressure product of ammonium nitrate and the partial pressure product predicted from ambient conditions and aerosol composition.

measured with an annular denuder and a denuder difference method, respectively, and the PM2.5 sulfate was collected on teflon filters. The sulfate was collected from a different PM2.5 cyclone than that used for the ammonium and nitrate measurements (Fitz and Zwicker, 1988). There are a number of potential sources of error in these measurements, and in this section, the effect of these errors on the calculation of PPP_p will be examined.

For solid particles that form NH_4NO_3(s), the partial pressure product is dependent solely on the ambient temperature, so the composition does not play a role as long as the gas-phase partial pressure product is high enough for NH_4NO_3(s) to form. Consequently, points were plotted in Figure 1 only when the aerosol phase concentrations of ammonium nitrate were significantly greater than zero. For aqueous phase particles osmotically dominated by ammonium nitrate (as is typical for the observations during SCAQS), moderate errors in the aerosol mass of ammonium nitrate do not substantially alter the molality of ammonium nitrate in the solution or the resulting partial pressure predictions, as discussed earlier. If the aerosol is not osmotically dominated by ammonium nitrate or if the errors are of a sufficient magnitude, PPP_p may have a substantial dependence on the measured aerosol ammonium, nitrate or sulfate mass.

At low aerosol nitrate values scatter in the data could be a result of proximity to the detection limit, since under this condition the filter blank values may be the same order as the collected values, or lack of ammonium nitrate in the aerosol phase. Figure 2 shows the ratio of predicted to measured partial pressure product versus mass of aerosol nitrate. The partial pressure product ratio is found to be independent of the aerosol nitrate mass and the scatter in the data is not significantly greater for the low nitrate values. Thus aerosol nitrate mass alone is neither a significant determinant of the partial pressure product, nor a significant factor

in the observed scatter in the data, and the two potential causes of scatter listed above do not appear to be significant.

Gas-Phase Measurements

During preliminary tests of the SCAQS sampler, a substantial coefficient of variation was observed in the gas-phase ammonia measurements (Fitz and Zwicker, 1988, p. 4-15) and this coefficient of variation was substantially larger than that of nitric acid. The magnitude of the coefficient of variation was partially attributed to the fact that the ambient ammonia concentrations present during the test sampling period were close to the detection limit of the ammonia annular denuder. Since the scatter about the solid line in Figure 1 shows a moderate increase with decreasing partial pressure, there is an indication that proximity of the gas-phase concentrations to the detection limit may increase data uncertainty. Some of the bias in the data may be due to loss of gas-phase ammonia or nitric acid to the cyclone, manifold, or tubing before collection, although tests of the apparatus prior to use during SCAQS indicated that only a few percent loss was to be expected (Fitz and Zwicker, 1988, p. 3-12 to 3-15).

Departure from Equilibrium

A possible explanation for the lack of agreement with the solid line in Figure 1 is departure from equilibrium. If departure from equilibrium is a cause of the disagreement in Figure 1 than for short values of τ_∞ we would expect PPP_p/PPP_m to cluster around unity, whereas at larger values of τ_∞ we might expect larger or smaller values in PPP_p/PPP_m due to greater departure from equilibrium. Figure 3 shows the ratio of the predicted partial pressure product to the observed partial pressure product versus the estimated values of τ_∞. Since the scatter appears to be larger at smaller values of τ_∞, there is no evidence for a departure from equilibrium.

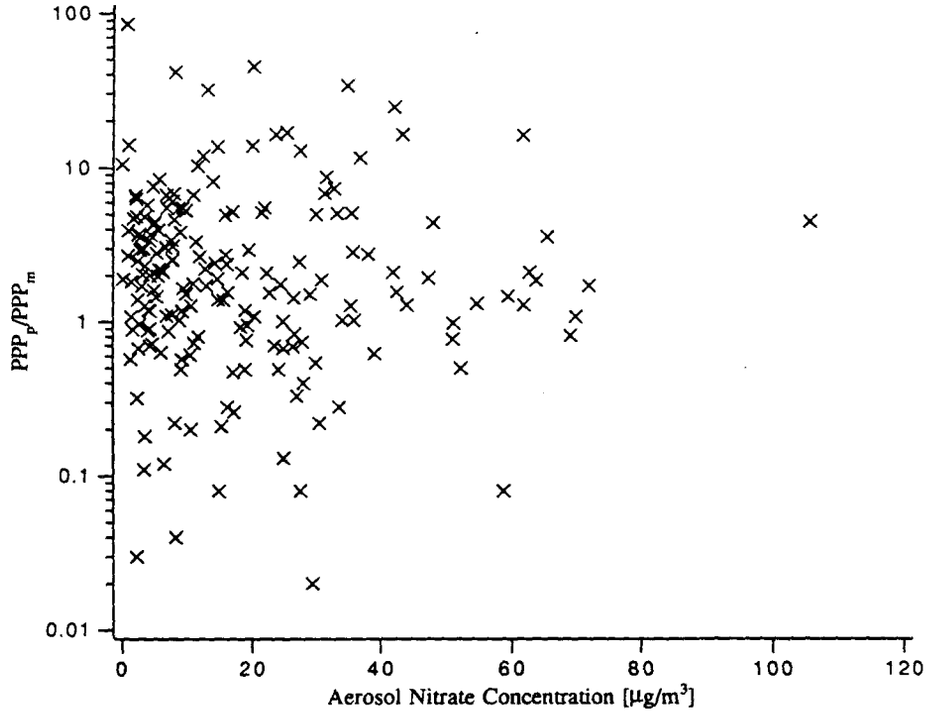

Figure 2. Ratio of predicted to measured partial pressure products as a function of the aerosol nitrate concentration.

In a subsequent section we present evidence for departure from equilibrium, but we are not able to discern it here.

Changes in Temperature and Relative Humidity during Collection

Over the three to four hour sample collection period typical during SCAQS, the ambient temperature and relative humidity often change. Increases in temperature typically result in decreases in relative humidity, which, for aqueous-phase aerosols, result in decreases in aerosol water content and concomitant increases in solute concentration. The increased temperature also has a direct effect on the ammonium nitrate equilibrium constant between gas and aqueous phases, serving to increase the ammonium nitrate vapor pressure. Thus increased ambient temperature increases the ammonium nitrate equilibrium constant both directly via changes in the equilibrium constant and indirectly via changes in relative humidity. For solid particles, temperature increases directly result in ammonium nitrate vapor pressure increases, via changes in the ammonium nitrate equilibrium constant between the gas and solid phases. These changes in ammonium nitrate vapor pressure over the course of the sampling periods may be the cause of the observed departure from the solid line in Figure 1.

In Figure 1 the triangular points designate samples collected during conditions of increasing ambient temperature, whereas the + and × points designate decreasing ambient temperature. The data collected during conditions of increasing temperature show slightly more bias than those collected during conditions of decreasing temperature, and the trend is more pronounced for aqueous-phase aerosols. These small trends may be due to mixing effects or departures from equilibrium, but there is insufficient evidence to select an explanation.

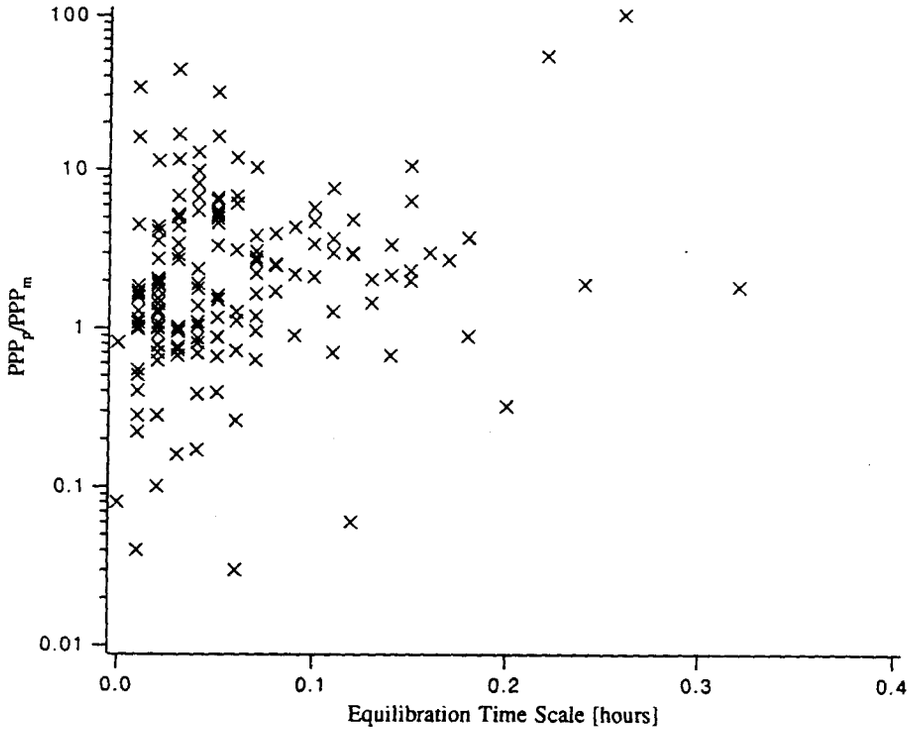

Figure 3. Ratio of predicted to measured partial pressure products as a function of the equilibration time scale τ_∞.

Mixed Solid Salts

The model that was used to predict the equilibrium partial pressure product corresponding to the measured aerosol compositions, AIM, is described by Wexler and Seinfeld (1991). This model does not consider mixed salts since the thermodynamic properties of these salts are not well known. Nevertheless, mixed ammonium nitrate – ammonium sulfate salts, such as $(NH_4)_2SO_4 \cdot 2NH_4NO_3$ and $(NH_4)_2SO_4 \cdot 3NH_4NO_3$, have been observed in atmospheric aerosols (Sturges et al., 1989), and the vapor pressure of ammonium nitrate over the mixed salts is less than over pure NH_4NO_3(s). If the ratios of nitrate to sulfate are such that all the ammonium nitrate is sequestered as one or more mixed salts, the model will overpredict the ammonium nitrate partial pressures. This overprediction provides a possible explanation for the bias in the data for the solid particle values in Figure 1. Since the thermodynamic properties of the mixed salts are not well known, we are not able to estimate the magnitude of this effect.

Aqueous Aerosol Mixing

In general, aerosol particles are expected to have a spectrum of compositions. The data of John et al. (1990) showed that the aerosol collected during SCAQS generally contained more sulfate in the smaller particles and more nitrate in the larger ones, and McMurry and Stolzenburg (1989) demonstrated that the aerosol is externally mixed in the particle diameter range 0.05 to 0.5 μm, even for particles of a similar size. Let us now examine how the observed deviation from equilibrium in the aqueous phase data may be due to the mixing of particles that occurs during sampling.

Assume for simplicity that we are sampling an aerosol containing particles with only two different compositions and that these two types of particles contain $M_{a,i}$

moles of ammonium, $M_{n,i}$ moles of nitrate, and W_i kilograms of water for particle compositions, $i = 1, 2$. If these two populations of particles are in equilibrium with gas-phase ammonia and nitric acid then

$$PPP_m = K_{an}\gamma_{an}^2 \frac{M_{a,1}M_{n,1}}{W_1^2} = K_{an}\gamma_{an}^2 \frac{M_{a,2}M_{n,2}}{W_2^2}, \tag{6}$$

where K_{an} is the equilibrium constant for aqueous ammonium nitrate and γ_{an} is the activity coefficient of ammonium nitrate. γ_{an} is a slowly varying function of the ionic strength, and since for atmospheric aerosols the ionic strength is primarily governed by the relative humidity and less so by the composition, we assume that the activity coefficients for the two types of particles are approximately the same.

Let us assume that upon mixing these two types of particles, the mixture is isolated from the environment so that the ammonium nitrate cannot evaporate. Although evaporation of ammonium nitrate may be a problem, depending on the apparatus employed, it has been demonstrated that both the SCAQS sampler (Fitz and Zwicker, 1988) and the Berner impactor (Wall et al., 1988) have limited evaporative losses.

We would like to compare the measured gas-phase partial pressure product with the partial pressure product inferred from the composition of the sample. In order to predict the ammonium nitrate partial pressure from the aerosol composition data, we must first predict the water content of the resulting mixture, W_{mix}. If the mixture is totally isolated from the environment then $W_{mix} = W_1 + W_2$. Using the ZSR relationship (Zdanovskii, 1948; Stokes and Robinson, 1966; Hanel and Zankl, 1979; Cohen et al., 1987; Pilinis and Seinfeld, 1987) we can show that if the water in the sample is allowed to equilibrate with atmospheric relative humidity, again the water content of the mixture is simply the sum of the individual water contents:

$$W_{tot} = \sum_j \frac{M_{tot,j}}{m_{0,j}(r.h.)}$$

$$= \sum_j \frac{M_{j,1}}{m_{0,j}(r.h.)} + \sum_j \frac{M_{j,2}}{m_{0,j}(r.h.)}$$
$$= W_1 + W_2, \tag{7}$$

where $m_{0,j}(r.h.)$ is the molality of species j that gives a solution of water activity $r.h.$ and $M_{j,i}$ are the moles of aerosol electrolyte j per m^3-air in particles of composition i. Thus the partial pressure product predicted from the composition of the collected sample is

$$PPP_p = K_{an}\gamma_{an}^2 \frac{(M_{a,1} + M_{a,2})(M_{n,1} + M_{n,2})}{(W_1 + W_2)^2}. \tag{8}$$

Combining Equations (6) and (8) and rearranging gives

$$\frac{PPP_p}{PPP_m} = 1 + (x + \frac{1}{x} - 2)\frac{W_1 W_2}{(W_1 + W_2)^2}, \tag{9}$$

where $x = \sqrt{\frac{M_{a,1}/M_{n,1}}{M_{a,2}/M_{n,2}}}$. The quantity $x + \frac{1}{x}$ has a minimum value of 2 when $x = 1$, in other words, when the two types of aerosol particles have the same ammonium to nitrate ratios, the mixing does not bias the calculated partial pressure product. At other x values, $x + \frac{1}{x}$ is greater than 2 so we find that the predicted partial pressure product always exceeds the measured partial pressure product when an external mixture is present,

$$\frac{PPP_p}{PPP_m} \geq 1. \tag{10}$$

This conclusion can be generalized to the mixing of any number of particles of differing ammonium nitrate compositions, such as would be found in a typical atmospheric sample.

Let us now try to estimate the magnitude of this effect. If sulfate is the other major ion in these aerosol particles, as is usually the case in Los Angeles, then charge balance gives

$$M_{a,i} \sim M_{n,i} + 2M_{s,i}, \tag{11}$$

where $M_{s,i}$ is the number of moles of sulfate in the aerosol of composition i. By assuming that all the nitrate is in solution as ammonium nitrate and all the sulfate as ammonium sulfate we can rewrite Equation (6) using Equation (7) as

$$\frac{PPP_m}{\gamma_{an}^2 K_{an}} = \frac{M_{a,i} M_{n,i}}{(M_{s,i}/m_{0,s} + M_{n,i}/m_{0,n})^2}. \tag{12}$$

By combining Equations (11) and (12) to eliminate $M_{s,i}$, we obtain

$$\frac{PPP_m}{\gamma_{an}^2 K_{an}} = \frac{M_{a,i}/M_{n,i}}{(\frac{1}{m_{0,n}} + \frac{1}{2m_{0,s}}(\frac{M_{a,i}}{M_{n,i}} - 1))^2}, \tag{13}$$

to find that for an aqueous ammonium nitrate – ammonium sulfate aerosol, the ratio $M_{a,i}/M_{n,i}$ is uniquely determined by the ammonium nitrate partial pressure product. Thus x is uniquely one for ammonium nitrate – ammonium sulfate aerosols in equilibrium with respect to gas-phase ammonia and nitric acid, and there should not be a significant bias due to mixing. Intuitively one would expect the quantity $M_{a,i}M_{n,i}$ to be determined by the partial pressure product, but since the water content of the particles also depends on the ionic components, the quantity determined by the partial pressure product is the ratio $M_{a,i}/M_{n,i}$.

If we now add one more degree of freedom, by allowing the aerosol to contain, say sodium, the next most prevalent ion in Los Angeles aerosols, then the ratio $M_{a,i}/M_{n,i}$ may differ for aerosols of different composition, depending on the mole fraction of sodium. At most locations in the SoCAB, sodium does not comprise a large portion of the ionic components of atmospheric aerosol (Eldering et al., 1990), especially in the PM2.5 aerosols examined here, so at these locations the ratio $M_{a,i}/M_{n,i}$ is determined by the partial pressure product alone. Long Beach is the closest site to the coast and thus is expected to have the highest aerosol sodium concencentrations of the SCAQS B sites. Figure 4 shows that the bias in the data from Long Beach is not noticeably different from that of the other sites.

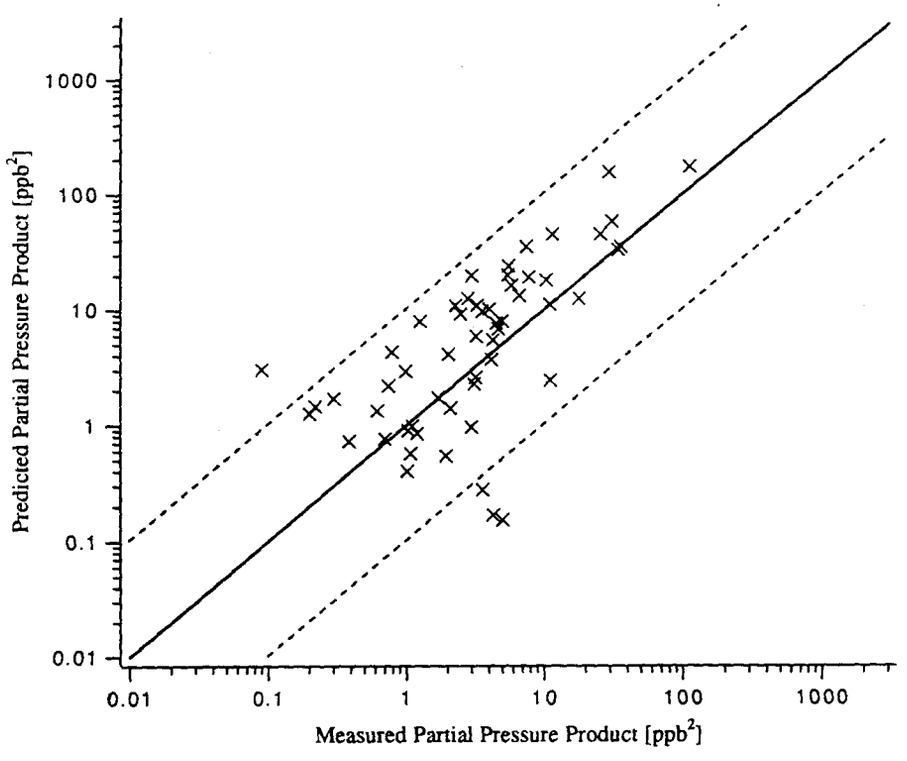

Figure 4. Comparison of the measured partial pressure product of ammonium nitrate and the partial pressure product predicted from ambient conditions and aerosol composition for Long Beach, CA.

Thus we conclude that if particles collected in the SoCAB are in equilibrium with gas-phase ammonium nitrate, but of different composition, they must have the same ratio $M_{a,i}/M_{n,i}$, and that mixtures of these particles are also in equilibrium with gas-phase ammonium nitrate. This fact is further employed in the next section where we examine equilibrium between particles of different size and composition.

Do the PM2.5 Data Support the Equilibrium Hypothesis?

When the measured and predicted partial pressure products were compared, a large scatter and some bias was found. Although some of the scatter may have been due to sampling error or simplifications used in the aerosol model AIM, a quantitative explanation for the scatter could not be found. Transport-limited departures from equilibrium are not supported by the data, since no correlation between PPP_p/PPP_m and τ_∞ was found. Since any correlation may have been obscured by scatter in the data caused by measurement artifacts, another approach to examining the lack of equilibrium is explored in the next section.

COINCIDENCE OF THE NITRATE AND AMMONIUM SIZE DISTRIBUTIONS

In the previous section we analyzed the PM2.5 inorganic data. Additional insight can be gained into the chemical and physical processes that govern the formation of these inorganic components by examining their size distributions. We showed in the previous section that 1) if a population of aqueous aerosol particles is in equilibrium with gas-phase ammonium nitrate and 2) if ammonium, nitrate, and sulfate make up the vast majority of the ionic components, as is usually observed in Los Angeles, then each particle has the same $M_{a,i}/M_{n,i}$ ratio. For a size distributed aerosol to be in equilibrium with respect to ammonium nitrate, the size distributions of ammonium and nitrate must be the same, since only then is the ratio $M_{a,i}/M_{n,i}$

independent of particle size. In order to obtain a quantitative measure of the degree of overlap of the ammonium and nitrate size distributions, let us define a coincidence factor, C_{an}, as

$$C_{an} = 1 - \frac{1}{2}\int_0^\infty \left| \frac{M_n(R_p)}{M_n^t} - \frac{M_a(R_p)}{M_a^t} \right| dR_p, \tag{14}$$

where $M_i(R_p)$ and $M_i^t = \int_0^\infty M_i(R_p)dR_p$ are the molar size distribution and total number of moles of nitrate, $i = n$, and ammonium, $i = a$. C_{an} is zero when the normalized size distributions do not overlap and unity when they coincide perfectly.

Column 8 of Tables 1-5 lists the coincidence factors derived from the inverted ammonium and nitrate distributions of John et al. (1990). We see that although there are many coincidence factors that approach unity, indicating equilibrium, there are also a substantial number of lower values that do not.

In the previous section we showed the absence of a correlation between τ_∞ and the ratio PPP_p/PPP_m. Is there a correlation between the values of τ_∞ and the coincidence factors? Figures 5-9 show the ammonium-nitrate coincidence factor plotted against the equilibration time scale τ_∞ for each of the sites. The lines are the linear best fits to the data. For all sites, when the estimated values of τ_∞ were short, the coincidence factors were high, and when they were long the coincidence factors were small. What are some of the implications of this finding?

When do Ammonium and Nitrate Have Different Size Distributions?

The estimated values of τ_∞ shown in Column 7 of Table 1-5 are all less than about 15 min. and values greater than about 5 min. correspond to the smallest coincidence factors. This 5 min. value does not necessarily indicate when equilibrium may be expected to hold. To estimate τ_∞ an accommodation coefficient value had to be assumed; the actual value may be one or two orders of magnitude lower than the 0.1 assumed depending on the effect of surface active organic compounds

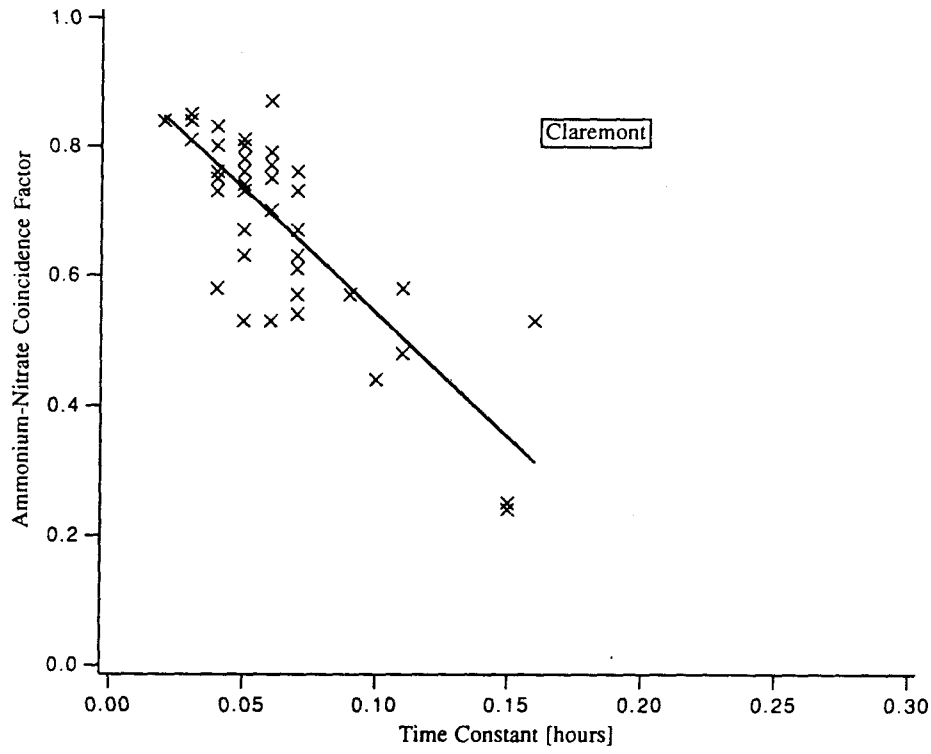

Figure 5. The ammonium nitrate coincidence factor as a function of the equilibration time scale τ_∞ for Claremont, CA.

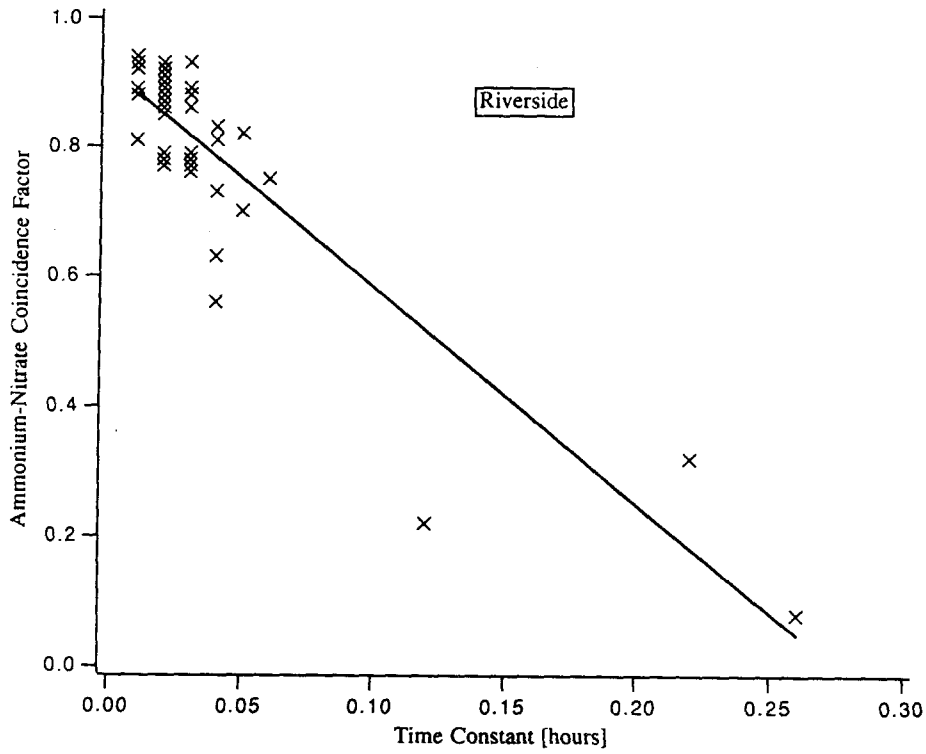

Figure 6. The ammonium nitrate coincidence factor as a function of the equilibration time scale τ_∞ for Riverside, CA.

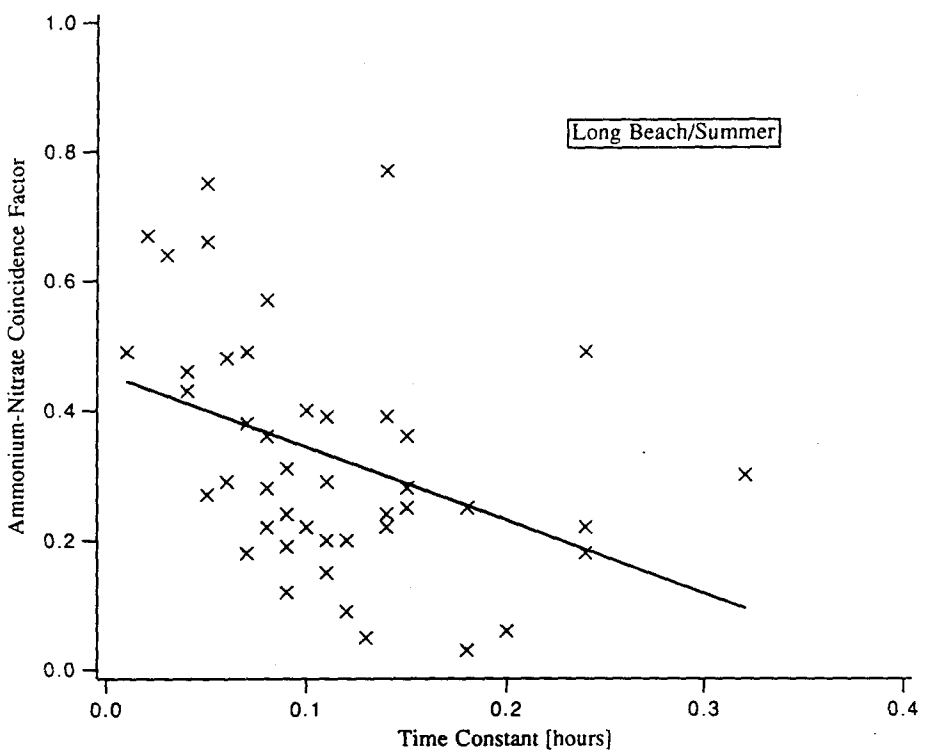

Figure 7. The ammonium nitrate coincidence factor as a function of the equilibration time scale τ_∞ for Long Beach, CA in the summer.

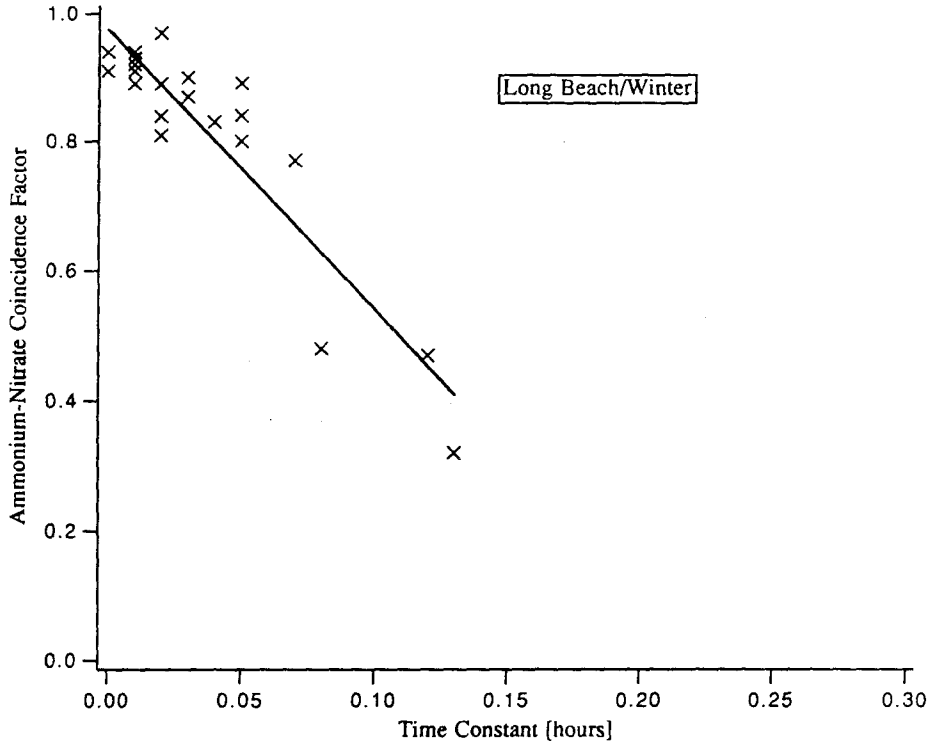

Figure 8. The ammonium nitrate coincidence factor as a function of the equilibration time scale τ_∞ for Long Beach, CA in the fall.

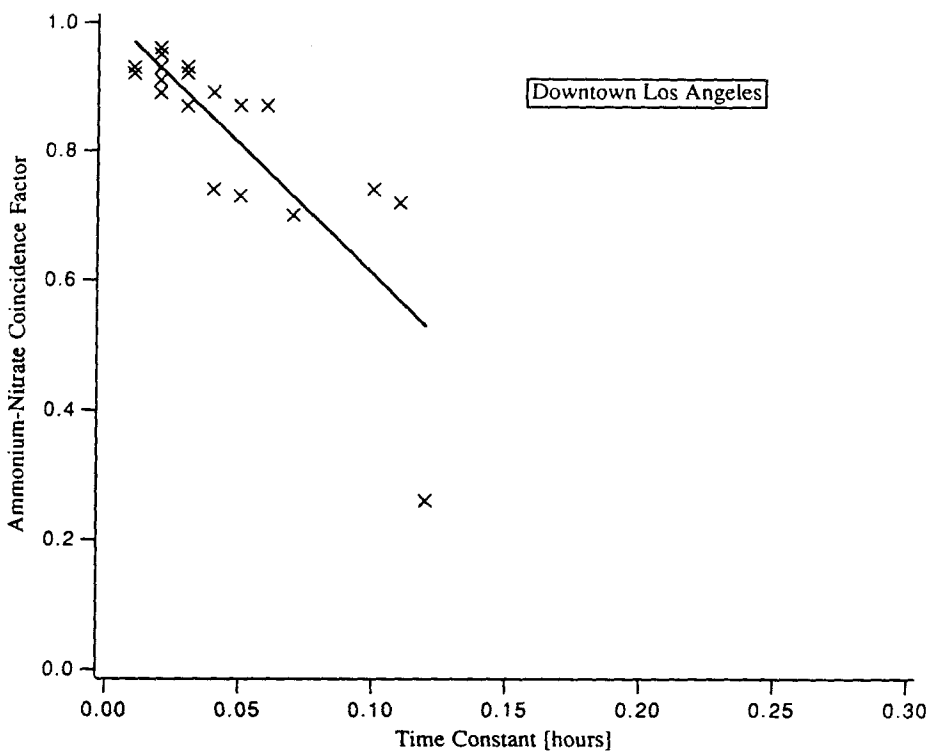

Figure 9. The ammonium nitrate coincidence factor as a function of the equilibration time scale τ_∞ for downtown Los Angeles, CA.

(Wexler and Seinfeld, 1990). Thus 5 min. is likely to be the minimum value of τ_∞ when lack of equilibrium is important, but it may be much longer.

Furthermore, the appropriate time scales for equilibration of aerosol particles of different composition are $\tau_{p,i}$, not τ_∞. The time constant, τ_∞, governs equilibration due to changes in the ambient concentrations. The time constants $\tau_{p,i}$ were not explicitly considered here and govern equilibration due to changes in the ammonium nitrate particle-surface partial pressure product. Although, equilibration between particles of different ammonium nitrate ratios occurs over times proportional to the $\tau_{p,i}$, these time constants can be related to τ_∞ for an osmotically benign, monodisperse aerosol of uniform composition by

$$\tau_p \sim \frac{W}{K}\tau_\infty, \tag{15}$$

where W is the aerosol water content and K is the equilibrium constant between the gas and aqueous form of the components. Thus, τ_∞ and τ_p may vary in a similar fashion, but they are of different magnitudes.

We postulated 1) that under warm, heavily polluted conditions indicative of inland Los Angeles regions, the aerosol is more likely to be in equilibrium with the gas phase, and 2) that under cooler, less polluted conditions indicative of a more coastal Los Angeles climate, the aerosol is less likely to be in equilibrium with the gas phase (Wexler and Seinfeld, 1990). In the summer, the two inland locations, Riverside and Claremont, show a much higher coincidence factor than the coastal location, Long Beach, although there is not a significant difference between the coincidence factors at the winter sites, Long Beach and Downtown Los Angeles. The inland locations were predicted to have shorter values of τ_∞ since there the mean aerosol size is smaller and the aerosol mass loading is higher, both of which provide a larger surface for transport to and from the aerosol phase. The coastal

locations were predicted to have longer τ_∞ values because there the mean aerosol size is larger and the aerosol mass small, both of which lead to a smaller surface area for transport. The data appear to support these earlier postulates.

Why do Ammonium and Nitrate Have Different Size Distributions?

As we discussed earlier, ammonium and nitrate appear to reside in different size distributions under conditions of long equilibration time constants, τ_∞. The question now arises as to the physical mechanisms that are responsible for appearance of these species in different size particles.

It has been proposed that the Kelvin effect may be an explanation for the observation that nitrate tends to appear in the larger particles and sulfate in the smaller particles under typical conditions in Los Angeles (Bassett and Seinfeld, 1984). We postulated that the Kelvin effect probably provides a minimal influence on the size distribution of ammonium nitrate (Wexler and Seinfeld, 1990). Under conditions when τ_∞ is short, the aerosols of various sizes and compositions are able to equilibrate with each other. If the Kelvin effect were significant, ammonium and nitric acid would preferably condense on larger particles, and the non-volatile sulfate would remain in smaller particles. But if the ionic components of the aerosol are primarily ammonium, nitrate, and sulfate then from Equation (11) we have

$$\frac{M_{a,i}}{M_{n,i}} \sim 1 + 2\frac{M_{s,i}}{M_{n,i}} \tag{16}$$

and we see that the ratio $M_{a,i}/M_{n,i}$ would be different for the large and small particles, and the observed coincidence factor would be small. What is observed though are high coincidence factors for short values of τ_∞, and thus the Kelvin effect does not appear to significantly influence the size distribution of ammonium nitrate in the atmosphere.

Another mechanism that may distribute ammonium and nitrate differently by size due to differences in the distribution of nitrate and sulfate is transport from the gas to aerosol phase. The single particle mass transport is given in Equation (2). Taking the ratio of this expression with itself for different size particles gives

$$\frac{J(R_{p,1})}{J(R_{p,2})} = \frac{R_{p,1}}{R_{p,2}} \frac{\alpha + Kn_2}{\alpha + Kn_1}. \tag{17}$$

Thus we see that the accommodation coefficient is the species dependent quantity that may influence the size distribution of a condensing species. Since nitrate usually appears in larger particles, and sulfate in smaller particles this implies that the accommodation coefficient for nitric acid must be less than that for sulfuric acid. The accommodation coefficients of highly soluble species on pure water are typically close to unity. Under atmospheric conditions the accommodation coefficients are typically lower due to surface active organics (Gill et al., 1983), and these surface active agents probably inhibit the accommodation of nitric and sulfuric acids to a similar degree. Thus different accommodation coefficients may explain the different distributions, but only if the sulfuric acid accommodation coefficient is significantly higher than that of nitric acid.

Another possible explanation for the different size distributions of nitrate and sulfate is heterogeneous sulfate formation, which has been proposed as a mechanism for sulfate formation in aqueous-phase particles (Hering and Freidlander, 1982). Most likely sulfite oxidation is reaction-limited in aerosol particles, that is, other physical processes such as transport and mixing are fast compared with the speed of the sulfite oxidation reaction (Schwartz, 1988), so heterogeneously formed sulfate should be size distributed proportional to the volume, or third, moment of the size distribution.

Sulfate and nitrate formed in the gas phase condenses on aerosol particles

according to Equation (2), so their distribution lies between the first and second moment of the aerosol size distribution, and we term this distribution the transport moment. Condensed sulfate or nitrate is size distributed according to the first moment for large particles with high accommodation coefficient and to the second moment for small particles, or particles with a low accommodation coefficient.

If heterogeneous sulfate formation is significant in the atmosphere, the sulfate should be present in the larger particles since its formation is proportional to the volume moment, and the nitrate should be present in the smaller particles since its formation is proportional to the transport moment (Hering and Friedlander, 1982; Seinfeld and Bassett, 1982). This is counter to the observation that the nitrate is usually observed in the larger particles and the sulfate in the smaller, which does not preclude heterogeneous formation of sulfate, but does lead to the conclusion that any heterogeneous sulfate formation is sufficiently small that it does not appear to influence its size distribution with respect to nitrate.

The volatility of nitrate may also affect its size distribution with respect to sulfate. Since the vapor pressure of sulfate is negligible, any sulfuric acid formed in the gas phase indiscriminantly condenses in a distribution proportional to the transport moment, subsequently increasing particle pH. This increased pH tends to increase the vapor pressure of volatile nitric acid, driving it to condense in particles where the sulfate does not prefer to condense. Since the transport moment tends to favor condensation of sulfate on smaller particles, this is a possible explanation for the observed lack of coincidence of the nitrate and sulfate, and the presence of nitrate in the larger size particles.

Is the relation between time scale and coincidence consistent with this proposal? Starting with a neutral-pH size-distributed aerosol, when the time scales are long, initial gas-phase sulfuric and nitric acid condense on the particles according to the

transport moment, but as the particle acidity increases the nitrate is effectively blocked from further condensation and instead tends to condense where the pH is higher. As the aerosol ages, the time scales typically decrease due to larger atmospheric aerosol loading, which gives opportunity for the larger particles rich in volatile nitrate to equilibrate with the smaller particles that are poor in nitrate.

Some of the wind trajectories in the Los Angeles basin carry pollutants over dairy feedlots that are large sources of ammonia. These ammonia rich air masses eventually reach the Riverside area heavily laden with aerosol due to the high ammonia concentration. Since ammonia tends to neutralize aerosol pH, aerosols collected in Riverside should have a higher level of coincidence than Claremont, which is a site with similar meteorologic conditions, but without the large source of ammonia downwind. Figures 5 and 6 show the Claremont and Riverside data. Although the coincidence factors are higher for Riverside, the values of τ_∞ are correspondingly smaller, such that the best fit lines have nearly the same slope and intercept. Thus, we cannot conclude from these data that sulfate condensing in smaller particles drives nitrate to the larger particles.

We have examined a number of possible mechanisms why sulfate appears in smaller particles and nitrate in larger ones. The data lead one to conclude that the Kelvin effect is not responsible, since under equilibrium conditions the size distributions tend to coincide. Aqueous phase oxidation of sulfite does not seem to be the explanation since this process would lead to more sulfate in larger particles, counter to many observations including those during SCAQS. Different accommodation coefficients for nitric and sulfuric acid may explain the distributions, but the accommodation coefficients of the two species must be significantly different to produce the observed distributions. Finally, acidification of aerosol particles due to sulfate condensation in smaller particles, may force the nitrate to condense in the

larger and more neutral particles.

Aerosol Particles are not in Equilibrium with Each Other

It is clear from Figures 5-9 that the aerosol during SCAQS had a wide range of coincidence factors and that the degree of coincidence correlates with the estimated time constant τ_∞. The lack of coincidence between the ammonium and nitrate size distributions indicates that the surface partial pressures of ammonia and nitric acid are different for particles of different size, and that these particles are not in equilibrium with each other. Since there is a strong correlation between this lack of equilibrium and the estimated values of τ_∞, we can conclude that, as predicted in earlier work, transport limitations cause the lack of equilibrium (Wexler and Seinfeld, 1990).

What does this correlation between C_{an} and τ_∞ say about equilibrium between the gas and aerosol phases? If the time constant for equilibration of the gas phase, τ_∞, is shorter than the time constants for equilibration of the aerosol phase, $\tau_{p,i}$, the gas-phase ammonium nitrate will tend to reach equilibrium with the aerosol before aerosol particles of different sizes equilibrate with each other. Once the gas phase has reached equilibrium with the aerosol phase, ammonium nitrate evaporates from particles with higher surface partial pressures and condenses on those with lower surface partial pressures. The gas phase acts as a conduit, passing ammonium nitrate among particles, while its ammonium nitrate concentration remains steady. Thus, even if aerosol particles are not in equilibrium with each other, the gas-phase concentration of ammonium nitrate may be in equilibrium with the transport-averaged aerosol surface partial pressures of ammonium nitrate, and therefore, the degree of equilibrium among aerosol particles does not indicate, one way or the other, equilibrium between the gas and aerosol phases.

IMPLICATIONS FOR AEROSOL MODELING: EQUILIBRIUM OR NOT?

The analyses we have just performed have a number of implications regarding the development of atmospheric aerosol models. The first regards models designed to predict the total mass of particulate matter (e.g., Russell et al., 1983, 1986, 1988). These models assume that 1) the volatile inorganic aerosol species are in equilibrium with their gas-phase counterparts, and 2) the gas-phase ammonia and nitric acid concentrations in equilibrium with the overall PM10 aerosol composition are the same as those in equilibrium with the full size distribution of particles. We have shown that a mixture of ammonium nitrate – ammonium sulfate aerosol particles has the same equilibrium surface partial pressures of ammonia and nitric acid as individual particles, so that modeling the total PM10 content of the aerosol yields the same equilibrium gas-phase concentrations of ammonium and nitric acid as would have been predicted by modeling the complete size distribution of the aerosol. Further we have shown that with the observed scatter in the ammonium nitrate partial pressure product, a departure from equilibrium between the gas and aerosol phases that correlates with the time constant τ_∞ cannot be discerned. Thus thermodynamic equilibrium is probably a reasonable assumption when modeling total PM10 aerosol, considering the uncertainty in the atmospheric measurements.

The second implication of this work concerns prediction of the size distribution of the volatile inorganic species. In previous work we showed that, even at equilibrium, transport between the gas and aerosol phases governs the size distribution of ammonium nitrate for solid particles or aqueous particles osmotically dominated by ammonium nitrate (Wexler and Seinfeld, 1990). In this work we demonstrate that during SCAQS different size particles were not in mutual equilibrium with respect to ammonium nitrate and that the lack of equilibrium correlated well with the magnitude of the time constant, τ_∞. Since a significant percentage of the samples

showed departure from mutual equilibrium, a full transport and equilibrium representation of the aerosol must be employed to accurately predict the size distribution of the volatile inorganics.

ACKNOWLEDGEMENT

This work was supported by the State of California Air Resources Board Agreement A932-054.

REFERENCES

Allen A. G., Harrison R. M. and Erisman J. (1989) Field measurements of the dissociation of ammonium nitrate and ammonium chloride aerosols. *Atmos. Environ.* **23** 1591-1599.

Bassett M. and Seinfeld J. H. (1983) Atmospheric equilibrium model of sulfate and nitrate aerosols. *Atmos. Environ.* **17** 2237-2252.

Bassett M. E. and Seinfeld J. H. (1984) Atmospheric equilibrium model of sulfate and nitrate aerosols – II. Particle size analysis. *Atmos. Environ.* **18** 1163-1170.

Cadle S. H., Countess R. J. and Kelly N. A. (1982) Nitric acid and ammonia in urban and rural locations. *Atmos. Environ.* **16** 2501-2506.

Chan M. and Durkee K. (1989) Southern.California Air Quality Study B-site operations. *California Air Resources Board* **A5-196-32** .

Cohen M. D., Flagan R. C. and Seinfeld J. H. (1987) Studies of concentrated electrolyte solutions using the electrodynamic balance. 2. Water activities for mixed-electrolyte solutions. *J. phys. Chem.* **91** 4575-4582.

Doyle G. J., Tuazon E. C., Graham R. A., Mischke T. M., Winer A. M. and Pitts J. N. (1979) Simultaneous concentrations of ammonia and nitric acid in a polluted atmosphere and their equilibrium relationship to particulate ammonium nitrate. *Environ. Sci. Technol.* **13** 1416-1419.

Eldering A., Solomon P. A., Salmon L. G., Fall T. and Cass G. R. (1990) Hydrochloric acid: A regional perspective on concentrations and formation in the atmosphere of southern California. *Atmos. Environ.* **submitted** .

Fitz D. and Zwicker J. (1988) Design and testing of the SCAQS sampler for the SCAQS study, 1987. *California Air Resources Board* **A6-077-32** .

Gill P. S., Graedel T. E. and Weschler C. J. (1983) Organic films on atmospheric aerosol particles, fog droplets, cloud droplets, raindrops, and snowflakes. *Rev. Geophys. Space Phys.* **21** 903-920.

Gray H. A., Cass G. R., Huntziger J. J., Heyerdahl E. K. and Rau J. A. (1986) Characteristics of atmospheric organic and elemental carbon particle concentrations in Los Angeles. *Environ. Sci. Technol.* **20** 580-589.

Grosjean D. (1982) The stability of particulate nitrate in the Los Angeles atmosphere. *Sci. Total Environ.* **25** 263-275.

Hanel G. and Zankl B. (1979) Aerosol size and relative humidity: Water uptake by mixtures of salts. *Tellus* **31** 478-486.

Harrison R. M. and MacKenzie A. R. (1990) A numerical simulation of kinetic constraints upon achievement of the ammonium nitrate dissociation equilibrium in the troposphere. *Atmos. Environ.* **24A** 91-102.

Hering S. V. and Friedlander S. K. (1982) Origins of aerosol sulfur size distributions in the Los Angeles basin. *Atmos. Environ.* **16** 2647-2656.

Hering S. V. and Blumenthal D. L. (1989) Southern California Air Quality Study (SCAQS) description of measurement activities. Final Report.. *California Air Resources Board* **A5-157-32** .

Hildemann L. M., Russell A. G. and Cass G. R. (1984) Ammonia and nitric acid concentrations in equilibrium with atmospheric aerosols: experiment vs theory. *Atmos. Environ.* **18** 1737-1750.

John W., Wall S. M., Ondo J. L. and Winklmayr W. (1989a) Acidic size distributions during SCAQS. *California Air Resources Board* **A6-112-32** .

John W., Wall S. M., Ondo J. L. and Winklmayr W. (1989b) Acidic aerosol size distributions during SCAQS. Compilation of data tables and graphs. *California Air Resources Board* **A6-112-32** .

John W., Wall S. M., Ondo J. L. and Winklmayr W. (1990) Modes in the size distributions of atmospheric inorganic aerosol. *Atmos. Environ.* **24A** 2349-2359.

Lawson D. R. (1990) The Southern California Air Quality Study. *J. Air Waste Manage. Assoc.* **40** 156-165.

McMurry P. H. and Stolzenburg M. R. (1989) On the sensitivity of particle size to relative humidity for Los Angeles aerosols. *Atmos. Environ.* **23** 497-507.

NOAA (1987) Local climatological data: Monthly summary. *National Oceanic and Atmospheric Administration* .

Pilinis C. and Seinfeld J. H. (1987) Continued development of a general equilibrium model for inorganic multicomponent atmospheric aerosols. *Atmos. Environ.* **21** 2453-2466.

Pilinis C., Seinfeld J. H. and Seigneur C. (1987) Mathematical modeling of the dynamics of multicomponent atmospheric aerosols. *Atmos. Environ.* **21** 943-955.

Pilinis C. and Seinfeld J. H. (1988) Development and evaluation of an Eulerian photochemicl gas-aerosol model. *Atmos. Environ.* **22** 1985-2001.

Russell A. G., McRae G. J. and Cass G. R. (1983) Mathematical modeling of the formation and transport of ammonium nitrate aerosol. *Atmos. Environ.* **17** 949-964.

Russell A. G. and Cass G. R. (1986) Verification of a mathematical model for aerosol nitrate and nitric acid formation and its use for control measure evaluation. *Atmos. Environ.* **20** 2011-2025.

Russell A. G., McCue K. F. and Cass G. R. (1988) Mathematical modeling of the formation of nitrogen-containing air pollutants. 1. Evaluation of an Eulerian photochemical model. *Environ. Sci. Technol.* **22** 263-271.

Saxena P., Seigneur C. and Peterson T. W. (1983) Modeling of multiphase atmospheric aerosols. *Atmos. Environ.* **17** 1315-1329.

Saxena P., Hudischewskyj A. B., Seigneur C. and Seinfeld J. H. (1986) A comparative study of equilibrium approaches to the chemical characterization of secondary aerosols. *Atmos. Environ.* **20** 1471-1483.

Schwartz S. E. (1988) Mass-transport limitation to the rate of in-cloud oxidation of SO_2: Re-examination in the light of new data. *Atmos. Environ.* **22** 2491-2499.

Stelson A. W., Friedlander S. K. and Seinfeld J. H. (1979) A note on the equilibrium relationship between ammonia and nitric acid and particulate ammonium nitrate. *Atmos. Environ.* **13** 369-371.

Stokes R. H. and Robinson R. A. (1966) Interactions in aqueous nonelectrolyte solutions. I. Solute-solvent equilibria. *J. phys. Chem.* **70** 2126-2130.

Sturges W. T., Harrison R. M. and Barrie L. A. (1989) Semi-quantitative x-ray diffraction analysis of size fractionated atmospheric particles. *Atmos. Environ.* **23** 1083-1098.

Tanner R. L. (1982) An ambient experimental study of phase equilibrium in the atmospheric system: aerosol H^+, NH_4^+, SO_4^{2-}, NO_3^- – NH_3(g), HNO_3(g). *Atmos. Environ.* **16** 2935-2942.

Wall S. M., John W. and Ondo J. L. (1988) Measurement of aerosol size distributions for nitrate and major ionic species. *Atmos. Environ.* **22** 1649-1656.

Wexler A. S. and Seinfeld J. H. (1990) The distribution of ammonium salts among a size and composition dispersed aerosol. *Atmos. Environ.* **24A** 1231-1246.

Wexler A. S. and Seinfeld J. H. (1991) Second-generation inorganic aerosol model. *Atmos. Environ.* **submitted** .

Zdanovskii A. B. (1948) New methods of calculating solubilities of electrolytes in multicomponent systems. *Zhur. Fiz. Khim.* **22** 1475-1485.

SECTION 6

MAJOR CONTRIBUTIONS

The primary contribution of this thesis is the discovery that transport processes play an essential role in determining 1) the gas-aerosol partition of ammonium nitrate and 2) the size distribution of the inorganic species. This thesis identifies and evaluates the time scales that govern equilibration between the gas and aerosol phases, and shows that these time scales may be too long under typical conditions in Los Angeles to permit the gas-aerosol equilibrium assumption to apply.

We show that even under conditions where overall equilibrium exists between the two phases that 1) thermodynamic equilibrium does not uniquely determine the size distribution of the volatile inorganics and 2) individual aerosol particles may not be in equilibrium with each other. The first conclusion applies to solid particles or aqueous particles osmotically dominated by ammonium nitrate, since for these particles the aerosol content of ammonium nitrate does not influence the particle-surface partial pressures of ammonia and nitric acid. The second conclusion is caused by the generally longer time scales associated with equilibration of the aerosol phase than associated with equilibration of the gas phase.

The secondary contribution of this thesis concerns the deliquescent behaviour of aerosol particles. We derive expressions for the temperature and composition dependence of the deliquescence point. It is shown that the deliquescence point may vary significantly with temperature and that this variation can be predicted from readily available thermodynamic data. The deliquescence point is also shown to vary with composition such that the mutual deliquescence point is always less than that of the individual components.

Most of the work in this thesis is generally applicable to urban and regional

atmospheric aerosol formation processes. In the future these principles and the aerosol inorganics model developed in this work should be incorporated into full atmospheric models of urban and regional polluted environments and used to predict the aerosol mass and size distribution of the inorganic species. Using such a model, the source-receptor relationships that govern the aerosol mass of these inorganics can be determined, and appropriate and cost-effective control measures applied.

APPENDIX A

AIM PROGRAM DOCUMENTATION

The AIM program was used in the comparisons in Sections 4 and 5 of this thesis. The primary component of AIM is the aerosol operator (subroutine aeropr) that models transport between the gas and aerosol phases of the condensible inorganic species. This appendix contains the call tree for the modules called by the subroutine aeropr and documents of each of these modules.

Call Tree for Aerosol Inorganics Operator

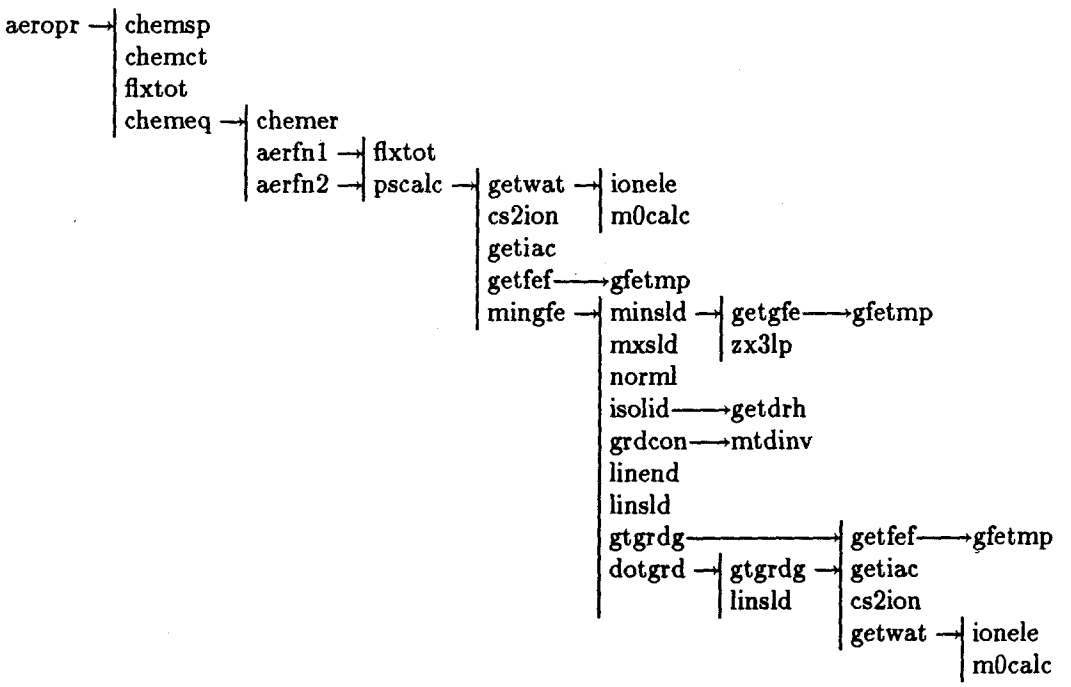

```
------------------------------------------------------------------

     block data aeapbd

 aerosol property block data

------------------------------------------------------------------

     block data aegpbd

 aerosol gas property block data

------------------------------------------------------------------

     subroutine aerfn1(acon,ratef,ratel,time)

 right hand side of ode's for mass of condensible/m^3 in aerosol

 inputs:
       acon    umoles/m^3 concentration of condensibles in aerosol phase
       time    time

 outputs:
       ratef   formation rate
       ratel   loss rate

------------------------------------------------------------------

     subroutine aerfn2(acon,ratef,ratel,time)

 right hand side of ode's for mass of condensible/m^3 in aerosol
```

inputs:

acon	umoles/m^3 concentration of condensibles in aerosol phase
time	time

outputs:

ratef	formation rate
ratel	loss rate

---

subroutine aeropr(tbeg,tend,gcon,aconc,rhd,tempd)

integerate from tbeg to tend moving stuff between gas and aerosol phases

inputs:

tbeg	time for beginning of integration [minutes]
tend	time for end of integration [minutes]
gcon	gas phase concentrations [umoles/m^3]
aconc	aerosol phase component concentrations [umoles/m^3]
rhd	relative humidity [0-1]
tempd	temperature [k]

outputs:

gcon	new gas phase concentrations
aconc	new aerosol phase concentrations

---

entry chemct (tmk)

write out the values of the various indicative counters that the program keeps.

argument list definition:

tmk	d.p.	a floating point number printed to identify the call.

output variable definition:

tmk	d.p.	floating point identifier.
fcount	integer	number of derivative subroutine calls since the last call.
acount	integer	number of times the asymptotic treatment was used since the last call.
rcount	integer	number of times stepsize was reduced since last call.
tfcnt	integer	total of fcount to this call.
tacnt	integer	total of acount to this call.
trcnt	integer	total of rcount to this call.

---

subroutine chemeq (dtchem, dfe, n, f, fmin)

originator: t.r. young nrl 1982

vax version: t.r. young nrl code 4040 may 1983

description: subroutine chemeq solves a class of "stiff" ode.s associated with reactive flow problems. these equations cannot be readily solved by the standard classical methods thus the selected asymptotic integration method is employed. the equations are divided into two catagories based on equilibration times and are integrated by either a low order classical method for the equations which have long equilibration times or a very stable step-centered method which helps preserve the asymptotic nature of the solutions when equilibration times are very short. an adaptive

stepsize is chosen to give accurate results for the fastest changing quantity. the routine assumes that all of the integrated quantites and the time step are positive.

argument list definition:

dtchem	d.p.	the interval of integration or the range of the independent variable. 0.0 c= t <= dtchem.
dfe	d.p.	the name of the derivitive function evaluator subroutine.
n	integer	the number of equations to be integrated. an error exisis if n ls greater than nd set by the parameter statement.
f(n)	d.p.	the initial values at call time i/o and the final values at return time.
fmin(n)	d.p.	minimum values for each function. i

language and limitations: although this subroutine is written in a fashion which promotes vectorization on vector computers, the fortran is nearly standard, and should work with minor modifications on any machine.

entry points: four entry points are provided for flexibility and optimum control.

chemeq: advances the equations the given increment 'dtchem'.

chemct: informative, prints the values of the indicative counters listed below:

1. the number of times asymptotics were used.

2. the number of derivative function evaluations.
3. the number times the integration step was restarted due to nonconvergence of the predictor-corrector scheme.

chemsp: provides the user with the option to reset the most important control parameters.

chempr: informative; prints out internal variables for diagnostic purposes.

subroutines referenced:

dfe whose actual name and definition are supplied by the user is called to obtain the derivitive functions.

call dfe(f, c, d, t)
argument list to dfe,

f(n)	d.p.	current values of the dependent variable.
c(n)	d.p.	calculated formation rates.
d(n)	d.p.	calculated loss rates.
t	d.p.	current value of the independent variable.

chemer: is called whenever an error is detected. currently the only error recognized is a time step that is too small.

call chemer(f, fmin, n)
argument list to chemer; (same definition as "chemeq"),

```
------------------------------------------------------------------

    subroutine chemer

stop if time step too small

------------------------------------------------------------------

    entry chempr (f, fmin, n)

 chempr (f, fmin, n)

 chempr may be called when ever an error occurs that can be
 attributed to the results of chemeq. a partial set of the internal
 variables is printed as a diagnostic.

 argument list definition:
 f(n)          r*4 current values of the dependent variable.
 fmin(n)       r*4 minimum values for each function.
 n             i*4 the number of entries in "f" & "fmin".

------------------------------------------------------------------

    entry chemsp (epsmn, epsmx, dtmn, tnot, pasy, tasy, prt)

 reset any local control parameters if their respective input
 values are greater than zero. default values are used if the
 input values are zero or less repectively.

 argument list definition:
    epsmn              d.p.      the maximum relative error allowed
                                 for convergence of the corrector step.
                                 default value: 1.0e-02
    epsmx              d.p.      thls number provides the basis for
```

		deciding weather convergence can be achieved with out added stepsize reduction. if eps/epsmin is greater than epsmx further reduction is applied. default value : 10.0	
dtmn	d.p.	the smallest stepsize allowed. default value: 1.0e-15	i
tnot	d.p.	the initial value of the independent variable t. default value: 0.0	i
pasy	d.p.	the percentage of the equations for which asymptotics will always be applied. equations with the smallest characteristic stepsize are chosen first.	
tasy	d.p.	asymptotics are applied if the characteristic stepsize of an equation is less than tasy. default value: 1.0e-02.	i
prt	d.p.	controls the output of chemsp. any non zero value suppresses all print output from this entry.	

---

subroutine cs2ion(rmcmp,rmsld,rmion)

calculate moles of ions in aerosol from total moles of components and solids

input

rmcmp moles of components

```
      rmsld   moles of solids

output

      rmion   moles of ions

-----------------------------------------------------------------

    subroutine dotgrd(rmcmp,rmsld,gradg,fac,temp,rh,msld,dot)

calculate dot product of constrained gradient and local gradient

inputs

      rmcmp   moles of components
      rmsld   moles of solids
      gradg   gradient of GFE
      fac     current position of steepest descent line
      temp    temperature [K]
      rh      relative humidity [0-1]
      msld    allowed solids

output

      dot     dot product

-----------------------------------------------------------------

    subroutine flxtot(acon,gcon,aconc)

convert aerosol concentrations to gas phase and aerosol compositions

input

      acon    aerosol and gas phase concentrations

outputs
```

```
      gcon    gas phase concentrations
      aconc   aerosol phase concentrations

-----------------------------------------------------------------

     subroutine getdrh(temp,drhout)

 calculate the deliquescence relative humidity of the aerosol solids
 data gleaned by tony in 1989

 input
     temp      temperature in degk

 output
     drhout    deliquescence points (0-1)

-----------------------------------------------------------------

      subroutine getfef(temp,fefsld,fefion,fefgas)
 this routine calculates the free energies of formation at temperature temp

 input
      temp   temperature in degrees kelvin

 output
      fefsld   free energy of formation of the solids at temp
      fefion   free energy of formation of the ions   at temp
      fefgas   free energy of formation of the gases  at temp

-----------------------------------------------------------------

     subroutine getiac(rmion,water,temp,gamma)

 calculate the ion activity coefficients in solution using meissner's method
```

```
 inputs
     rmion      moles of each component
     water      mass of water in solution [kg]
     temp       temperature degk

 outputs
     gamma      activity coefficient of each electrolyte

 written by tony 1/90

-----------------------------------------------------------------
     subroutine getwat(rmion,rh,temp,water)

 calculate the water content of the aerosol given the component molalities.
 this routine is designed to calculate the water content of the aerosol
  by assuming that all the bisulfate is actually protons and sulfate.
  this way we can calculate the water content without knowing the results
  of the sulfate equilibrium.

 inputs
         rmion  - moles of ions
         rh     - relative humidity
         temp   - temperature

 output
         water  - kilograms of water

-----------------------------------------------------------------
     function gfetmp(gf,hf,cp,temp)
```

```
calculate the free energy of formation divided by rt at temperature temp

input
      temp    temperature [k]
      hf      enthalpy
      cp      heat capacity

output
      gf      free energy of formation at temperature t

-----------------------------------------------------------------
    subroutine grdcon(gradg,rmcmp,rmsld,rmsldx,msld,slds)

apply the constraints to the gradient vector
this algorithm follows that of
        david russell, optimization theory, w. a. benjamin, inc. 1970

inputs:
      gradg   unconstrained gradient
      rmcmp   normalized moles of components [sum(rmcmp(i)**2)=1]
      rmsld   moles of solids
      rmsldx  maximum moles of solids
      msld    which solids may exist due to deliquescence
      slds    solid stoichiometry

outputs:
      gradg   constrained gradient

-----------------------------------------------------------------
    subroutine gtgrdg(rmcmp,rmsld,temp,rh,msld,gradg)
```

```
calculate the gradient of the gfe

inputs
      rmcmp   moles of components
      rmsld   moles of solids
      temp    temperature [k]
      rh      relative humidity [0-1]
      msld    allowed solids

output
      gradg   gradient of gfe

-----------------------------------------------------------------

    subroutine ionele(rmion,rmele)

convert moles of ions to moles of electrolyte

input
      rmion   moles of ions

output
      rmele   moles of electrolyte

-----------------------------------------------------------------

    subroutine isolid(rh,temp,msld)

check which salts may be in solid form

inputs:
      rh      - relative humidity
      temp    - temperature
```

```
output:
      msld   - solids that may exist

-----------------------------------------------------------------

     subroutine linend(rmcmp,rmsld,gradg,msld,slds,facend)

find out what value of facend makes the equation rmsld(i)-gradg(i)*facend
  hit the first constraint

inputs
      rmcmp   moles of components
      rmsld   moles of solids
      gradg   gradient of the gfe
      msld    allowed solids

output
      facend  value of fac that hits first constraint

-----------------------------------------------------------------

    subroutine linsld(rmsldc,gradg,fac,rmsld)

calculate position on line

inputs:
      rmsldc - initial point
      gradg  - direction from point
      fac    - how much to go

output:
      rmsld  - final point
```

```
------------------------------------------------------------------

     subroutine m0calc(rh,temp)

 calculate the molality of the salt that has activity equal to rh

 inputs:
     rh   relative humidity 0-1.0
     temp temperature in degrees kelvin

 output:
     rm0  vector of molalities set in common block /m0cb/

 note: rm0 does not vary much with temperature (cohen and seinfeld,
       j. phys. chem. 91:4569) and so we will use the values
       calculated by chris pilinis in his sectional equilibrium codes
       and ignore temperature variations.  i've added in nitric and
       hydrochloric acids.

------------------------------------------------------------------

     subroutine mingfe(rmcmp,temp,rh,rmsld,epscnv,nbisct,maxits)

 minimize the gibb's free energy

 inputs:
     rmcmp  - mole of components
     temp   - temperature degk
     rh     - relative humidity
     epscnv - convergence criterion
     nbisct - number of bisections
     maxits - maximum number of iterations before convergence given up
```

```
 outputs:

     rmsld  - moles of each solid

-----------------------------------------------------------------

     subroutine minsld(rmsld,msld,temp,slds)

 minimize gibbs free energy in solid phases by linear programming

 inputs

       rmsld   moles of solids

       msld    allowd solids

       temp    temperature

       slds    stoichiometry of solids

 output

       rmsld   revised moles of solids

-----------------------------------------------------------------

    subroutine mtdinv(n,a,x,eps,indic,nrc,deter,irow,jcol,jord,y)

 this routine started out as the simul routine on page
 290 of applied numerical methods.  it was modified by
 tony in nov. 1984 to be much faster.

 args:

    n       dimension of matrix to invert

    a       array containing matrix to invert

                    n=2,indic=1(max=3):  |1 3|5|

                                         |2 4|6|
```

```
x       solution vector
eps     if the pivot is less than eps, bombo
indic   flag which chooses mode for matinv
     <0 computes inverse in place
     =0 computes inverse in place and computes solution
        vector from a(i,n+1) vector
     >0 computes solution vector from a(i,n+1) vector
        only. inverse is not computed
nrc     actual dimension of array a
deter   the determinant of the array
irow    integer scratch array dimensioned n
jcol    integer scratch array dimensioned n
jord    integer scracth array dimensioned n
y       d.p. scratch array dimensioned n.  the same area can be used for
          both jord and y since they are not used simultaneously.  in
          general y has twice as many bytes as jord though.
```

```
     subroutine mxsld(rmcmp,msld,rmsldx)

 calculate maximum moles of each solid

 inputs
      rmcmp   moles of components
      msld    allowed solids

 output
      rmsldx  maximum moles of each solid
```

```
      subroutine norml(veci,len,veco)

 normalize a vector (this may blow if vec elements too big)

-----------------------------------------------------------------

      subroutine pscalc(rmcmpd,rmsld,rh,temp,ps,water,ppac,ppan)

 calculate the surface partial pressures given the aerosol composition

 inputs
       rmcmpd    umoles/m^3 of components
       rh        r.h.
       temp      temperature [k]

 outputs
       rmsld     umoles/m^3 of solids
       ps        surface partial pressure [umoles/m^3]
       water     kg of water
       pphc      partial pressure product for ammonium chloride [umoles/m^3]^2
       pphn      partial pressure product for ammonium nitrate [umoles/m^3]^2

-----------------------------------------------------------------

      block data sldstc

 data statements describing solid stoichiometry
```